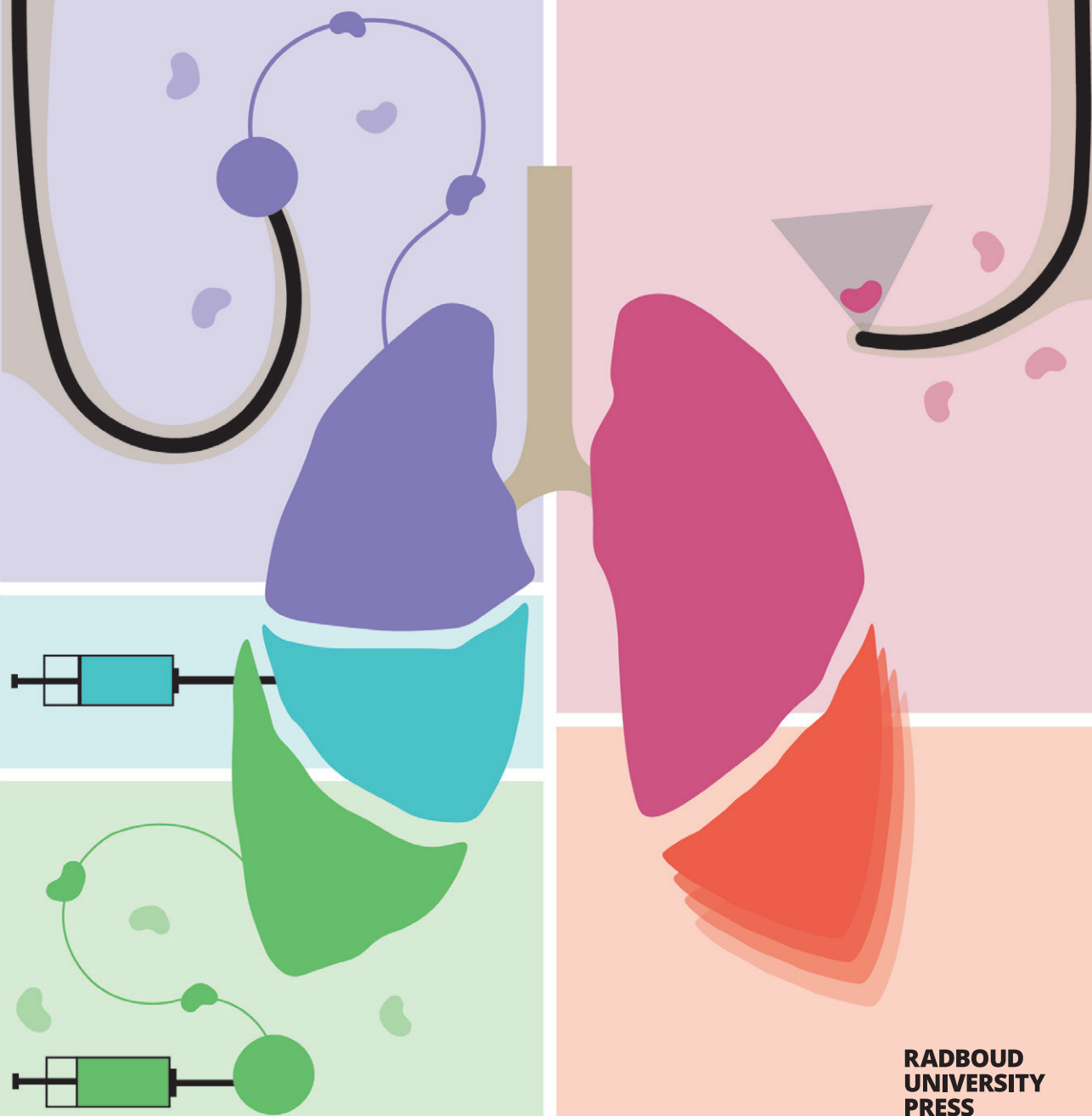


Advanced image-guided diagnosis and staging in patients with early-stage lung cancer



Desi K. M. ter Woerds

**RADBOD
UNIVERSITY
PRESS**

Radboud
Dissertation
Series

Advanced image-guided diagnosis and staging in patients with early-stage lung cancer

Desi ter Woerds

**Advanced image-guided diagnosis and staging
in patients with early-stage lung cancer**

Desi ter Woerds

Radboud Dissertation Series

ISSN: 2950-2772 (Online); 2950-2780 (Print)

Published by RADBOUD UNIVERSITY PRESS
Postbus 9100, 6500 HA Nijmegen, The Netherlands
www.radbouduniversitypress.nl

Design: Proefschrift AIO | Guus Gijben

Cover: Desi ter Woerds

Printing: DPN Rikken/Pumbo

ISBN: 9789465150451

DOI: 10.54195/9789465150451

Free download at: <https://doi.org/10.54195/9789465150451>

© 2025 Desi ter Woerds

**RADBOUD
UNIVERSITY
PRESS**

This is an Open Access book published under the terms of Creative Commons Attribution-Noncommercial-NoDerivatives International license (CC BY-NC-ND 4.0). This license allows reusers to copy and distribute the material in any medium or format in unadapted form only, for noncommercial purposes only, and only so long as attribution is given to the creator, see <http://creativecommons.org/licenses/by-nc-nd/4.0/>.

Advanced image-guided diagnosis and staging in patients with early-stage lung cancer

Proefschrift ter verkrijging van de graad van doctor
aan de Radboud Universiteit Nijmegen
op gezag van de rector magnificus prof. dr. J.M. Sanders,
volgens besluit van het college voor promoties
in het openbaar te verdedigen op

dinsdag 9 december 2025
om 16:30 uur precies

door

Desi Karina Maria ter Woerds
geboren op 20 juli 1995
te Enschede

Promotoren:

Prof. dr. H.F.M. van der Heijden

Prof. dr. A.F.T.M. Verhagen

Copromotoren:

Dr. E.H.J.G. Aarntzen

Dr. R.L.J. Verhoeven

Manuscriptcommissie:

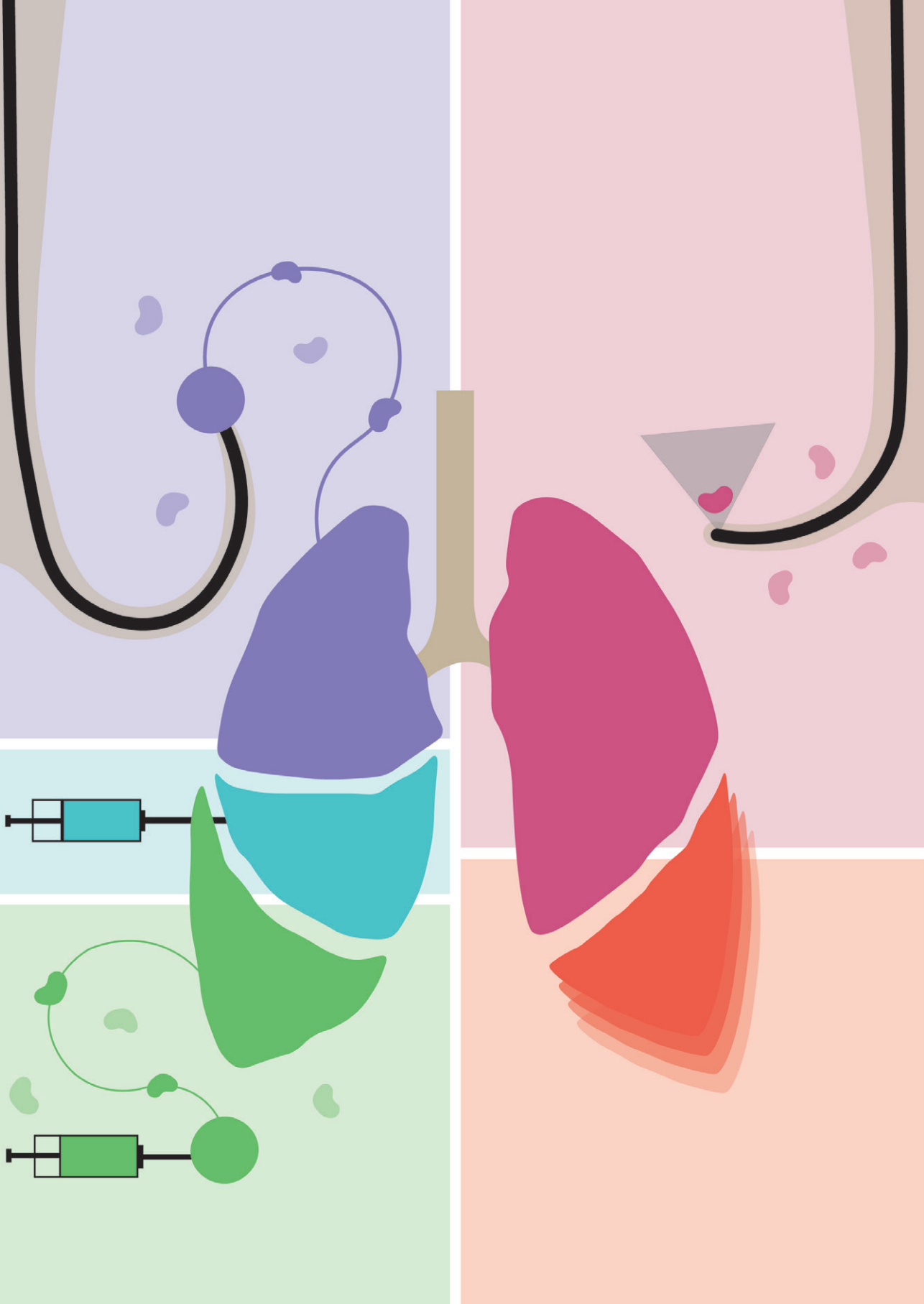
Prof. dr. J.J. Fütterer

Prof. dr. J.T. Annema (Amsterdam UMC)

Dr. O.C.J. Schuurbiers-Siebers

Table of contents

Chapter 1	General introduction and outline of thesis	7
Part I	Feasibility and added value of a sentinel lymph node procedure in lung cancer	
Chapter 2	Ex-vivo exploration of an endobronchial sentinel lymph node procedure in lung cancer for optimizing workflow and evaluating feasibility of novel imaging tools <i>Journal of Thoracic Disease, 2023;15(2):291-299</i>	23
Chapter 3	Feasibility of Non-Invasive Sentinel Lymph Node Identification in Early-Stage NSCLC Through Ultrasound Guided Intra-Tumoral Injection of ^{99m} Tc-Nanocolloid and Iodinated Contrast Agent During Navigation Bronchoscopy <i>Cancers (Basel), 2024;16(22):3868</i>	37
Chapter 4	Feasibility of intraoperative Indocyanine green injection to identify lymph nodes at risk of metastatic disease for early-stage lung cancer <i>JTCVS Techniques, 2025;35:172-181</i>	59
Part II	Evaluating current diagnostic and staging practices	
Chapter 5	Endobronchial Ultrasound Staging During Navigation Bronchoscopy for Peripheral Pulmonary Nodules in the Real World: Which Patients Will Benefit? <i>Cancers (Basel), 2025;17(10):1700</i>	77
Chapter 6	Diagnostic Challenges in a Cohort of Screen-detected Nodules Referred for Navigation Bronchoscopy: prevalence of second primary disease <i>Submitted</i>	103
Chapter 7	Summary, general discussion and future perspectives	119
References		133
Appendices	Nederlandse samenvatting	146
	Research data management	150
	List of publications	152
	PhD portfolio	154
	Curriculum Vitae	156
	Dankwoord	158



Chapter 1

General introduction
and thesis outline

As an introduction to this thesis, the following chapter describes our current knowledge and standard practices of diagnostic and staging efforts in patients with lung cancer and other cancer types. By describing current practice in lung cancer and novel practices performed in other cancer types, this introduction aims to reveal the knowledge gaps in lung cancer care that form the rationale behind the research performed in this thesis.

1.1 Lung cancer

Lung cancer is diagnosed in almost 2.5 million patients every year and caused more than 1.8 million deaths in 2022, making it the leading cause of cancer-related mortality. Despite advances in treatment for advanced-stage disease over the past decade, prognosis for patients diagnosed at a late stage remains poor, with limited curative options available.[1, 2] Additionally, the rising complexity and cost of treatments for late-stage lung cancer underline the importance of early detection. Diagnosing lung cancer at an earlier stage could therefore not only improve survival outcomes, but also lead to broader health and societal benefits.[3, 4] Fortunately, the number of patients where the disease is discovered in an early stage is expected to increase due to a larger amount of incidental findings emerging from the widespread use of high-resolution imaging techniques and possible future screening programs.[5, 6]

1.2 Lung cancer stages and types

Lung cancer can be broadly divided into small cell lung cancer (SCLC), accounting for approximately 15% of cases, and non-small lung cancer (NSCLC), accounting for approximately 85% of cases. Compared to NSCLC, SCLC is a more aggressive form of cancer, with an overall 5-year survival rate of 5%.[7] The most common types of NSCLC can be subdivided into adenocarcinoma (AC), squamous cell carcinoma (SCC), and large cell carcinoma and sees a higher overall 5-year survival rate, depending on the extent of disease at discovery.[4] Disease extent is classified into stages I to IV, according to the TNM system (see Figure 1). Firstly, the primary tumor (T) is classified as Tis, which is a group of abnormal cells, to T4, which includes a tumor > 7 cm. Secondly, the regional lymph nodes (N) are classified N0, meaning no metastases, to N3, involvement of contralateral lymph nodes. Lastly, distant metastasis (M) is classified as M0, no distant metastases or M1, distant metastases, including non-mediastinal lymph nodes. The disease stage, defined by the TNM

descriptors, will determine a patient's prognosis. The 5-year survival of patients where only a small pulmonary nodule is found (stage IA) is 82%, while patients with distant metastasis (stage IVB) have a 5-year survival rate of just 7%. Accurate diagnosis and staging is therefore important to determine prognosis and propose the correct treatment.[1]

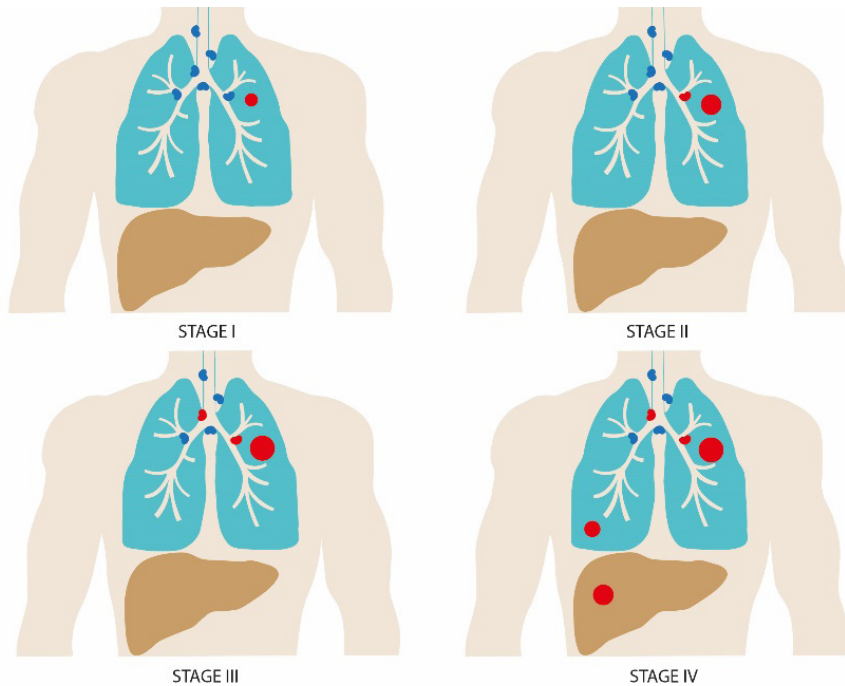


Figure 1: The four stages of lung cancer according to the International Association for the Study of Lung Cancer (IASLC).[1]

1.3 Lung cancer diagnosis

The widespread use of imaging techniques has led to a growing number of incidentally detected pulmonary nodules. The number of patients in whom pulmonary nodules were detected in chest CT scans increased from 38% in 2008 to 50% in 2029.[6] When a pulmonary nodule is detected on a Computed Tomography (CT) scan, either accidentally or through screening, the patient is referred to the hospital where it is crucial for the pulmonary physician to determine the malignancy risk. A Positron Emission Tomography (PET)/CT-scan can subsequently be performed to provide further guidance on risk stratification.[8] Prior to the PET scan, the patient receives an injection with the radiotracer 2-deoxy-2-[^{18}F]

fluoro-D-glucose (^{18}F FDG) which mimics the functionality of glucose, used for the metabolism in the body. Upon radioactive decay, it emits positrons that are annihilated into photons, which can be imaged by the detector of the PET scanner. Increased ^{18}F FDG-uptake in a lung lesion represents elevated metabolic activity, indicating an active process within the body. Whereas an active process can indicate both a benign as well as a malignant process, it often warrants further investigation when combined with clinical characteristics. In malignant disease, the amount of ^{18}F FDG-uptake is strongly associated with tumor aggressiveness and migration of the disease to the lymph nodes.[9] Patient and nodule characteristics as collected through CT and ^{18}F FDG-PET imaging can be used to determine whether a lung nodule could be malignant and warrants (image-guided) biopsy to determine disease origin.[8, 10]

When the risk of malignancy is high, a biopsy of the lesion can be taken to determine the origin of the nodule. Generally, three options exist: surgical biopsy, image guided trans-thoracic needle aspiration and navigation bronchoscopy. A surgical biopsy is relatively invasive and preferably avoided.[11] The currently available minimally invasive options to obtain a biopsy of a peripheral lung nodule are CT-guided transthoracic needle biopsy (TTNB), whereby a needle is inserted into the chest from the outside, and navigation bronchoscopy (NB), which uses the endobronchial paths to reach the lesion. TTNB has an overall diagnostic yield of around 79.0%, but also sees a pneumothorax rate of 28.3% of which 11.5% of patients require a chest tube. [12] Navigation bronchoscopy has emerged as a relatively new, minimally invasive, diagnostic method to obtain tissue from a (peripheral) lung lesion and has shown a diagnostic yield of 73.6-95.3% with only a 3.3% risk of pneumothorax.[12, 13] During a navigation bronchoscopy, both endobronchial as well as trans-parenchymal navigation can be performed using extended working channels for passing of tools through a bronchoscope or robotic assisted bronchoscopy systems. Many technologies and innovations have been developed to confirm the location of the tools as well as to improve tissue sampling, reporting variable diagnostic yields.[14] For example, a radial endobronchial ultrasound (EBUS) mini probe, real-time cone-beam CT (CBCT) guidance with augmented fluoroscopy (AF, see Figure 2A), electromagnetic navigation technology, virtual bronchoscopy navigation (VBN), ultrathin bronchoscopy (UTB) and robotic assisted bronchoscopy (RAB) can be used.[15] Tissue can be obtained by multiple biopsy tools; a hollow needle, brush, cryoprobe, or forceps, see Figure 2B. The cytological specimens obtained by a needle or brush can be analyzed by Rapid On-Site Evaluation (ROSE), where information about the quality of the biopsy and possibility of malignancy is provided intra-procedurally.[16, 17]

1.4 Lymph node staging

Lymph nodes are small, bean-shaped structures that play a crucial role in the immune system by filtering lymphatic fluid and trapping pathogens, foreign particles, and malignant cells. In lung cancer, the lymph nodes in the mediastinum and hilar regions are often the first sites where metastases occur, following lymphatic drainage from the primary tumor. Assessing these nodes is a critical step in determining the extent of disease and guiding treatment decisions.[18] The endobronchial ultrasound (EBUS-)bronchoscope (Figure 3A) is flexible and has an integrated convex ultrasound transducer at the tip.[19] It scans parallel to the insertion direction of the bronchoscope, allowing for real-time visualization of structures of interest, e.g., lymph nodes or tumors. The EBUS-bronchoscope can visualize stations 2, 3p, 4, 7, 10 and 11 via the trachea and stations 5 and 8 via the esophagus, called EUSb (Figure 3B).[20] The size and imaging features of these lymph nodes as determined via ultrasound are used as indicators for possible lymph node involvement and therewith warrant transbronchial needle biopsy (TBNA) and ROSE.[20]

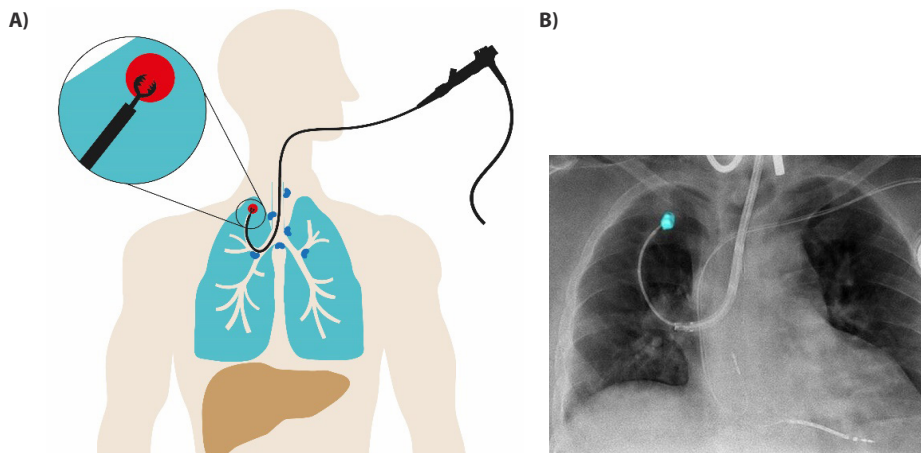


Figure 2: A) The bronchoscope and catheter visible in the thorax, and a lesion as depicted by augmented fluoroscopy (AF). Augmented fluoroscopy uses the known location of the lesion to project it over the 2D fluoroscopy image to guide the bronchoscopist. B) Schematic visualization of a biopsy by forceps during NB.

Since the introduction of EBUS around two decades ago, the purpose of EBUS and EUSb have slowly shifted from a purely diagnostic procedure to confirm metastatic disease to a staging procedure where the objective is to rule out metastatic disease. Staging by EBUS is recommended when a central lesion is found, the N1 nodes are suspected to be involved (see Figure 3B) or in the case of a tumor > 3 cm.[21] In

some cases EBUS cannot reach the lymph nodes or provides insufficient evidence of metastatic disease.[22] A cervical mediastinoscopy could then be performed to assess the lymph nodes more invasively, but this has been deemed unnecessary in most cases after systematic EBUS/EUSb by recent evidence.[23] An EBUS procedure can be combined with navigation bronchoscopy in a single anesthesia procedure, but since lesions of patients referred for primary navigation bronchoscopy are typically < 3 cm, this is often not necessary. The combination is technically easy and attractive, because it allows for simultaneous diagnosis and staging, potentially streamlining clinical workflows. However, no research has yet been performed to determine which patients would benefit from this combination and how time and effort could be used most efficiently.

Treatment plans in the case of early-stage lung cancer predominantly consist of surgery or stereotactic ablative radiotherapy (SABR). Unfortunately, SABR does not allow secondary evaluation of tissue pathology and metastatic disease extent. In the case of surgery, a (lobe-specific) complete lymph node resection is performed alongside primary tumor resection. Resection allows for pathological assessment and staging, which determines if additional therapy is necessary.[24] Even after extensive preoperative staging by an [¹⁸F]FDG-PET/CT-scan, systematic EBUS and EUSb or mediastinoscopy unexpected lymph node metastases are unfortunately found in as much as 23.1% of surgical patients after pathological evaluation of the resected tissue and lymph nodes. Of all occult metastases, up to 54.5% can occur in lymph node regions that are inaccessible for evaluation by current diagnostic procedures, i.e., EBUS and surgical mediastinoscopy.[25-27] The high incidence of upstaging after surgery and the high recurrence rate, implies undetected disease dissemination. One could argue based on these results that our guideline concurrent staging algorithms of using [¹⁸F]FDG-PET/CT and EBUS are of suboptimal quality in the work-up of patients with early-stage lung cancer. Thus, there is a strong reason for further studying methods that could improve detection rate. To improve staging of the lymph nodes in lung cancer, we can look at procedures performed in other cancer types as part of clinical practice to explore the possibility to extent their mechanism to the work-up for patients with (suspected) lung cancer.

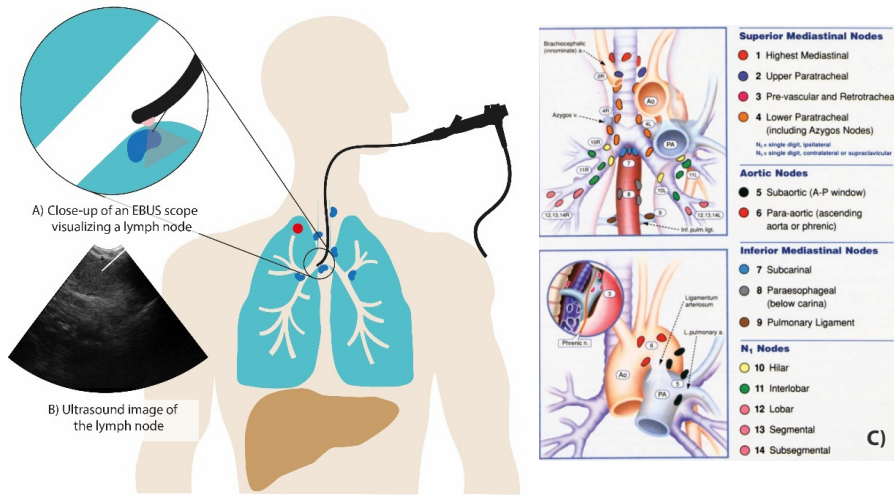


Figure 3: Visualization of an EBUS scope when performing TBNA, with a close up of the tip of the scope, with a needle protruding (A) and an ultrasound image of a lymph node with an imaginary needle (B).[19] C) Categorization of lymph nodes stations in the chest, adapted from Mountain and Dresler (1997), with permission.[20]

1.5 A sentinel lymph node procedure

In for example breast cancer, head and neck cancer and melanoma, a sentinel lymph node (SLN) procedure is routinely performed. The SLN procedure or biopsy usually consists of the injection of a tracer into or surrounding the tumor and follow its lymphatic drainage into the lymph nodes nearby for more detailed evaluation of these lymph nodes after removal. The rationale is to identify the path where tumor cells would metastasize to and determine the lymph nodes where they would most likely harbor first, outside the primary tumor. Specifically in breast cancer, resection of multiple lymph nodes can cause complications like oedema. By removing only the lymph nodes that are necessary for staging or treatment of disease, these complications can be avoided as much as possible.[28]

1.5.1 A sentinel lymph node procedure in lung cancer

In lung cancer, the SLN procedure could be useful to improve the detection rate of lymph node metastases and reduce the chance of recurrence. However, while these procedures are implemented in clinical practice for other cancer types, the transposition to lung cancer is challenging due to anatomical variation of the pulmonary lymphatic vessels and the physiological and physical characteristics of the thorax and lungs. Additionally, there is significant heterogeneity on tracer

type, imaging timepoints, injection location, injection volume and injection method amongst literature on the SLN procedure in lung cancer, making readily implementation difficult.[29] In this thesis, two novel methods that employed different tracer types and injection methods to perform the SLN procedure in lung cancer were explored.

1.5.2 Tracer and injection characteristics for a sentinel lymph node procedure

The injection method, tracer type and identification modality used to find the tracer, but also time between tracer injection and visualization differ per cancer type and purpose of the procedure. In breast cancer, injection protocols have been developed for injection through the skin in the tumor (intratumorally) or around the tumor (peritumorally) in an intradermal, subdermal or peri-subareolar fashion.[28] When the tracer is then visualized, this lymph node can be marked for removal during surgery. If assessment during surgery states that this lymph node is free from tumor cells, all other lymph nodes can remain in situ, without the risk of tumor cells being left behind. This allows for specific and limited lymph node resection. The choice of tracer for a given staging procedure depends on the preferred time between tracer injection and tracer detection, availability of the tracer, evidence of tracer drainage and available detection methods. The time between tracer injection and visibility in the lymph nodes or washout of the lymph nodes depends on the drainage speed and retention of the tracer in the lymph nodes. These characteristics depend on several physical and chemical properties like size, shape, charge, and coating of the particles containing contrast or imaging agents, see Figure 4.[28, 30]

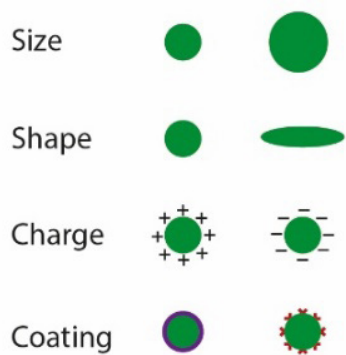


Figure 4: Physical and chemical properties of contrast or imaging particles.

1.5.3 Radioactive tracers for a sentinel lymph node procedure

The majority of the tracers used for SLN procedures are radioisotopes that are visible on single-photon emission computed tomography (SPECT). The most commonly used radioisotope is Technetium-99m (^{99m}Tc), which is frequently combined with colloid-based structures, resulting in a radiotracer that can vary in size.[28] Most hospitals have an elution system that produces ^{99m}Tc on a daily basis, ensuring a steady supply for the production of radiopharmaceuticals used in medical imaging and diagnostics. ^{99m}Tc decays by isomeric transition, with a pure γ -ray emission of 140 keV and a half-life of 6 hours.[31] A SPECT scanner consists of two γ -cameras in a 180° geometry that detect these γ -rays in a 360° orbit, see Figure 5. By combining and reconstructing the detected γ -rays, a 3D image of the radioisotopes is made.[32] In the Netherlands, SLN procedures using ^{99m}Tc -based tracers are routinely performed in breast cancer and melanoma patients. This typically involves a two-day protocol in which the radiotracer is injected the day before surgery. Following injection, SPECT imaging is used to visualize the lymphatic drainage pathway(s) towards the SLN. On the day of surgery, the tracer could be visualized by a hand-held gamma-probe.[33] In breast cancer, the identification rate of SLN is 94%, while in melanoma, identification rates as high as 99% have been reported using similar radiocolloids.

The applicability of the SLN procedure using ^{99m}Tc -based compounds in lung cancer has previously been studied and obtained some satisfactory results in a small number of centers. One of the first groups was Liptay et al. (2000), who injected ^{99m}Tc -sulfur-colloid (15–100 nm) in all four quadrants of the tumor in 54 NSCLC patients and identified SLN in 83% of patients with a hand held gamma detector, approximately one hour after injection.[34, 35] A systematic review and meta-analysis by Taghizadeh Kermani et al. (2013) on the SLN procedure in lung cancer reports a pooled detection rate of 84.4% for radiotracers.[36] However, despite these encouraging results, clinical implementation has not been embraced over the following years.

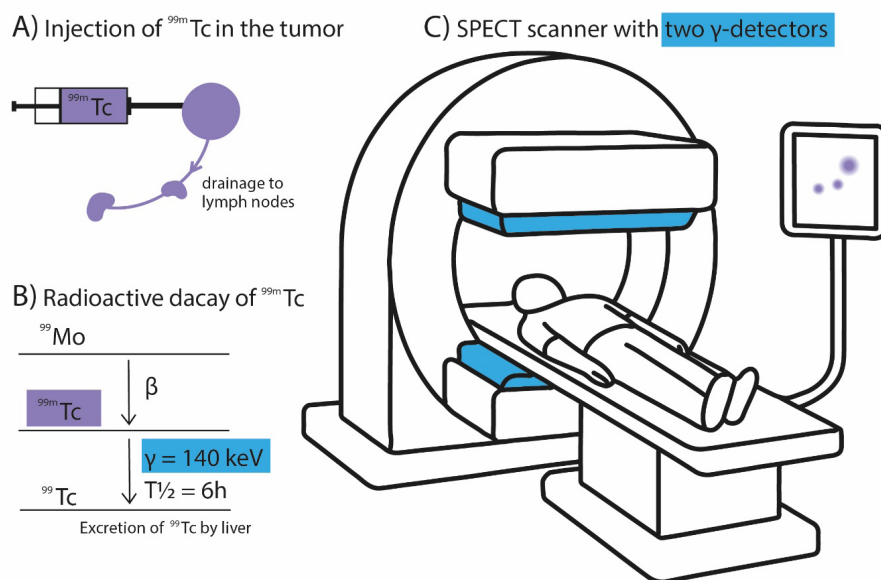


Figure 5: A) Injection of ^{99m}Tc -nanocolloid in or around the lung tumor. B) Radioactive decay of ^{99}Mo to ^{99m}Tc , which takes place in the elution system in the hospital and emits β -radiation; and the radioactive decay of ^{99m}Tc to ^{99}Tc , which emits γ -radiation with an energy of 140 keV and a half-life of 6 hours. C) After injection, the γ -radiation emitted by ^{99m}Tc -(nanocolloid) is detected in the SPECT/CT-scanner and drainage to the lymph nodes can be visualized.

1.5.4 Fluorescent tracers for a sentinel lymph node procedure

The most used fluorescent tracer is indocyanine green (ICG), which is invisible to the naked eye.[37] To be able to visualize the fluorophore, it is excited with a light wavelength of around 775 nm and the subsequently emitted light of 830 nm is measured as the fluorophore relaxes to a lower energy state by radiative decay. Both of these wavelengths are in the near-infrared range, see Figure 6.[38] ICG has a hydrodynamic diameter of 1.2 nm and SLN can be seen around 15 minutes after injection with a tissue penetration depth of up to 1 cm.[39] In cervical cancer, the identification rate of SLN by ICG is 90–100%.[40] In breast cancer, ICG obtains an SLN detection rate of 69–100% and a higher number of SLN can be removed per patient using this method compared to methods with radiotracers.[41] Advantages of ICG are the affordability, easy production, ability to image in a high resolution in real-time, absence of radiation exposure and the fact that it does not stain the surgical field. A disadvantage is the limited tissue penetration depth, see Figure 6, and difficulty in visualizing the complete drainage pattern because of light-tissue reactions like interface reflection, scattering, absorption, and tissue autofluorescence.[38, 42]

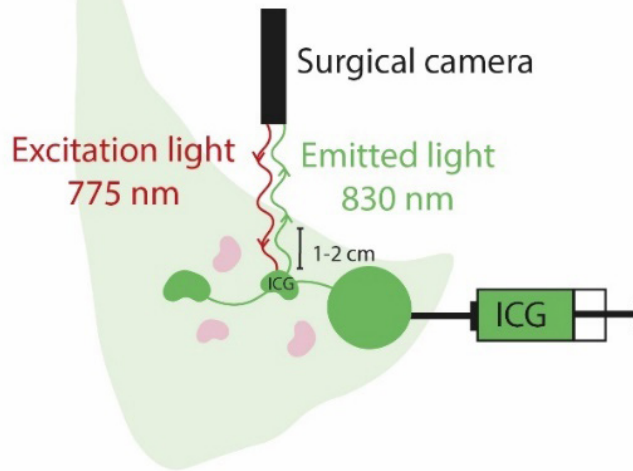


Figure 6: Injection of ICG in the tumor in the lung lobe, followed by drainage to the lymph nodes. Light with a wavelength of 775 nm is used to excite the fluorophore and as it relaxes to a lower energy state by radiative decay it emits light of 830nm which can be measured by a surgical camera. ICG can be detected at a maximal tissue depth of 1–2 cm.

While a two-day protocol includes imaging visualization of the (radioactive) tracer beyond superficial structures, ICG could be used directly in the surgical field because of the fast drainage of the molecule. Both methods are therefore explored in this thesis to determine the feasibility of implementation of both methods in lung cancer and explore these limitations but also the added value for lung cancer staging.

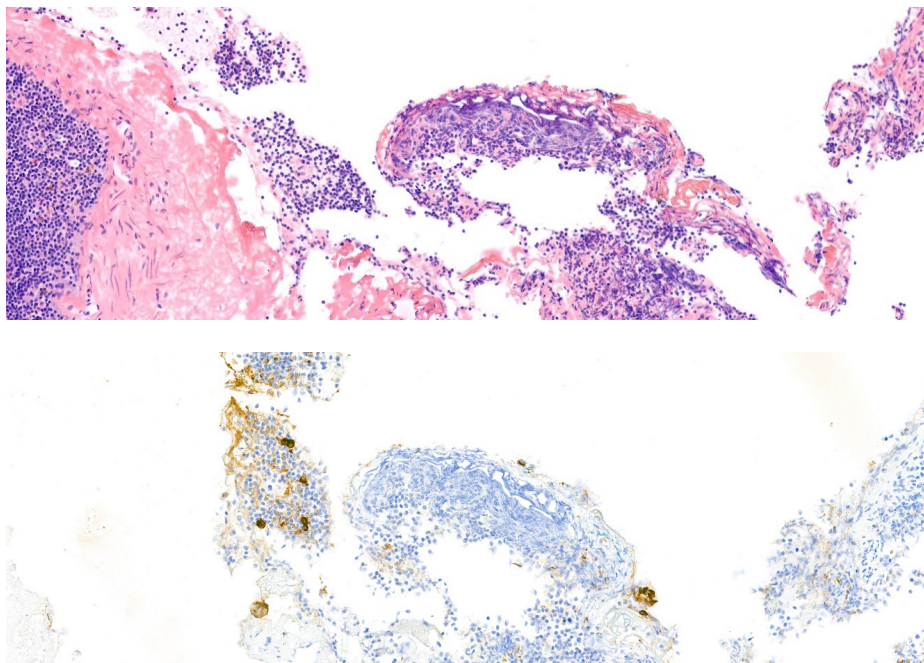


Figure 7: Image of a lymph node stained by H&E (upper image) and cytokeratin (lower image), which shows cytokeratin-containing cancer cells in brown.

1.6 From macro-metastatic to micro-metastatic disease

Performing the SLN procedure, could not only allow for a less extensive lymphadenectomy, but the tracer also provides the first location of possible metastases. After surgery, lymph nodes are evaluated by the pathologist, to check if there are cancer cells present and therewith determine if additional treatment is necessary. Currently, Dutch guidelines state that surgically removed lymph nodes should be cut in thin slices to maximize the chance of finding tumor cells. Microscopic evaluation routinely includes one hematoxylin-eosin (H&E-) stained section and the assessment of the pathologist is based on recognizing the morphology of tumor cells in the removed lymph nodes. Since lymph nodes vary in size, one single H&E stained slice per lymph node might not include possible tumor cells that are present just outside the slice for example, making them more likely to be overlooked and patients more likely to be understaged.[43, 44] The current guidelines have also stated that nodal status (N) is affected when micrometastases are found (< 2.0 mm) but not when isolated tumor cells (ITC, < 0.2 mm) are detected.

New pathological techniques have become available that can detect these micrometastases and ITC in the lymph nodes, which may help improve staging accuracy. Immunohistochemistry (IHC) is frequently used to detect occult metastatic spread by using antibodies specific for cytokeratin (a marker of epithelial cell origin). These antibodies specifically mark cells containing cytokeratin, which do not normally occur in the lymph nodes, making them more visible for pathologists by staining them a different color (See Figure 7).[34] Additionally, reverse transcriptase polymerase chain reactions (RT-PCR) analyzes the gene expression of histologic markers specific for lung cancer metastases. These genes are fundamentally expressed in lung tissue and therefore have low to no expression in lymph nodes.[45]

A systematic review reporting on studies using IHC and/or RT-PCR to detect metastatic cells of lung cancer showed that 0.4%-20.9% of routinely assessed negative lymph nodes contained (micro)metastasis or ITC after additional IHC or RT-PCR. They advise pathologists to consider implementing a more sensitive method, such as serial sectioning in combination with IHC, as the standard diagnostic method for evaluation of lymph nodes in patients with NSCLC might be insufficient.[44] While these techniques hold great potential, they are very time consuming and costly. Performance of the SLN procedure during surgery could offer efficiency by enabling targeted pathological work-up of only those lymph nodes that are most likely to contain metastases. By focusing the pathological and IHC evaluation on these lymph nodes, the additional efforts and costs could be minimized. Implementing this method could improve staging accuracy and reduce the risk of recurrent disease by making patients with previously undetected (micro) metastases eligible for adjuvant treatment.

1.7 Recurrent disease versus second primary disease

When patients are diagnosed at an early stage, curation of disease is often still possible, and the survival rate is significantly higher compared to late-stage disease. The longer survival period of these patients unfortunately also makes them susceptible to the development of new primary lung cancers during follow-up. After curative treatment of lung cancer, patients are followed for several years to be able to detect disease recurrence early but also to allow early detection of second primary lung cancer (SPLC).[46] While the risk of recurrence diminishes over time after treatment, the risk of developing SPLC remains present.[47-49] Distinguishing between recurrent disease and SPLC is not possible on imaging

only, but has profound implications for choice of treatment. A tissue biopsy including pathological and/or additional staining, molecular- or clonal analysis must be performed to determine the origin of the secondary disease and propose the best treatment plan. Unfortunately, this is not always an (available) option and therefore many tumors are treated without pathological confirmation nor analysis of their relation to prior cancer(s).[50] Since it is often unclear whether a second tumor is recurrent disease of SPLC, the incidence of these diseases are also not unambiguously known. The last part of this thesis focusses on the incidence of SPLC and recurrence in a specific patient cohort with a high incidence of (early-stage) lung cancer and a high proportion of patient with a history of lung cancer. Not only patient specific treatment plans but also follow-up conditions and future healthcare needs are based on patient volume, tumor types, survival rates and risk of recurrent and metastatic disease. We aim to better understand in which ways diagnosis and staging could be improved as well as provide predictions on the future care needs of these patients and the (possible) future burden on the healthcare system.

1.8 Thesis outline

This thesis aims to improve diagnostic and staging techniques in early-stage lung cancer. Inspired by SLN procedures successfully implemented in other cancer types, the adaptation and implementation of this technique in early-stage lung cancer patients is explored by two methods in the first part of the thesis. In the second part, current practices are evaluated to provide recommendations on the use of staging and diagnostic procedures to make optimal use of our healthcare resources. By exploring the use of alternative imaging and pathological strategies, this work seeks to close the knowledge gaps mentioned in this chapter and contribute to more personalized care for lung cancer patients and reduce their risk of developing recurrence.

Part I - Feasibility and added value of the SLN procedure in lung cancer

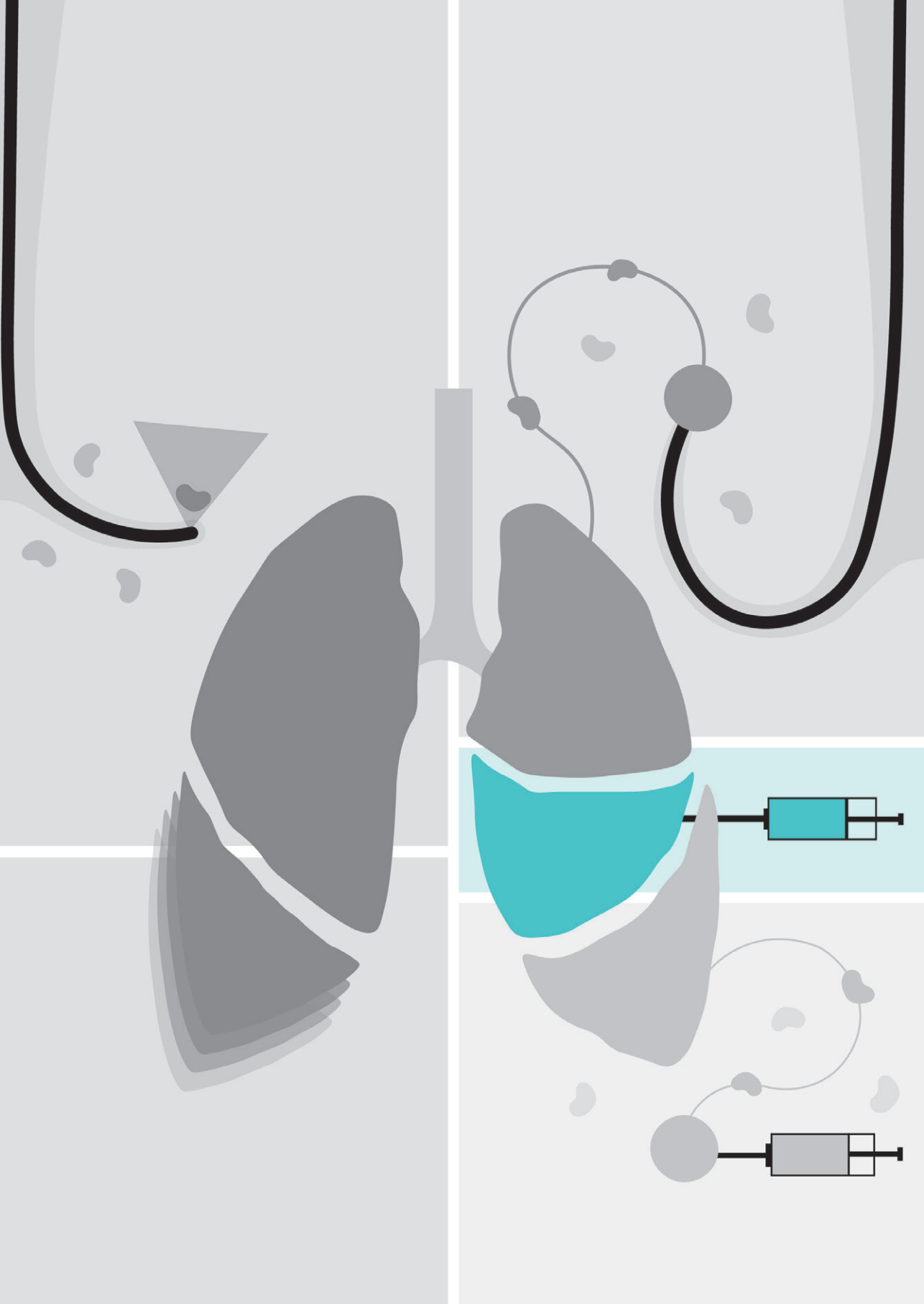
In other cancers, the SLN procedure has been proven to aid in staging and treatment, but the added value of this procedure has not been proven in lung cancer in such a way that it is embedded in clinical practice. Part I of this thesis focusses on the technical aspects of the SLN procedure in lung cancer by exploring new technological advancements to detect lymph node location and involvement. The possibility to identify the SLN is evaluated firstly during diagnostic 3D-image guided navigation bronchoscopy and subsequently during surgical resection.

Chapter 2 explores the SLN procedure for lung cancer by reporting on an *ex vivo* study to determine whether an endobronchial injection with a novel radial ultrasound tool would be feasible in patients with early-stage NSCLC. This research is translated to an *in vivo* setting in **Chapter 3** where we investigate the feasibility of this technique in patients with suspected early-stage lung cancer undergoing navigation bronchoscopy. The novel catheter is used to perform injections of ^{99m}Tc -nanocolloid endobronchially, and subsequent SPECT/CT-imaging is performed to determine feasibility of SLN identification. **Chapter 4** describes a clinical trial in early-stage lung cancer patients undergoing surgery, where NIR imaging was used after the injection of ICG was injected during surgery to find the SLN in lung cancer patients. The found SLN were subjected to additional pathological and immunohistochemical evaluation to determine if more metastatic disease is found and establish the added value of this procedure.

Part II - Evaluating current diagnostic and staging practices

The second part focusses on a detailed analysis of diagnostic and staging procedures already embedded in clinical practice to improve healthcare utilization. While the value of mediastinoscopy after EBUS was already proven to be minimal, the performance of EBUS in patients with a small peripheral nodule referred for a navigation bronchoscopy was investigated in **Chapter 5**. In many of the patients in this cohort, lymph node involvement is not expected and eventually found in even fewer patients. Selecting patients for the combination of EBUS during a diagnostic navigation bronchoscopy procedure based on imaging features could improve the use of OR-time and personnel without decreasing diagnostic accuracy. Lastly, **Chapter 6** describes the incidence of second primary lung cancer and recurrence in a cohort of patients undergoing navigation bronchoscopy that have been subjected to follow-up. By exploring the incidence of SPLC and recurrence, the necessity of additional diagnostic procedures and lung cancer treatments for these patients and the burden on the healthcare system can be better predicted.

In **Chapter 7**, the above-mentioned work is summated, the findings are discussed further and future perspectives involving staging as well as possible treatments are given.



Chapter 2

Ex-vivo exploration of an endobronchial sentinel lymph node procedure in lung cancer for optimizing workflow and evaluating feasibility of novel imaging tools

Desi K.M. ter Woerds, Roel L.J. Verhoeven, Stefan M. van der Heide, Ad F.T.M. Verhagen, Erik H.J.G. Aarntzen and Erik H.F.M. van der Heijden

Published in Journal of Thoracic Disease (2023)

2.1 Abstract

Background: Early-stage lung cancer is treated with curative intent by surgery or radiotherapy. However, upstaging is frequently seen after surgery in clinical N0 lung cancer patients, and despite curative intent, 2-year recurrence rates of 9–28% are reported. A sentinel lymph node (SLN) procedure could improve the staging accuracy. We explored the feasibility of performing a navigation bronchoscopy based SLN procedure in human ex vivo lung cancer specimens to optimize procedural parameters and assess a novel injection tool.

Methods: Ten lung resection specimens were included and allocated to either peri- or intratumoral injection of a tracer combining ^{99m}Tc -nanocolloid and indocyanine green (ICG) while varying the injection volume. A Pioneer Plus catheter with a pre-angulated 24G needle and an ultrasound (US)-element was used to perform real-time US guided transbronchial injections at multiple locations. Thereafter, single photon emission computed tomography/computed tomography (SPECT/CT)-scanning was performed to image injection depots and to assess their location relative to the tumor.

Results: An average volume of 0.7 mL (range, 0.3–1.2 mL) with an average activity of 89.5 MBq ^{99m}Tc (range, 35.4–188.0 MBq) was injected. Intratumoral injections in non-solid and solid tumors were successful in 100% and 64.3% respectively, while 100% of peritumoral injections in solid tumors were successful. The US-element of the catheter allowed real-time imaging and was able to visualize all tumors and 67.4% of all injections. SPECT/CT-scanning visualized 76.7% of the injection depots.

Conclusions: A navigation bronchoscopy mediated SLN procedure seems technically feasible. The Pioneer Plus is a suitable catheter to place tracer depots at multiple intra-/peri-tumoral sites, while receiving real-time feedback on the needle localization in relation to the tumor. The next step of in vivo injections will determine if tracer drainage to the SLN can also be detected on pre- and per-operative imaging.

2.2 Introduction

Non-small cell lung cancer (NSCLC) accounts for 85% of all diagnosed lung cancers. Its 5-year survival rate is highly depended on the stage of disease and ranges from > 77% in stage IA disease to 10% in stage IVA disease.[4] A minority of NSCLC patients are diagnosed at an early stage and these tumors are treated with curative intent, receiving surgery or stereotactic ablative radiation.[7] Even in this early stage, 2 years after intended curative treatment, a recurrence rate of 9.4–28.3% is observed.[51, 52] Moreover, up to 23.1% of clinically N0-staged patients are upstaged to N1 or N2 lymph nodal involvement based upon routine pathological examination of surgically resected material.[25] These results indicate that the presence of occult disease — albeit micro- or macro-metastatic — might be underestimated in early-stage NSCLC, resulting in undertreatment and inferior outcomes.[53]

A technique that could improve the staging accuracy and that is increasingly used in other clinical fields is a sentinel lymph node (SLN) procedure. An injection of a radioactive, fluorescent, or paramagnetic tracer is administered in, or surrounding the tumor area which subsequently drains via the lymphatic system to the locoregional lymph nodes. These tracers are then visualized on imaging before or during surgery to help identify and retrieve the first draining ('sentinel') lymph node, allowing further specific evaluation. ^{99m}Tc -nanocolloid and/or indocyanine green (ICG) are most often used, but other methods can also be applied.[37] The literature on SLN procedures in lung cancer by radioactive tracers or ICG suggests an identification rate of around 90%, while varying approaches are reported.[29, 36, 54] Despite this published success, an SLN procedure has not been implemented into routine surgical treatment, mainly due to the complexity and lack of clinical consequences since lobectomy still is the cornerstone of curative surgery.[55] However, with the raised interest in sublobar resection and the upcoming interest in minimal invasive, image guided local therapy, the importance of research revolving around SLN is considerably increased.

Since an SLN procedure is not part of clinical practice for lung cancer, no standardized protocol has been established. The need for a robust and accurate protocol to standardize the injection, identification and dissection of SLN has been addressed by multiple authors in the past.[29, 56, 57] This will be essential to determine the added value of an SLN procedure in lung cancer treatment. In NSCLC, both peri- and intratumoral tracer injections have been successfully

performed before and during surgery to identify the SLN, but there is often no specific rationale for choosing one above the other.[45, 58]

Nowadays, patients with a peripheral pulmonary nodule suspected of lung cancer are increasingly often diagnosed through cone-beam computed tomography (CBCT)-based navigation bronchoscopy programs.[16, 59-61] These procedures may facilitate the opportunity to perform an SLN procedure in patients with small peripheral pulmonary lesions during diagnostic work-up.[62] A pre-operative identification of the SLN could possibly decrease operation time and improve SLN localization, particularly in patients with atypical drainage patterns or with an SLN outside the surgical field.[63] In this *ex vivo* study, we aim to assess multiple parameters that are relevant for a standardized SLN procedure through transbronchial injection.

2.3 Methods

2.3.1 Study design

This is a prospective, single-center study using *ex vivo* lung resection specimens that examined the feasibility of an endobronchial SLN procedure in lung cancer patients. Multiple procedure parameters were varied in small subsets of explants and adjusted to optimize a protocol that could be implemented in clinical practice. Furthermore, a novel device was used to test its clinical value as an endobronchial injection tool.

Patients undergoing lung cancer resection, either by segmentectomy, lobectomy or pneumectomy, were eligible to participate in the study. The study was conducted in accordance with the Declaration of Helsinki (as revised in 2013). The Research Ethics Committee of the Radboud University Medical Center agreed upon study design and confirmed that no formal ethical approval is required for this research (Reference No. 2020-6946). All patients gave informed consent for use of resected lung specimen within this feasibility study prior to study enrollment. A total of 10 patients were included. Patient demographic and nodule characteristics were collected.

2.3.2 Radioactive tracer

A dual-labelled radioactive-fluorescent tracer (^{99m}Tc -ICG-nanocolloid, GE Healthcare) was used for injection. For the purpose of this study, the fluorescent component of this tracer was not utilized. To test the retention of tracer volume (i.e., spillage)

and repeatability of injection, we varied injection volume — previously described as feasible in literature — while taking tumor size into account by not injecting the largest volume in the smallest tumor.[56, 58] Volumes and dose activity were obtained from pooled commercially available single syringes pre-filled with ^{99m}Tc -ICG-nanocolloid. All used materials and the syringe were measured before and after the injections to calculate the total injected activity.

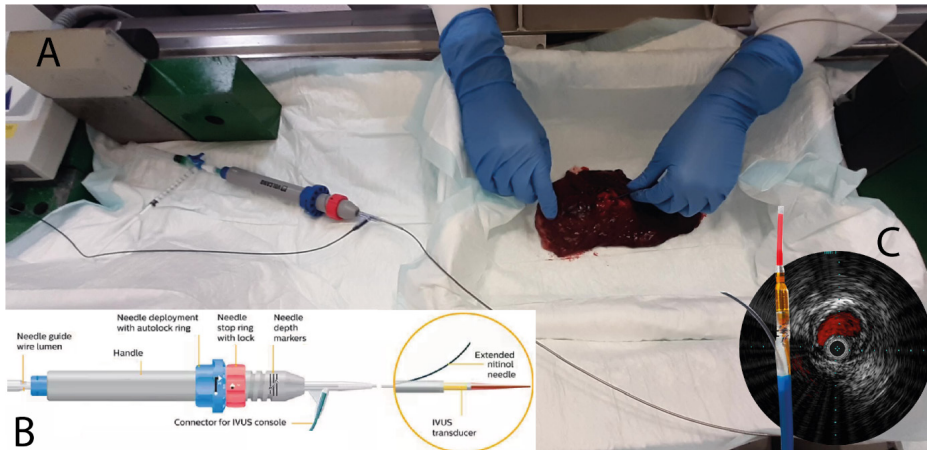


Figure 1: Visualization of the experimental set-up. (A) Experiment set-up with on the left a syringe filled with ^{99m}Tc -ICG-nanocolloid and a syringe filled with saline connected with a three-way valve to the Pioneer Plus catheter leading to the resected lung tissue on the right. (B) Pioneer Plus catheter features with a needle guidewire lumen that has a Luer-lock. (C) Example IVUS-image obtained with the transducer, as depicted in yellow.[64] (B,C) were adapted from Philips product information with the permission of Philips. IVUS, intravascular ultrasound; ICG, indocyanine green.

2.3.3 Tracer injection method

Tissues were injected with the tracer either in or around the tumor — intra- or peritumoral — to evaluate which method would be preferable in a clinical setting. Of 10 obtained specimens, 5 were injected intratumorally and 5 peritumorally, which was allocated in a non-randomized fashion to match lesion size in both groups. Since non-solid lesions are less dense and have a much more compressible compound than soft tissue, it was hypothesized that these lesion types could allow for better retention of tracer volume compared to solid tumors that are dense and compressed. Therefore, in addition, all non-solid lesions were allocated to intratumoral injections.

2.3.4 Tracer injection tool

There are currently no commercial endobronchial instruments that allow for needle placement and/or tracer injection under direct ultrasound (US)-visualization in the

periphery of the lung. Precise placement and location confirmation are important in order to adequately inject tracers within the tumor area. For this reason, an intravascular ultrasound (IVUS) catheter, the Pioneer Plus (Philips, The Netherlands; manufactured by Viant, USA) was used endobronchially (Figure 1). The Pioneer Plus is a torquable device that combines US-guidance with an angulated 24G needle that has an outer diameter of 2.1 mm (6F sheath compatibility).[64] This could facilitate reaching multiple parts of the tumor in one procedure and allow for US-visualization of tumor location and needle placement.

2.3.5 Workflow

A syringe filled with a ^{99m}Tc -ICG-nanocolloid solution was attached to the Pioneer Plus and the working volume of around 0.3 mL (as measured previously) was filled up with tracer solution. The catheter was connected to the IVUS-console to obtain radial US-images. See Figure 1 for a visualization of the set-up. With the needle retracted in-sheath, the catheter was navigated through the bronchial tree to a location near the tumor. This was confirmed both on the US-imaging and by palpation, as the tumor and catheter were palpable in the soft lung tissue. The tumor was visualized on US-imaging and depending on the injection method, the needle was fully extended while the tumor was visible (intratumorally) or while the tumor was not visible (peritumorally). This was confirmed again by palpating the location of the tumor and catheter before attempting to inject the tracer, based on the defined dose escalation protocol.

Subsequently, the catheter was navigated to new locations near or in the tumor to place multiple tracer depots. Using this approach, an attempt to administer the tracer in or around four quadrants of the tumor was made.[65] A flowchart of the study procedures can be found in Figure 2. The real-time US-images of lung tumor and tracer injection were recorded in addition to documentation on visibility of the tumor and successfulness of the injection. Unsuccessful injections were defined as injections where the plunger of the syringe could not be moved due to pressure at the needle tip, or, when there was visible leakage of tracer. Additionally, photo- and video-graphic material was collected during the experiment to capture difficulties and points of improvement.

Informed consent was obtained before surgery. After surgery, the *ex vivo* lung tissue specimen was injected with ^{99m}Tc -ICG-nanocolloid before undergoing a SPECT/CT-scan and conventional pathological assessment.

2.3.6 SPECT/CT imaging

Since *ex vivo* lung tumor tissue was used, there was no drainage of the tracer to the lymph nodes. A single photon emission computed tomography/computed tomography (SPECT)/CT-scan was made to visualize the injection depots and optimize the imaging protocol. SPECT acquisition parameters included a 360° orbit with 180° detector geometry, 256×256 matrix size, and 9° angle step with 30 s/view and 20 views. After acquisition, an iterative reconstruction with 6 iterations, 16 subsets and a gaussian filter of 8.4 mm was used to obtain the final SPECT/CT-images.

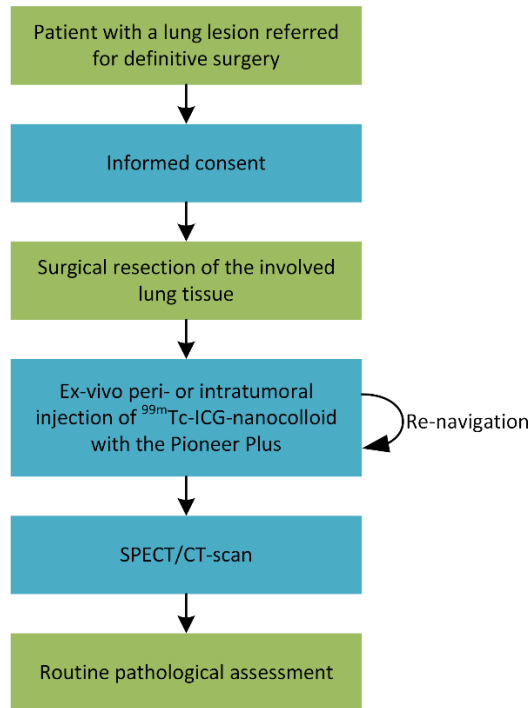


Figure 2: Flowchart of conventional treatment (in green) and study activities (in blue). ICG, indocyanine green; SPECT/CT, single photon emission computed tomography/computed tomography.

2.3.7 Pathological assessment

All tissues were fixed with formalin after scanning. Histological sections were assessed by a pathologist to evaluate tumor size, origin and lymph nodal involvement, following routine clinical practice. These outcomes were collected.

2.3.8 Statistical analysis

This was an explorative feasibility study and descriptive analysis were performed in Excel (Microsoft version 16.0, Redmond, WA, USA).

2.4 Results

2.4.1 Tracer injection method

Intratumoral injections were performed in two non-solid and three solid tumors and were successful in 7 out of 7 (100%) and 9 out of 14 injections (64.3%), respectively. Peritumoral injections were performed in five solid tumors and all 22 performed injections were successful (100%). A total of 5 injections were unsuccessful; 3 were due to visible tracer leakage during injection and 2 were due to an inability to inject, because the plunger of the syringe could not be moved when the needle was extended in the tissue.

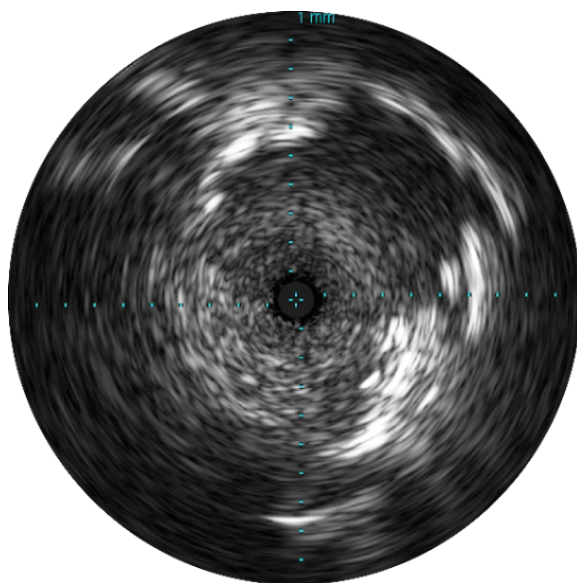


Figure 3: Visualization of lung tumor tissue on IVUS-imaging, similar to that of rEBUS mini probe imaging as currently available in navigation bronchoscopy. The needle can be extended up until 7 mm. The radial US image is calibrated such that the needle is positioned at 12 o'clock.

Table 1: Visualization of experimental outcomes. Of the 10 included specimens, eight were solid tumors and two were non-solid lesions. Final pathology showed seven adenocarcinomas, two squamous cell carcinomas and one benign lesion. The median tumor size was 30 mm. An average total volume of 0.7 mL (range, 0.3–1.2 mL) was injected, with an average of 0.16 mL per depot. The injection speed ranged from 2 to 10 s, depending on volume and resistance during injection. Pathological assessment was not hindered by tracer injection, as scored by the pathologist. No samples or data were excluded from analysis.

Specimen number	Gender	Age	Lesion type (on CT)	Lesion size (mm)	Intra- or peritumoral	Injected tracer volume (ml)	Number of injections	Successful injections	Injections visible on IVUS-images	Pathological outcome
1	M	74	Solid	41	Intratumoral	0.5	4	4	3	Acinar AC
2	M	74	Non-solid	32	Intratumoral	0.3	3	3	3	Lepidic AC
3	F	80	Sub-solid	30	Peritumoral	0.6	3	3	2	Lepidic AC
					Intratumoral		1	0	1	
4	F	48	Solid	16	Peritumoral	0.6	4	4	1	Benign
5	F	64	Solid	41	Peritumoral	0.5	4	4	2	SCC
6	M	75	Solid with cavitation	53	Peritumoral	1.2	6	6	3	SCC
7	M	73	Solid	66	Intratumoral	0.4	3	3	3	AC
					Peritumoral		1	1	0	
8	F	48	Non-solid	42	Intratumoral	0.9	4	4	4	AC
9	M	65	Solid	27	Peritumoral	0.8	4	4	4	Solid AC
10	M	72	Solid	26	Intratumoral	1.1	6	2	3	Acinar AC

AC, adenocarcinoma, CT, computed tomography, F, female, IVUS, intravascular ultrasound, M, male, SCC, squamous cell carcinoma.

2.4.2 Tracer injection tool

The Pioneer Plus catheter and console were able to visualize all tumors, both solid and non-solid. Figure 3 shows a tumor on US-imaging. The needle always exits at the 12 o'clock position in the US-image and because the catheter is torsionally rigid, rotation of the catheter will change the orientation of the image and therefore the needle location when extended. Based on the distance indicator presented in mm on the image (see Figure 3), the desired needle depth — up to 7 mm — can be determined. Controlling the Pioneer Plus was considered easy and no training additional to reviewing the manual was necessary. A short instruction to familiarize with the imaging console was completed, but the control panel is largely self-explanatory.

Injections were visible in 17/21 intratumoral injections and 12/22 peritumoral injections. When the catheter was placed peritumoral, the overall US-visibility was inferior due to air in the parenchyma whereas an intratumoral catheter location provided better overall visibility. When the injection is visible on the US-image, the location and possible leakage can be monitored.

2.4.3 SPECT/CT imaging

An average total radioactivity of 89.5 MBq was injected. The radioactivity in the tissues ranged from 35.4 to 188.0 MBq as a dose escalation protocol was used and the tracer had a fixed radioactive concentration. The scanning protocol with a SPECT-scan of around 17 min and a low-dose CT-scan provided enough resolution to locate individual injection depots. Of all injected radioactive depots, 76.7% (33/43) could be individually identified on SPECT/CT-images (see also Figure 4). The amount of radioactivity did not affect the visibility of tracer depots.

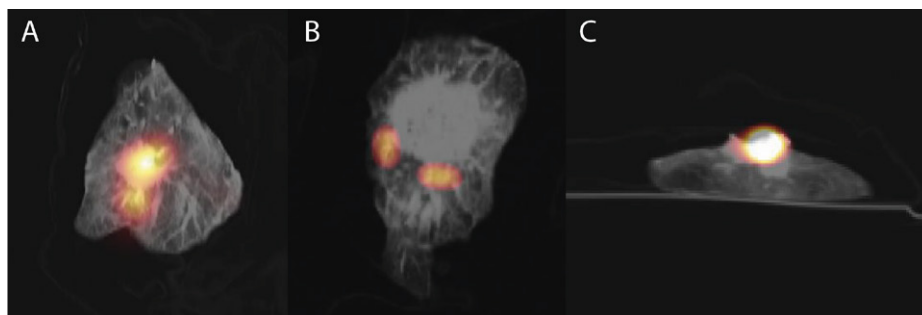


Figure 4: SPECT/CT-imaging of three *ex vivo* lung tissues. Visualization of intra- (A) and peritumoral (B) injections in the lung cancer specimen in the coronal plane on SPECT/CT-imaging. (C) shows tracer leakage from an intratumoral injection which is seen as a depot on top of the tissue in the transversal plane. SPECT/CT, single photon emission computed tomography/computed tomography.

2.5 Discussion

Our *ex vivo* results suggest that performing an SLN imaging procedure by navigation bronchoscopy is feasible when using a novel hybrid imaging and injection device and a radiotracer. While intratumoral injections seem successful in the majority of lesions, peritumoral injections were always successfully applied. Several parameters and workflow settings were explored.

There are a range of tracer types available to perform an SLN procedure. Magnetic tracers for example, have been explored in the past, but the identification rate of SLN during surgery has remained between 73% and 84%. Visible dyes on the other hand report an identification rate of only 22–50% as it is difficult to visualize dyes in anthracotic nodes. Additionally, CT lymphography can provide exceptional spatial resolution to distinguish SLN from an injection depot but cannot be used intraoperatively.[66] During this experiment, we used ^{99m}Tc -ICG-nanocolloid, but the ICG was not used for visualization purposes as there was no drainage in this *ex vivo* experiment. Depending on the use of the tracer after injection, either pre- or perioperatively, these tracers could also be used individually or in combination with other tracer types.

In breast cancer, where an SLN procedure is guideline recommended clinical practice, there is still debate on the site of tracer injection. Intracutaneous injections can be placed successfully subareolar, intra- or peritumorally.[33] In a systematic review and meta-analysis on SLN procedures in lung cancer, Taghizadeh Kermani et al. in 2013 found peritumoral injection of a tracer to perform best in terms of sensitivity and detection rate when compared to intratumoral injections.[54] This resonates with our results, where 100% of peritumoral injections were successful compared to 76% of all intratumoral injections. Tumor characteristics on CT have not yet been correlated to injection successfulness. We do however hypothesize that choosing an injection method pre-procedurally based on CT-characteristics could be difficult and that peritumoral injections would be a safer option to establish successful injections.

Injections were only determined to be unsuccessful when leakage was seen at the injection site or when intratumoral resistance was too high and the plunger of the syringe could not be moved. Leakage into the bronchi when injecting in a peripheral tumor could therefore not be properly assessed during the procedure.

The intended number of injections was adjusted periprocedural in three specimens because the tumor area was already covered (specimen 2), because more injections were needed to cover more possible drainage patterns (specimen 3) or because multiple injections failed (specimen 10). Additionally, the peritumoral region proved to be difficult to reach in a large and more centrally located tumor (specimen 3) and we have therefore performed an intratumoral injection to cover more possible drainage patterns. Uribe-Etxebarria Lugariza-Aresti et al. in 2017 could also not complete 4 peritumoral injections in all quadrants in two very central tumors, although they injected transpleurally.[67] Adjusting the protocol per-procedurally seems inevitable and should be considered when the injections are not considered to cover the tumor and possible drainage patterns adequately. A formal volume escalation protocol is difficult to realize due to heterogeneous tumor characteristics (i.e., size, solidity, density), and the protocol used can therefore be described as a feasibility protocol.

One specimen that was assigned to the intratumoral injection group (specimen 7) was injected peritumorally once by accident, as the actual needle location was discovered after injection of the tracer.

The Pioneer Plus was able to image all tumors and is therefore considered to be a valuable tool when performing endobronchial tracer injections. The handling of the device and imaging quality are up to standard when compared to clinically used endobronchial US-devices. The standardized orientation in which the needle always deploys in the 12 o'clock position, makes determining needle position easy and possibly safer, even if the needle or injection itself are not visible. Moreover, the angulated needle seems essential in enabling the placement of injections in multiple places in or around the tumor. Therefore, the use of this catheter should be further investigated in a clinical setting to determine its added value as an endobronchial catheter to perform injections.

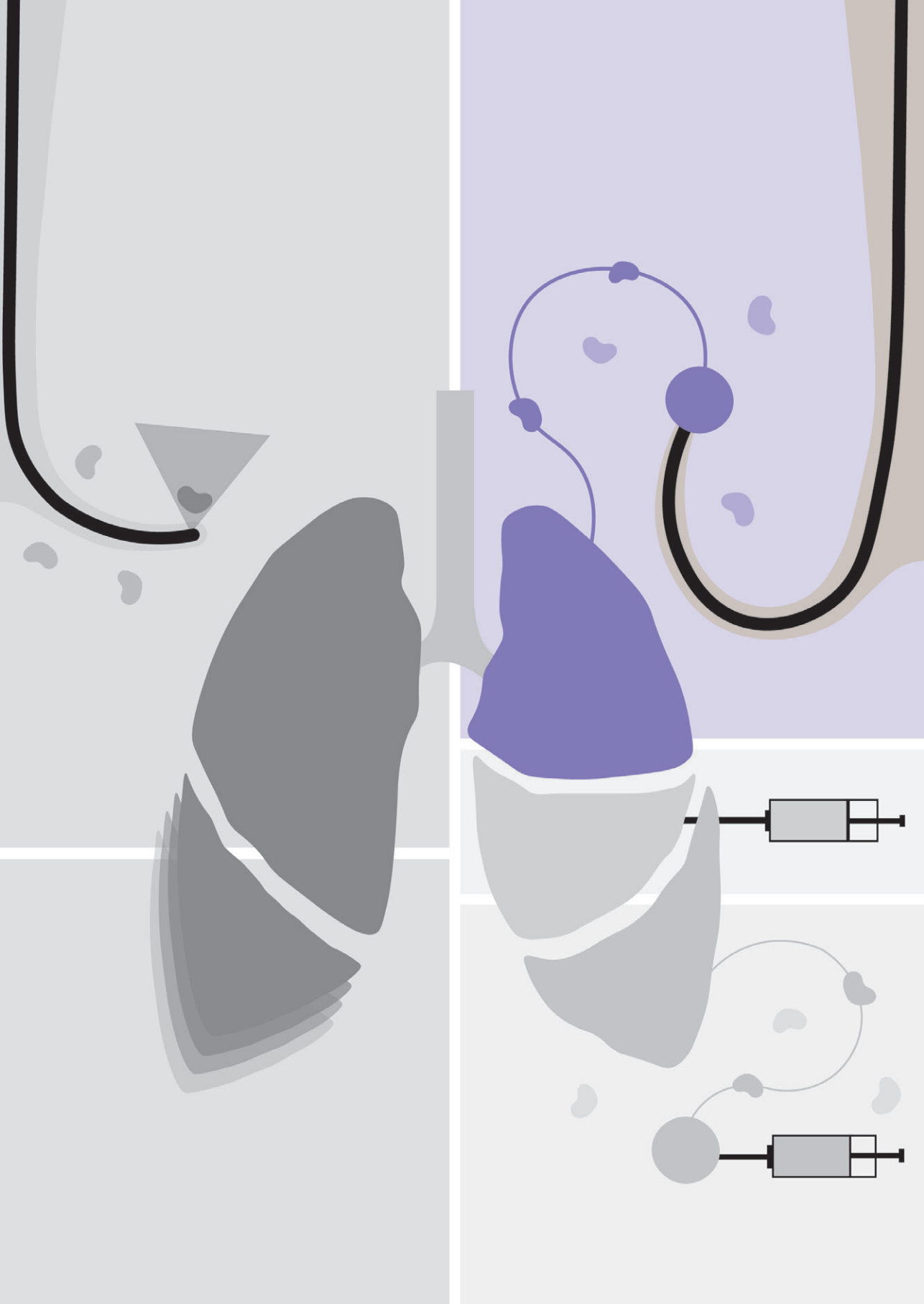
The lung was deflated, and no ventilation was performed, which makes it difficult to evaluate possible injection diffusion in the tissue in a clinical setting. Gilmore et al. in 2012 found that lymphatic migration was unreliable when injecting ICG intraoperatively into deflated lung parenchyma.[56] They were able to improve the consistency of lymphatic migration and SLN identification by ventilating the lung for < 3 min. This should therefore be considered when developing a clinical protocol.

There was limited attenuation of the radioactivity during scanning, as would be the case when the tissue is surrounded by the thorax wall. In a patient, the resolution

of SPECT-imaging could therefore be inferior when scanning the same amount of radioactivity and injection depot volumes. Additionally, when considering the time the tracer needs to drain to the lymph nodes, the half-life of ^{99m}Tc should be considered. This could result in the use of more activity or a longer scan time to be able to detect the amount of tracer drained to the SLN in a clinical setting. Future clinical studies will determine if the SLN would be visible using these doses and imaging settings.

2.6 Conclusion

An SLN procedure carried out in a minimally invasive, endobronchial manner seems feasible. The Pioneer Plus is a suitable catheter to perform injections endobronchially at multiple locations, while being able to view the injected area. Peritumoral injections seem more successful than intratumoral injections, while a SPECT/CT-scan is able to visualize all radioactive injection depots. Future research should determine the applicability, lymphatic tracer drainage and visibility for SLN detection and its added clinical value in a large patient cohort.



Chapter 3

Feasibility of Non-Invasive Sentinel Lymph Node Identification in Early-Stage NSCLC Through Ultrasound Guided Intra-Tumoral Injection of ^{99m}Tc -Nanocolloid and Iodinated Contrast Agent During Navigation Bronchoscopy

Desi K.M. ter Woerds, Roel L.J. Verhoeven, Erik H.J.G. Aarntzen
and Erik H.F.M. van der Heijden

Published in Cancers (2024)

3.1 Abstract

Background: As the first sentinel lymph nodes (SLN) in lung cancer are most likely to harbor metastasis, their non-invasive identification could have a significant role in future treatments. We investigated the feasibility of adding an SLN procedure to a diagnostic navigation bronchoscopy.

Methods: Thirty-one patients were included for injection of ^{99m}Tc -nanocolloid and an iodinated contrast agent intra-/peritumorally and assessment of tracer dissipation via SPECT and CBCT imaging. Injections were performed endobronchially using a multi-modal catheter (Pioneer Plus), combining radial ultrasound and an angulated retractable needle to place injections under fluoroscopy and real-time ultrasound.

Results: The injection of an imaging tracer was feasible in all cases using the catheter. Ultrasound visualized 29/30 tumors, and tracer injection was performed in 100% of patients. An SLN was subsequently identified in 10 out of 31 cases (32.3%) via SPECT/CT imaging. Iodinated contrast agent injection under CBCT imaging prior to ^{99m}Tc nanocolloid injection visualized dissipation pathways and enabled needle relocation for subsequent ^{99m}Tc -nanocolloid injection.

Conclusions: Performing imaging tracer injections with a multi-modal catheter provided safe and local depot placement immediately following diagnostic navigation bronchoscopy. SPECT/CT imaging using ^{99m}Tc -nanocolloid showed inconsistent results for SLN identification.

3.2 Introduction

While advancements in medicine have improved cancer treatments, overall lung cancer survival is still abysmal. Moving towards early-stage disease detection and treatment optimization are considered key strategies to tackle non-small cell lung cancer (NSCLC).[68] In the early stages of NSCLC, it is paramount to determine the extent of disease, as this has profound implications for the survival of patients. While the size of the primary tumor impacts survival, i.e., 5-year survival for stage IA (10–30 mm) disease is 88% and for stage IB (30–40 mm), it is 78%, lymph node involvement has an even more detrimental effect. The 5-year survival for patients with stage IA disease (88%) decreases to 68% as soon as an N1-node is involved and to 50–61% when N2-disease is discovered.[1] Unfortunately, current lymph node staging strategies are suboptimal. We and others have shown that guideline-concordant staging via the combined availability of positron emission tomography/computed tomography (PET/CT) imaging, systematic endobronchial ultrasound (EBUS), and/or mediastinoscopy is accurate in only 65.5% of resectable early-stage (cN0) NSCLC. Occult lymph node metastases were found in 9% to 23.1% of patients after surgery with curative intent.[23, 25, 69]

It is known that lymphatic spread often starts in lymph nodes which are beyond the reach of EBUS and thus cannot be assessed during diagnostic work-up. These lymph nodes, which are most likely to harbor lymphatic spread, are called the sentinel lymph nodes (SLN), and they should be accurately identified.[66] Imaging procedures to identify the SLN are routinely implemented in other tumor types, such as breast and skin cancer.[41, 70] During an SLN procedure, several intra- and/or peritumoral injections of a tracer with radioactive, fluorescent, or magnetic properties are administered, which drains via the lymphatic system and accumulates in lymph nodes over time. This tracer can be visualized before or during surgery to guide SLN identification.[71]

With the advent of neoadjuvant drug therapy in early-stage lung cancer, as well as knowing that only surgery would allow for resection for further exploration of the nodes, a universal minimally invasive approach is preferred. An approach that allows for the identification of such nodes on non-invasive imaging such as single-photon emission computed tomography (SPECT), PET, or CT imaging prior to therapy could prove beneficial, particularly in early-stage disease. Additionally, given the further development of image-guided navigation bronchoscopy (NB) procedures in recent years, minimally invasive access to small primary lung cancers has improved.[72-74] Ideally, the SLN would be visualized on imaging immediately

following an NB for diagnostic purposes, which may allow for a better patient selection for local treatments.

To integrate an SLN procedure into an NB procedure requires specific endobronchial instruments. The placement of an injection should preferably be performed when the operator is confident that the tracer is injected into the lesion or its direct surroundings. As larger lesions can drain to a greater area, repeat local repositioning of the injection instrument into different areas of the tumor or its surrounding tissue should be feasible.[75] Additionally, injections should preferably be guided by real-time 3D imaging to allow for understanding of the positioning of instruments relative to the tumor.[67, 76, 77] At present, commonly used devices for bronchoscopy do not meet all these requirements. An ultrathin bronchoscope can visualize an additional 3–4 bronchial generations beyond those captured by a conventional bronchoscope, but some lesions might still be unreachable, the camera can be obscured by mucus or (local) bleeding, or the bronchoscope could become wedged. Radial EBUS (rEBUS) is widely available and is a valuable tool for local position confirmation, as it can visualize structures beyond the bronchial wall, but it does not provide directional support for real-time tissue acquisition or injection guidance like linear EBUS-systems.[15, 67]

In this single-center explorative study, we evaluated the feasibility of adding an SLN procedure to NB by introducing a novel instrument that combines radial ultrasound (US) and a retractable angulated needle that enables intra- and peritumoral injections under real-time imaging. We evaluated (1) the possibility of injecting a radiotracer and iodinated contrast agent in peripheral pulmonary lesions using this instrument, and (2) whether these tracers allow for subsequent identification of drainage to the SLN on SPECT/CT imaging.

3.3 Methods

3.3.1 Study design and patient cohort

This is a prospective, single-center clinical feasibility study of an endobronchial SLN procedure following a diagnostic NB procedure in patients suspected of having early-stage lung cancer. Patients that were referred for a diagnostic navigation bronchoscopy to diagnose a lung lesion of 10 to 50 mm, with or without ipsilateral hilar node involvement (stage IA-IIIB), were eligible. Patients aged < 18 years, with an ASA score > 4, previous treatment for lung cancer, or a known allergy to contrast agents were excluded. Pre-procedural staging was based on

combined fluorodeoxyglucose ($[^{18}\text{F}]\text{FDG}$)-PET/CT or contrast chest CT imaging alone. Patients with imaging-based suspicion of N2 or N3 lymph node metastases were excluded. Patients were enrolled between December 2022 and May 2024 after providing informed consent. This trial was approved by the Local Medical Research Ethics Committee (Reference No. 2022-13640 on 29 November 2022) and followed the ethical principles of the Declaration of Helsinki (clinicaltrials.gov identifier NCT05555199).[78]

3.3.2 Navigation bronchoscopy procedure

All patients underwent a diagnostic NB in which a therapeutic bronchoscope (19-J10 endoscope, Pentax Medical, Tokyo, Japan) and a pre-angulated extended working channel of 180 degrees or medial curvature (Medtronic EWC, Minneapolis, MN, USA) were navigated to the lesion under cone beam computed tomography (CBCT-, Philips Azurion Flexarm or Siemens Artis Pheno), augmented fluoroscopy (AF-), and radial endobronchial ultrasound (rEBUS) guidance (Olympus, Tokyo, Japan), as reported previously.[15, 79] Biopsies of the lesion for tissue diagnosis were taken by TBNA and/or forceps and were assessed by rapid on-site evaluation (ROSE), as per clinical practice. When no benign diagnosis was found by ROSE, and the lesion was still suspected of lung cancer, the patient was further enrolled in the study. If CBCT imaging after biopsy showed any grade of blood in the surrounding lung parenchyma prior to imaging tracer injection, this was noted. Finally, a systematic EBUS was performed to assess the involvement of hilar and mediastinal lymph nodes, following routine clinical practice (EB-19-J10U, Pentax Medical, Japan).

3.3.3 Study procedure

Pioneer Plus radial ultrasound

Prior to this study, an explorative *ex vivo* study was performed to test the feasibility of using the intravascular ultrasound (IVUS) Pioneer Plus catheter (Philips IGT-D, Amsterdam, The Netherlands) for radial US-guided injection in resected human lung tissue with $^{99\text{m}}\text{Tc}$ -ICG-nanocolloid.[64, 80] Having evaluated the feasibility of injection via varying volumes and imaging parameters, the Pioneer Plus was used outside of its intended use, with permission of the medical ethics committee, for evaluation in this clinical feasibility study.

The Pioneer Plus was originally designed as an intravascular catheter intended to identify and re-enter the true vessel lumen based on IVUS imaging. It does so by using a 20 MHz ultrasound transducer with solid-state piezo-electric crystals,

allowing a maximum imaging diameter of 20 mm. The Pioneer Plus further includes a nitinol-based needle that, upon extension outside of the sheath, comes out from the catheter at a 90° angle at a maximum needle extension of 7 mm (see Figure B1). The catheter is torsionally stiff and can thus be rotated for adequate needle (re)positioning. The ultrasound probe is calibrated into the catheter such that the angulated needle does not come into the direct imaging plane of the ultrasound imaging upon full extension but stays just proximal of the transducer (~2 mm). The imaging plane is perpendicular to the needle extension, and the needle will always extend out of the sheath at the 12 o'clock angle in the ultrasound image. This calibration allows for validation that the catheter is correctly positioned relative to the tumor such that adequate injection can take place under real-time imaging.

Imaging tracer injection

An intention to inject multiple tracer depots was established based on pre-procedural planning and intra-procedural findings. To perform the injections, the working volume of the Pioneer Plus catheter of 0.3 mL [80] was pre-filled using a 3 mL Luer-lock syringe filled with 2 mL ^{99m}Tc -nanocolloid solution. The Pioneer Plus was inserted into the pre-angulated catheter that remained positioned near or inside the lesion. Using the IVUS-console (Core M2, Philips, The Netherlands), the lesion and injections could be imaged using radial US. Upon verifying the positioning of the catheter and lesion on continuous US imaging and/or (augmented) fluoroscopy (Figure 1), the target location is fixated at the 12 o'clock position. Injection(s) were placed either in the tumor — intratumorally — or surrounding the tumor — peritumorally. Both approaches were performed to assess feasibility, also depending on the feasible positions of the catheter, as concluded during the navigation bronchoscopy procedure. The 7 mm (angulated) reach of the needle was used in all injections to ensure sufficient penetration beyond the bronchial wall. After the first injection, the needle was retracted, and the catheter was navigated to new locations near or in the lesion to place multiple tracer depots, when possible. After the last injection, the needle was retracted, and all radioactive tracer in the working volume was removed by placing a vacuum on the syringe proximally.

Using this approach, an attempt to evenly administrate the tracer in or around the lesion in multiple depots was made using visualization of the lesion on radial US and fluoroscopy.[65] The injected volume and number of injections was varied to study the characteristics for a successful injection, but tumor volume was taken into account to prevent injecting more than 50% of the total tumor volume.

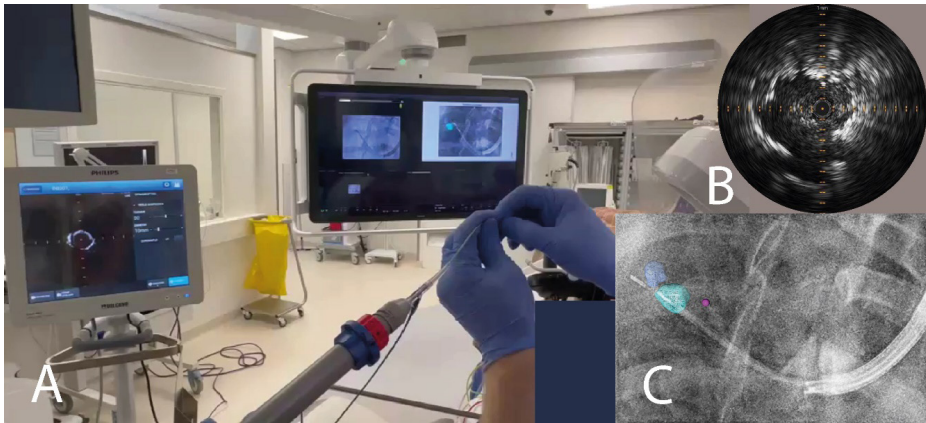


Figure 1: Visualization of the Pioneer Plus catheter in patient. (A) with a view of the radial US image (B) and augmented fluoroscopy (C) in a suite equipped with a Philips Azurion Flexarm CBCT system. Augmented fluoroscopy depicts two parts of the lesion in dark and light blue and a pink dot for the catheter position on CBCT, used for navigation and sampling. The US transducer (distal) and needle shaft (proximal) can be seen as radiopaque in image C. CBCT, cone beam computed tomography; US, ultrasound.

Protocol amendment

At the start of the study, all subjects underwent at least one injection of ^{99m}Tc -nanocolloid (Nanocoll, GE Healthcare, Eindhoven, The Netherlands). Interim analysis after the treatment of 10 patients showed that the SLN could not always be visualized on SPECT/CT following the injections (6/10 patients). It was thereby concluded that immediate, real-time visualization to gain feedback on tracer dissipation may improve injection accuracy. Subsequently, an iodinated contrast agent for CT im-aging, Iomeron 300 (300 mg iodine/mL, Bracco Imaging Deutschland GmbH, Konstanz, Germany), was added to the injection protocol (with ethical committee approval) from subject 15 onwards. When, despite US guidance during injection, fluoroscopy showed endobronchial or direct vascular leakage of Iomeron 300, the position of the needle could be adjusted prior to ^{99m}Tc -nanocolloid injection.

SPECT/CT imaging and SLN identification

Initially, two SPECT/CT scans were performed within a window of 1 to 6 h after injection to allow for the evaluation of appropriate scan time frame(s) (for imaging parameters, see Appendix A). During the interim analysis, the optimal timing of SPECT/CT scanning was evaluated, whereafter all other patients received one SPECT/CT scan at an optimal interval. The lymphatic drainage and uptake of ^{99m}Tc -nanocolloid and Iomeron in the lymph nodes as observed via SPECT/CT imaging was assessed by a nuclear medicine physician (EHJGA).

Data analysis

Patient, lesion, and injection characteristics; fluoroscopy-, CBCT-, radial US- SPECT/CT imaging; and pathological outcome were collected of all patients. This was an explorative feasibility study, and only descriptive statistics are described.

3.4 Results

A total of 34 patients were included in the study. Three patients were excluded due to a lack of intra-operative confirmation or suspicion of malignancy by ROSE. Thirty-one patients with a median lesion size of 18.7 mm underwent the study procedure following successful NB. The patient and lesion characteristics are depicted in Table 1. The study procedure added around 15 min to the procedure time, making the total procedure time a median of 1 h 45 min; see Table 2.

Table 1: Pre-procedural patient and lesion characteristics.

¹ Cyst/cavity was scored positive when gas-containing structures were found within the tumor or its direct surroundings. ² PET imaging showed slightly elevated FDG-avidity in nodal regions 5/6 in two cases.

	Characteristic		Frequency
Patient characteristics	Age, median (\pm IQR)		71 (\pm 14)
	Gender, <i>n</i> (%)	Male	21 (67.7%)
		Female	10 (32.3%)
	BMI, median (\pm IQR)		26 (\pm 5)
	FEV1, median (\pm IQR)		88 (\pm 31)
	DLCO, median (\pm IQR)		84 (\pm 23)
Lesion characteristics	Lesion size on CT, median (\pm IQR)		18.7 (\pm 9.6)
	Lobe, <i>n</i> (%)	Upper	25 (80.6%)
		Lower	6 (19.4%)
	Lesion type, <i>n</i> (%)	Solid	19 (61.3%)
		Part-Solid	4 (12.9%)
		GGO	7 (22.6%)
		Cystic	1 (3.2%)
	Cyst/cavity, <i>n</i> (%) ¹		5 (16.1%)
	Imaging-based pre-procedural stage, <i>n</i> (%)	iN0	24 (77.4%)
		iN0–1	5 (16.1%)
		iN1–2 ²	2 (6.5%)

BMI, body mass index; CT, computed tomography; DLCO, diffusing capacity of the lungs for carbon monoxide; FEV1, forced expiratory volume in the first second; GGO, ground-glass opacity; IQR, interquartile range.

Table 2: Study characteristics regarding the use of the Pioneer Plus catheter, ^{99m}Tc -nanocolloid, and Iomeron 300 injection.

³ Bleeding after biopsies was scored positive when intra-parenchymal bleeding was visible on CBCT imaging and was furthermore noted in one case based on videoscopic observation after diagnostic navigation bronchoscopy but prior to tracer injection.

Characteristics		Frequency
Pioneer Plus catheter	Duration of NB, hh:mm, median (\pm IQR)	01:45 (\pm 00:26)
	(Intraparenchymal) bleeding after biopsies, <i>n</i> (%) ³	11 (35.5%)
	Tracer injection device, <i>n</i> (%)	
	Pioneer Plus catheter	30 (96.8%)
	Conventional TBNA needle	1 (3.2%)
	Tumor visibility on radial US imaging, <i>n</i> (%)	29 (96.7%)
	Real-time radial US visibility of tracer injection, <i>n</i> (%)	0 (0.0%)
	Multi-depot placement, <i>n</i> (%)	
^{99m}Tc -nanocolloid	Yes (> 1 injection)	22 (73.3%)
	No (1 injection)	8 (26.7%)
	Number of patients with injection(s), <i>n</i> (%)	31 (100%)
	Number of injections, median (\pm IQR)	2 (\pm 1)
	Injection type, <i>n</i> (%)	
	Intratumoral	16 (51.6%)
	Peritumoral	7 (22.6%)
	Intra- and peritumoral	8 (25.8%)
Iomeron 300	Injection volume, mL, median (\pm IQR)	0.43 (\pm 0.5)
	Radioactivity, MBq, median (\pm IQR)	28.0 (\pm 21.7)
	Total injection time per depot, seconds, median (\pm IQR)	9 (\pm 9)
	Number of patients with injection(s), <i>n</i> (%)	15 (48.4%)
	Number of injections, median (\pm IQR)	1 (\pm 1)
	Injection type, <i>n</i> (%)	
	Intratumoral	11 (73.3%)
	Peritumoral	3 (20.0%)
	Intra- and peritumoral	1 (6.7%)
	Injection volume, mL, median (\pm IQR)	0.30 (\pm 0.20)
	Injection visible on fluoroscopy, <i>n</i> (%)	15 (100%)
	Total injection time per depot, seconds, median (\pm IQR)	12 (\pm 7.25)
	Leakage visible on fluoroscopy, <i>n</i> (%)	4 (26.7%)

EBUS, endobronchial ultrasound; US, ultrasound; IQR, interquartile range; NB, navigation bronchoscopy; TBNA; transbronchial needle aspiration.

3.4.1 Pioneer Plus radial ultrasound

The Pioneer Plus was used to perform tracer injection(s) in 30 out of 31 patients (Table 2). A conventional aspiration needle was used once when a non-solid lesion was located directly at the tip of the extended working channel, and the angulated needle of the Pioneer Plus catheter could only achieve a peritumoral injection (where intratumoral injections are preferred in non-solid lesions [80]). Radial US imaging could visualize 29 out of 30 lesions (96.7%). One lesion of 20.6 mm in the LUL was not visible on radial US imaging due to loss of contact with the lesion because of deformation of the extended working channel upon insertion of the relatively rigid Pioneer Plus catheter through its lumen, which rendered the US imaging unusable for guiding the injection (fluoroscopy/CBCT imaging was used instead). Figure 2 visualizes the radial US imaging of different lesion types. Unfortunately, none of the injections itself were visible on radial US, as the needle extension did not result in in-plane visualization, as known from linear-EBUS, and injected tracers were echolucent.

Figures B1 and B2 indicate the visibility of the radial US Pioneer Plus on the fluoroscopy and CBCT images.

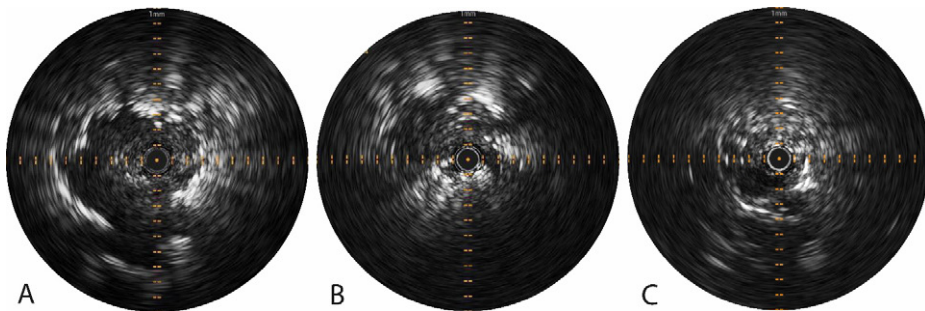


Figure 2: Visualization of a solid lesion (A), part-solid lesion (B), and GGO (C) on radial US imaging via the Pioneer Plus catheter after having completed diagnostic navigation bronchoscopy, pre-injection. (A) The solid lesion is clearly visualized. Beyond the lesion, some intra-parenchymal bleeding following previous sampling altered the echogenicity of the lung parenchyma. (B) The part-solid lesion is visualized, along with the GGO component that can be predominantly seen from 9 to 12 o'clock. Some hyper-echoic speckle is seen at the 4 to 7 o'clock position, following minor bleeding after biopsy. (C) The image of the GGO not only shows a mixed blizzard sign (as mentioned by Park et al. [81]) but also a clear (pulsating) vessel from the 6 to 9 o'clock position. The vessel should be out of the vicinity of the needle at the 12 o'clock position and should therefore stay in the 3 to 9 o'clock position during injection. GGO, ground-glass opacity; US, ultrasound.

3.4.2 Imaging tracer injection

^{99m}Tc-nanocolloid injection

A median of two injections (range, 1–4) with a volume of 0.4 mL (range, 0.2–1.0 mL) and a Technetium-99m activity dose of 43.9 MBq (range, 8.1–51.6 MBq) were administered in 31 patients. Placement of multiple depots was performed in 22 out of 31 patients (73.3%). The other nine patients received an injection of imaging tracer(s) at a single location, as multiple depot placement was not considered to be of additional value due to catheter placement next to the lesion ($n = 2$) or previous intra-parenchymal bleeding from diagnostic biopsy hampering the clear distinction of the lesion from the parenchyma ($n = 7$).

Iodinated contrast injection

A median of one Iomeron 300 injection (range, 1–4) with a volume of 0.3 mL (range, 0.3–1.0 mL) was performed in 15 patients. Iomeron visualized leakage to a vessel on fluoroscopy that was not visible on radial US imaging in 4 out of 15 patients (26.7%). This enabled the relocation of the needle to a different location to ensure an accurate intra- or peritumoral injection of ^{99m}Tc-nanocolloid for drainage to the lymph nodes. As can be seen in Figures B3 and B4, the injected depot of Iomeron 300 can be visualized on CBCT and subsequent low-dose CT imaging.

3.4.3 SPECT/CT imaging and SLN identification

In the first ten patients, two SPECT/CT scans were performed (see also Figure B5 for a flowchart of patients and study procedures). Early scans were performed between 1 and 3 h after injection, and a secondary late scan was performed between 3 and 6 h after injection. Example images are given in Figure 3. After ten patients underwent two SPECT/CT scans following ^{99m}Tc-nanocolloid injection, an interim analysis was performed to determine the need for two time frames. Only one patient had an SLN identified in the late scan (at 04:44 h), which was not visible in the early scan. It was therefore concluded that the optimal scanning time frame was after at least 4 h, and that one scan would suffice (exact timing was always co-dependent on scanner availability and logistics).

In total, an SLN was identified on SPECT/CT imaging (early as well as late scan times) in 10 out of 31 patients (32.3%); see Table 3. When an SLN was identified on SPECT imaging, it was only one lymph node in seven patients (22.6%) and two lymph nodes in three patients (9.7%).

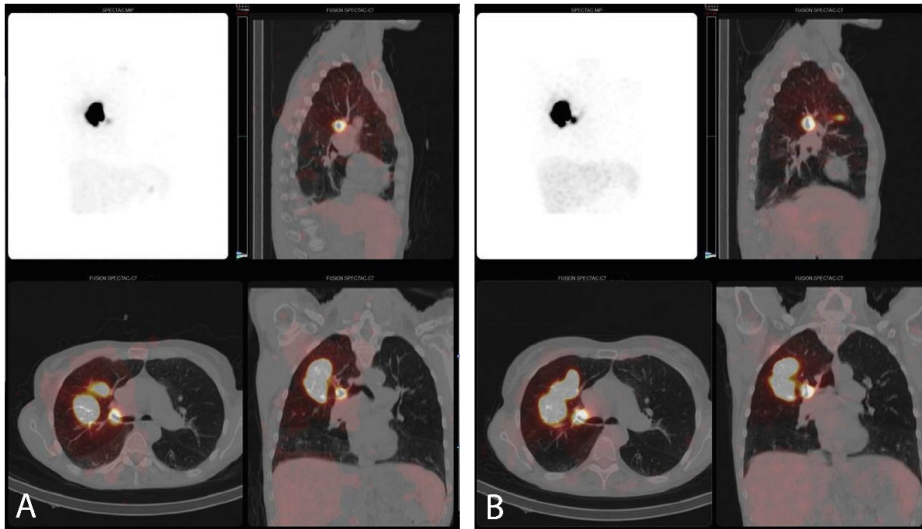


Figure 3: Visualization of the ^{99m}Tc -nanocolloid detection in the coronal plane (upper left) and combined SPECT and low-dose CT images in the sagittal (upper right), transversal (lower left) and coronal plane (lower right) in one patient with an early scan time of 02:09 h (A) and a late scan time of 04:09 h (B). The SLN is visible in both scans, although more of the ^{99m}Tc -nanocolloid seems to have drained to the lymph node in the late scan. CT, computed tomography; SLN, sentinel lymph node; SPECT, single photon emission computed tomography

Since an SLN could be identified on SPECT/CT in only a minority of patients, the imaging acquisition time was prolonged by 120% (from 10 min to 22 min) in the last four patients to check whether this would increase sensitivity. An SLN was identified in only one of these patients (25%).

Leakage of ^{99m}Tc -nanocolloid itself could not be visualized on fluoroscopy, CBCT, or radial US imaging. However, scattering of the radioactivity of ^{99m}Tc -nanocolloid throughout the lung or segment was visible in nine patients (36.0%) on SPECT/CT, suggesting endobronchial leakage.

Table 3: Post-navigation bronchoscopy parameters with scan times; SLN identification on SPECT imaging; pathology outcome of lesion and received treatment.

⁴ One patient had only a late scan-time and an extra late scan time at 23:51, which has been left out of the median and IQR calculations. ⁵ In one patient, an SLN could be identified on the early scan, but no late scan was performed due to logistical limitations. ⁶ based on SPECT imaging showing radioactivity throughout the ipsilateral lung.

Characteristics		Frequency	
SPECT/CT imaging	Patients with an early scan, <i>n</i> (%)	10 (32.3%)	
	Early scan time, hh:mm, median (±IQR)	02:28 (±01:02)	
	Patients with a late scan time, <i>n</i> (%)	30 (96.8%)	
	Late scan time, hh:mm, median (±IQR) ⁴	04:19 (±00:55)	
	SLN identification, all scan times, <i>n</i> (%)	10 (32.3%)	
	SLN identification early scan, <i>n</i> (%)	5 (50.0%)	
	SLN identification late scan, <i>n</i> (%) ⁵	9 (30.0%)	
	Endobronchial leakage, <i>n</i> (%) ⁶	9 (29.0%)	
Staging and treatment	Pathology outcome of lesion after NB, <i>n</i> (%)	AC	19 (61.3%)
		SCC	5 (16.1%)
		NSCLC	2 (6.5%)
		Benign	4 (12.9%)
		Non-representative	1 (3.2%)
	Treatment, <i>n</i> (%)	Surgery	15 (48.4%)
		Other	16 (51.6%)
	Subgroup: pathological lymph nodal stage after surgery, <i>n</i> (%)	pN0	12 (80.0%)
		pN0(i+)/isolated tumor cells	2 (13.3%)
		pN1	0 (0.0%)
		pN2	1 (6.7%)

AC, adenocarcinoma; CT, computed tomography; IQR, interquartile range; NB, navigation bronchoscopy; NSCLC, non-small cell lung cancer; SCC, squamous cell carcinoma; SPECT, single-photon emission computed tomography; SLN, sentinel lymph node.

3.4.4 Lesion and lymph node outcomes

One patient was diagnosed with station 4L involvement through same-procedure EBUS post-navigation bronchoscopy (but did not show an SLN on SPECT imaging).

As per multidisciplinary team decision, fifteen patients underwent surgical resection, allowing for histopathological confirmation. Post-operative detailed assessment of lymph node involvement was found in three patients (Table 3). One patient was found to have macro-metastatic disease in stations 3 and 5 (pN2), and

two patients were diagnosed with isolated tumor cells (ICTs). In none of these three patients was an SLN found on SPECT/CT imaging, making determination of a true SLN impossible.

3.4.5 Safety, risks, and adverse events

The study procedure involved additional radiation by means of fluoroscopy-guided needle placement and injection, which comprised approximately one to two minutes. A maximum of two extra CBCT scans were additionally made to visualize tool-in-lesion and the dissipation of Iomeron in and around the lesion in the study setting. The radiation dose and safety of CBCT-guided NB has been previously described by Verhoeven et al. (2021) and Wijma et al. (2024).[16, 82] The injection of ^{99m}Tc -nanocolloid with a maximum dose of 100 MBq adds ~0.5 mSv to the procedure but is predominantly localized near the lesion itself, resulting in a minimal increase in total effective dose per patient. After NB, up to two low-dose CT scans of around 3.3 mSv each are performed to provide anatomic reference to the detected ^{99m}Tc .

One serious adverse event was observed. Upon symptoms, a patient returned two days after the procedure with a pneumonia in the biopsied area. In this specific patient, a Nashville grade 2 bleeding had occurred during NB, for which adrenaline was successfully locally applied through the catheter prior to the study procedure using ^{99m}Tc -nanocolloid injections.[83] It is therefore thought to be caused by the biopsies taken before the study procedure and not by the use of the Pioneer Plus catheter or the placing of the imaging tracer depots.

3.5 Discussion

This single-center explorative study shows that an SLN procedure can be performed following a diagnostic NB procedure through use of a novel multi-modal catheter that allows for the accurate intra-/peritumoral injection of tracers under US and fluoroscopic guidance. The multi-modal Pioneer Plus catheter was able to visualize all tumors and allowed for the injection of imaging tracers in all cases. The combination of secondary imaging techniques, such as using iodinated contrast, fluoroscopy, and CBCT imaging, further allowed for the evaluation of tracer leakage beyond the ultrasound plane. While the injection of intra-/peritumoral tracers was feasible in all cases, subsequent drainage of tracers into an SLN could not be uniformly identified on SPECT/CT imaging. ^{99m}Tc -nanocolloid and/or SPECT imaging as an imaging tracer might not provide suitable ingredients for a non-invasive

SLN procedure in lung cancer when employed immediately following diagnostic navigation bronchoscopy.

3.5.1 Real-Time US-Guided Endobronchial Injection

The Pioneer Plus catheter, originally designed and approved as a vascular lumen re-entry catheter, proved to be an effective and safe device that could be used for the endobronchial injection of radiotracers, as used in this study. During the design and conduction of this trial, there were no other devices available that combined US and a needle for real-time injection. However, as of 2023, the iNod Ultrasound Guided Biopsy Needle (Boston Scientific, Marlborough, MA, USA) became available in the USA for image-guided biopsy, although it is not (yet) available in the EU.[84] The iNod is similar to the Pioneer Plus catheter but exhibits some differences in regards to its technical aspects. While the Pioneer Plus has an angulated 24 G needle that stops just before the US field of view, the iNod has a 25 G needle that exits at an 11° needle ramp and is within the US field of view. The iNod uses a single-element rotational transducer with a frequency of 30 MHz, classifying it as an ultra-high frequency device, whereas the Pioneer Plus employs a 20 MHz transducer with continuous radial ultrasound generated by 64 fixed elements.[85] Due to its lower frequency and continuous imaging at all angles, the Philips system potentially provides better overall image quality and a larger imaging diameter, which can potentially improve the view of the lesions further away from the bronchi when used endobronchially.

The Pioneer Plus catheter has been demonstrated to be safe and effective in injecting imaging tracers in or around peripheral lung lesions. The combination of radial ultrasound and a needle also makes this type of device necessary when moving towards local treatments. Real-time visualization of the tumor by radial US, in combination with the 3D imaging possibilities of CBCT for precise positioning and confirmation, could provide the essential support for safely administering therapeutic agents locally.

3.5.2 Imaging Tracers and Other Particles

Over the past two decades, several research groups have studied the feasibility of an SLN procedure for lung cancer, with heterogenous approaches and results. These protocols have varied in several aspects, including whether the radiotracer was injected intraoperatively (one-day protocol) or transthoracically by CT guidance before surgery (two-day protocol). Additionally, differences are observed in the injected volume, activity, methods of injection, and time to detection. Various particles, namely ^{99m}Tc -sulfur-colloid (61–445 nm) or ^{99m}Tc -tin-colloid (100–1000 nm),

were used.[86-92] Kim et al. hypothesize that the ideal particle size for SLN mapping is in the range of 10–50 nm, suggesting that larger particles may be retained at the injection site, while smaller sizes are cleared from the injection site too quickly.[93]

In our study, ^{99m}Tc -nanocolloid (Nanocoll, GE Healthcare, The Netherlands) was used (particle size of 6.5–68 nm, with 99% < 13 nm), which could be considered to be within the ideal particle size range.[28, 71] Despite this, while previous studies using gamma probe detection achieved SLN identification over 60%, our SLN identification rate on SPECT imaging by ^{99m}Tc -nanocolloid remains at only 32.3%.[86-92] There are multiple factors that influence the clearance and retention of particles in the lymph nodes, e.g., coating, surface charge, colloidal stability, and biological compatibility. However, the ideal particle for an SLN procedure and the best method of detection remain unclear,[94] as is further corroborated by our findings. Future research is needed to pinpoint the specific dynamics of individual tracers and carriers, which would allow for evidence-based protocols for SLN imaging identification.

3.5.3 Imaging Modalities

To the best of our knowledge, three studies have used a transthoracic injection of a radiotracer for SPECT imaging of sentinel lymph nodes in lung cancer patients. Romano et al. injected 10 mL of ^{99m}Tc -tilmanocept intra- and peritumorally under CT guidance. They performed a SPECT scan in six patients after a median of four hours. Lymph node uptake was detected in four patients (66.7%).[95] In addition, they used a gamma probe intraoperatively and detected an SLN in all patients. Nomori et al. performed a similar procedure and found an SLN in 39 out of 63 patients (62%) on SPECT imaging around 16 h after administration. They also used a gamma probe during surgery and detected an SLN in 48 patients (78%).[90] Lastly, Abele et al. performed SPECT imaging 1, 2, or 3 h after CT-guided injection and found an SLN in 12 out of 24 included patients (50%).[63] These groups found similarly low identification rates via SPECT imaging, and the two groups that included gamma probes identified more SLN intra-operatively than those observed via pre-operative SPECT imaging. This might be due to the SPECT spatial resolution and the long acquisition time of SPECT imaging, which can result in breathing artefacts, attenuation, and scattering of radioactivity by surrounding tissue and detector geometry. Therein, intraoperative gamma probes may offer advantages, as these can be located closest to the lymph node, significantly increasing sensitivity. Given that previous research on SLN identification using gamma probes reported significantly higher detection rates (61.5% to 86%) compared to our findings using SPECT imaging, more sensitive non-invasive imaging modalities should be considered for further exploration.[86-92] PET imaging, for example, offers superior

resolution compared to SPECT and could potentially achieve higher detection rates for SLN, but there is currently no PET tracer available for this purpose. Additionally, the complexity of producing positron-emitting nuclides poses challenges for routine use in SLN procedures. To improve lymph node staging in the future, further exploration of alternative imaging modalities and protocols, in combination with optimized particle characteristics, is essential.

3.5.4 Strengths and Limitations

This study demonstrates that performing an SLN procedure in combination with an NB is technically feasible and can be performed through endobronchial access with a novel device that allows for real-time ultrasound visualization of the tumor, combined with simultaneous needle placement. However, there are still limitations that should be mentioned. This was a single-center study, making assessment of reproducibility difficult. We found that injection has consistently been shown to be feasible, but due to low overall SLN detection rates, the potential influence of injection volume on detection rates could not be investigated, as is the same for other injection and acquisition parameters in this exploratory study. Due to the low detection rate, and since we excluded patients with prior local or systemic cancer treatments, this study does not allow for conclusions to be drawn regarding the feasibility of SLN imaging in respect to (down-)staging after neo-adjuvant treatments.

After an interim analysis, we decided to check for injection dissipation by including iodinated contrast prior to ^{99m}Tc -nanocolloid injection. With Iomeron 300, we were able to visualize the dissipation of the injected tracer and found leakage after first-attempt needle placement in 4 out of 15 patients, which was not expected based on real-time radial US imaging. Although the exact cause of leakage (bigger vessels, capillaries, or direct endobronchial leakage) was not clear in all patients, the location of Iomeron was always visible on fluoroscopy, even at low volumes (0.1–0.45 mL per injection).

We were successfully able to inject radiotracers in all patients. The attempted injection volume was based on predefined criteria ensuring that no more than 50% of the tumor volume was injected into a single lesion, as we hypothesized that higher volumes would increase the chance of endobronchial leakage. However, radioactivity was detected in other parts of the lung via SPECT imaging in nine patients (29.0%) throughout the study, which could be an indicator for intrabronchial leakage by post-procedural coughing. As the authors could not find studies that provided recommendations regarding volume, future studies of the

optimal injection volume when related to lesion size and the chance of leakage should be performed.

To minimize the potential impact on patients but maximize the impact of sentinel node detection on clinical decision making, we choose to perform an SLN procedure at the end of a diagnostic NB, in contrast to previous studies reporting on SLN detection using intraoperative methods during surgery. Unfortunately, we could only detect an SLN in a minority of patients (32.2%), which led us to conclude that our current approach is insufficient. Lesion aspects like solidity and the presence or absence of cysts/cavities (25.8% in our cohort) or their combination with diagnostic sampling prior to tracer injection, which inherently results in minor (intra-parenchymal) bleeding (visible on CBCT in 38.7% of patients), are factors that may alter the local environment before attempting imaging tracer injection. However, our sample size is too small to explore such correlations. To prevent possible biopsy-related leakage, an SLN imaging protocol in which an NB procedure is performed solely to inject the (radio)tracer could increase the identification rate, but this would also significantly increase patient burden and the amount of effort required.

3.6 Conclusion

The injection of a (radio)tracer endobronchially using a device that combines radial US and an angulated needle is feasible, with an SLN identification on SPECT/CT imaging of 32.3%. The Pioneer Plus catheter was able to visualize all tumors and provided guidance while injecting imaging tracers. Iomeron could readily visualize the dissipation of the injected fluid in the lung. The obtained SLN identification by SPECT/CT imaging is lower than that obtained in other studies that focused on identification via more localized imaging (intra-operative gamma probe). Multiple parameters were varied and studied in this trial, but no protocol parameter could be optimized. Future research should be performed to find alternative, more sensitive, non-invasive SLN imaging techniques.

3.7 Supplementary data

3.7.1 Appendix A: SPECT/CT imaging parameters

SPECT acquisition parameters included a 360° orbit with 180° detector geometry 256x256 matrix size, and 9° angle step with 30 sec/view and 20 views. One patient was scanned at 24h with a detection time of 60 sec/view to determine tracer retention and SLN identification improvement after a longer time period. In four patients, a different protocol with an angulation step of 3°, 22 sec/view and 60 views was used.

A low dose CT scan was made for anatomical reference. After acquisition, an iterative reconstruction with six iterations, 16 subsets and a gaussian filter of 8.4 mm was used to create the final SPECT/CT images.

3.7.2 Appendix B: Supplemental Figures

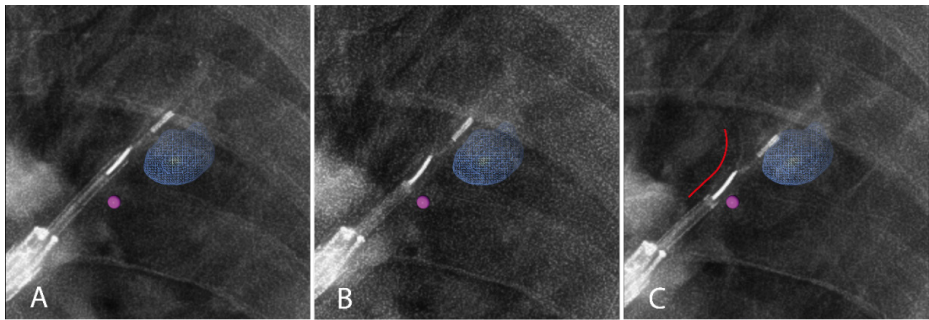


Figure B1: Visualization of the Pioneer Plus catheter near the lesion on AF with the needle in sheath (A), the needle deployed (B) and the catheter moved more distal to push the needle further into the tissue to enhance angulation (C). The needle sheath and US-transducer appear to be radiopaque, whilst the needle is (minimally) radiopaque. A peritumoral injection was performed here. A red line is added for reference of the needle position. AF, augmented fluoroscopy; US, ultrasound.

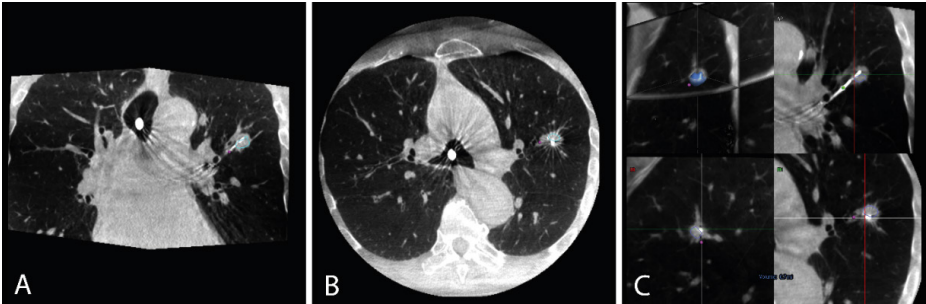


Figure B2: Visualization of the Pioneer Plus catheter on CBCT imaging in the transversal plane (A), coronal plane (B), and adjusted planes (C). The needle visibly protrudes into the lesion in (A) and (C, lower right) at the ten o'clock position of the radial US-transducer. An intratumoral injection was performed here. CBCT, cone-beam computed tomography; US, ultrasound.

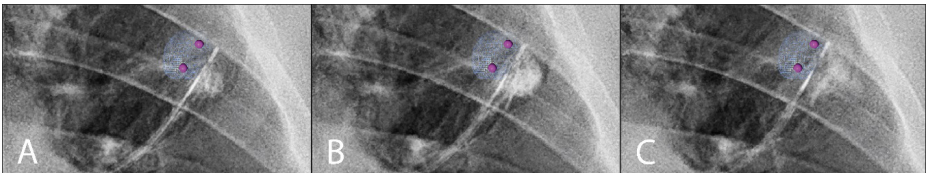


Figure B3: Visualization of an lomeron injection, during injection (A), right after injection (B) and 2 minutes after injection (C). A depot of lomeron 300 is slowly formed and also partially washes out within 2 minutes.

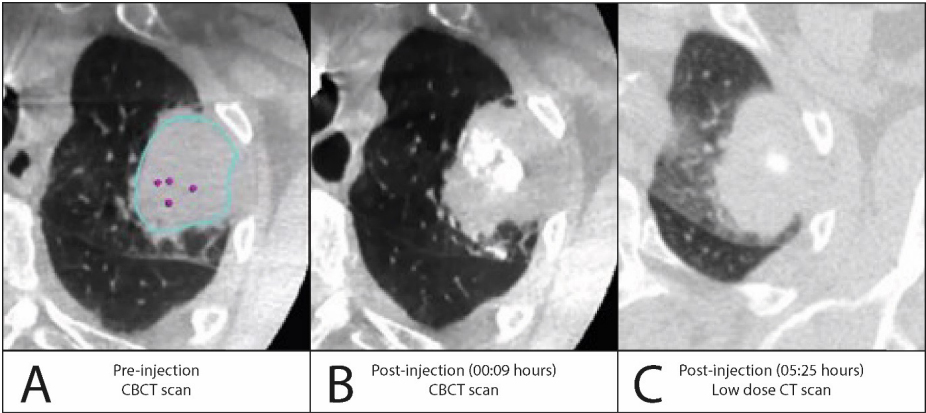


Figure B4: Visualization of the visibility of lomeron 300 before injection (CBCT scan) directly after injection on a CBCT scan and after 05:25 hours on a low dose CT scan. We can clearly see the dissipation of lomeron 300 in the first scan and at a later scan time, the contrast agent as almost completely dissolved. (CB)CT, (cone-beam) computed tomography.

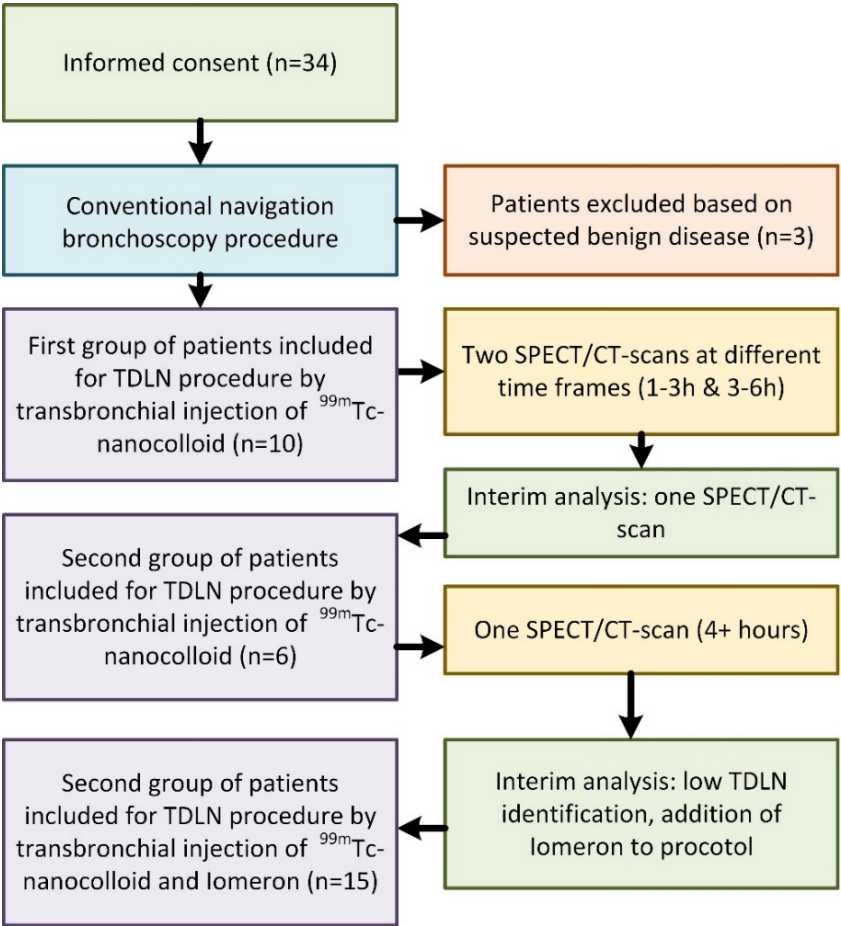
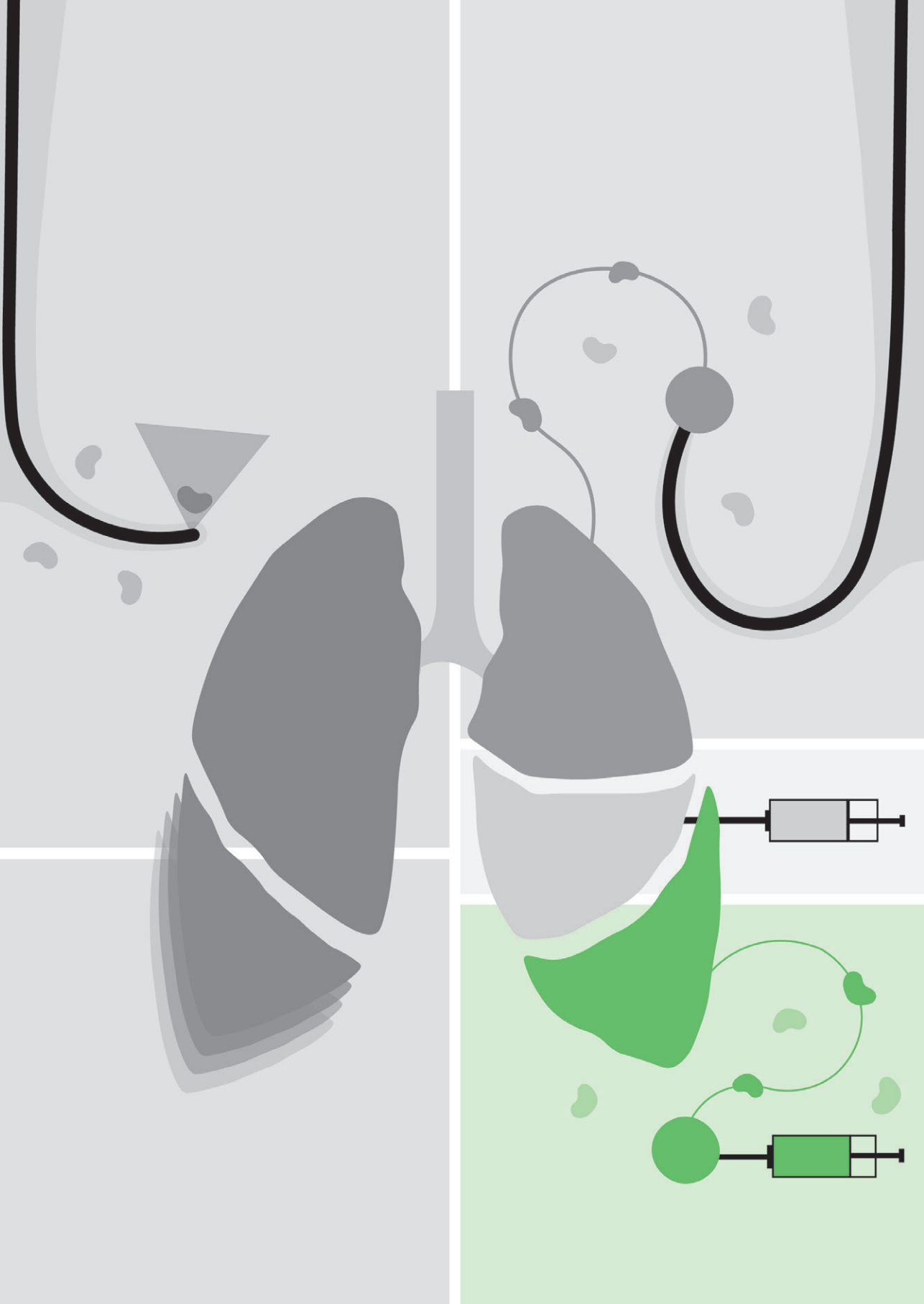


Figure B5: Flowchart of study procedures, interim analysis and adjustment done to reduce patient burden and increase knowledge on injection dissipation and SLN identification. CT, computed tomography, SPECT, single-photon emission computed tomography; TDLN, tumor-draining lymph node.



Chapter 4

Feasibility of intraoperative Indocyanine green injection to identify lymph nodes at risk of metastatic disease for early-stage lung cancer

Desi K.M. ter Woerds, Roel L.J. Verhoeven, Stefan M. van der Heide, Erik H.J.G. Aarntzen, Monika G. Looijen-Salamon, Shoko Vos, Ad F.T.M. Verhagen and Erik H.F.M. van der Heijden

Published in The Journal of Thoracic and Cardiovascular Surgery Techniques (2025)

4.1 Abstract

Background: Despite surgical resection and mediastinal lymph node dissection, 34% of stage IB-IIIB non-small cell lung cancer (NSCLC) patients demonstrate recurrence within 3.5 years, indicating disease dissemination undetected by current staging methods. Although 23.1% of clinical N0-patients are upstaged to pN1- or pN2-disease after surgery, occult disease may still be present in pN0-patients. The aim of this research was to explore implementation of a sentinel lymph node (SLN) procedure to identify lymph nodes at risk and determine its effect on staging.

Methods: In this single-center prospective study, cN0-patients with resectable NSCLC underwent intraoperative indocyanine green (ICG) injection followed by the identification of up to three SLN with near-infrared imaging. All lymph nodes were analyzed by conventional hematoxylin and eosin (HE) staining and the SLN were additionally analyzed by serial sectioning and cytokeratin staining to detect tumor cells that may be missed by conventional analysis.

Results: SLN were successfully identified in all 48 patients (100%). In three cases, injections were however incorrectly positioned possibly leading to incorrect SLN identification. Eight patients were diagnosed with pN1- or pN2-disease post-operatively: all detected by conventional pathological assessment. Analysis of correctly performed SLN procedures showed negative SLN were 100% indicative of absence of metastatic spread downstream. In two patients serial sectioning and cytokeratin staining of the SLN revealed isolated tumor cells (ITC) in one N1 node.

Conclusions: An intraoperative SLN procedure using ICG is feasible with an identification rate of 100%. A negative SLN was an indicator for absence of metastases in lymph nodes downstream.

4.2 Introduction

The preferred treatment for early-stage non-small cell lung cancer (NSCLC) is surgical resection with complete mediastinal lymph node dissection.[68] However, despite curative intent, recent data shows a 34% recurrence rate within 3.5 years for stage IB-IIB NSCLC patients,[44, 96] which may indicate hematogenous- and or lymphatic dissemination that remained undetected by pre-operative staging. In the absence of distant metastases, lymph node staging is currently based on contrast enhanced computed tomography (ceCT) and 2'-deoxy-2'-[¹⁸F]fluorodeoxyglucose ([¹⁸F]FDG) positron emission tomography (PET) imaging, followed by systematic endobronchial ultrasound (EBUS). Accurate assessment of lymph node involvement is essential for effective treatment planning and prognosis. Alarming, we and others report that despite systematic staging in accordance with the guideline, up to 23.1% of clinical stage N0-patients are upstaged to pN1- or pN2-disease after surgery.[23, 25, 69] Conventional diagnostic techniques that are based on hematoxylin and eosin (HE) staining detect macro-metastatic disease, but are postulated to overlook micro-metastatic disease. A systematic review by Sun et al. (2022) reported that micro-metastases were found in 9.3%-62.5% of patients when immunohistochemical (IHC) and/or polymerase chain reaction (PCR) techniques were used.[97] This highlights the limitations of current staging practices and the possibility of improving techniques to detect lymphatic spread in NSCLC.

A procedure to find the sentinel lymph nodes (SLN) has become routine clinical practice in other cancer types, like breast cancer and melanoma.[41, 70] The SLN are defined as the first lymph nodes with an individual lymphatic drainage from the tumor lesion, making it a reference point for assessing locoregional lymphatic dissemination. The SLN can be identified by administration of a tracer via an intra- and/or peritumoral injection, which drains via the lymphatic system and accumulates in lymph nodes over time.[71]

SLN procedures have been explored in lung cancer using various techniques, including an injection with radiolabeled tracers combined with a gamma probe in a two-day protocol, which has logistical challenges.[86, 89, 91] Ideally, the SLN procedure would be performed during surgery to allow for immediate identification and additional pathological evaluation of lymph nodes most at risk. Near-infrared (NIR) fluorescent tracers, specifically indocyanine green (ICG), show promise towards achieving this goal. While this has been studied by multiple groups, a procedure to identify the SLN using ICG has not yet been widely implemented in clinical practice.[56, 98]

In this study we aim to evaluate the feasibility of SLN identification using ICG injection and NIR imaging during lung surgery in patients with early-stage NSCLC and determine if more metastases could be identified through additional pathological work-up of the SLN identified by intra-operative ICG.

4.3 Methods

4.3.1 Study Design and Patient Selection

In a prospective single-center study, the feasibility of an intraoperative SLN procedure in patients with resectable NSCLC was assessed. cN0 Patients with a tumor size of 10–50 mm referred for lung resection with complete mediastinal lymph node dissection were eligible for inclusion. Exclusion criteria were previous treatment for lung cancer (neoadjuvant treatment or other) or known allergy to iodinated contrast agents or indocyanine green. The study was approved by the local Medical Research Ethics Committee (Reference No. 2022-13640, approved on November 29, 2022) and followed the ethical principles of the Helsinki Declaration (clinicaltrials.gov identifier NCT05555199).[78] All patients provided written informed consent for publication of anonymized study data before participation. Enrollment took place between December 2022 and August 2024. Procedural follow-up of at least two weeks was available from all patients; clinical follow-up will continue for at least 5 years after study participation. Patients could be injected with ICG either via navigation bronchoscopy directly preceding surgery or transpleurally during surgery.

In our surgical practice, lobe-specific systematic node dissection is always performed to the best of our abilities, according to the ESTS guidelines.[99, 100]

4.3.2 Navigation bronchoscopy procedure to perform ICG injection

When tumor identification through a surgical approach was deemed difficult or impossible, an endobronchial approach was performed when logistically feasible. After full sedation of the patient, a bronchoscope with an extended working channel (Medtronic EWC, Minneapolis, USA) and radial EBUS (rEBUS), or an ultrathin bronchoscope (UTB) was inserted to attempt navigation to the lesion, under fluoroscopy guidance. When the lesion was visualized by either the UTB or rEBUS, a 21G Periview Flex (Olympus Corporation, Tokyo, Japan) was inserted to inject 1.0 ml of ICG in multiple intra- and/or peritumoral depots to ensure even distribution in or around the lesion. After ICG injection, the surgery continued as mentioned below. Ventilation of both lungs proceeded until collapse of the lung during surgery.

4.3.3 Transpleural ICG injection, surgery and SLN identification

Patients were fully sedated using standard general anesthesia and single-lung ventilation was achieved using a double-lumen endotracheal tube. Surgery was performed via (robotic) video-assisted thoracoscopic surgery ((R-)VATS, either uniportal or multiportal) or thoracotomy. Following lung isolation, 25 mg of indocyanine green (ICG) powder (Verdye, Diagnostic Green GmbH, Aschheim-Dornach, Germany) was reconstituted in 25 mL of sterile water. A syringe of 1 mL was filled and connected to a 23G DeFlux Needle (Link Medical Products Pty Ltd, Auckland, New Zealand) or a 23G butterfly needle (Sol-care, Chicago, USA), depending on surgeon preference. See Figure 1 for illustrated examples. An attempt to inject 1.0 mL of ICG evenly divided over up to four depots in the surrounding quadrants of the tumor was performed to cover all possible drainage patterns. If spillage outside of the injection location occurred, this was aspirated before ventilating the lung for three minutes. The optimal dose of ICG and ventilation time was taken from the dose-escalation study by Gilmore et al. in 2012.[56] Surgery continued as per routine clinical practice, removing the tumor and performing a complete mediastinal lymph node dissection. Lymph nodes were collected in separate containers.

After removing all lymph nodes, immediate *ex vivo* near-infrared (NIR) imaging by VATS optics (Karl Storz, Tuttlingen, Germany) or by R-VATS optics (Intuitive Surgical, Sunnyvale, USA) was conducted in the OR to determine the subjective signal intensity of ICG uptake in the lymph nodes. Up to three most fluorescent lymph nodes were considered SLN and were processed as SLN by the pathology department.

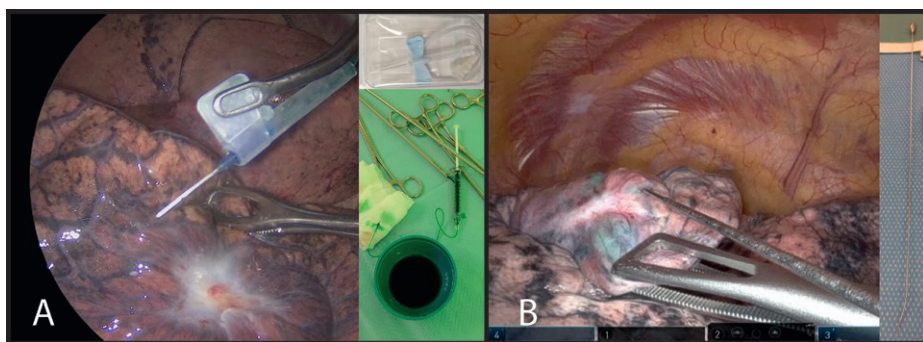


Figure 1: A butterfly needle (A) and DeFlux needle (B) can both be used for transpleural injections depending on surgeon preference and the angle at which the lesion is located from the trocar.

4.3.4 Pathological Examination

Non-SLN lymph nodes were assessed by one HE stained slide, as per routine clinical practice. The SLN were subjected to serial sectioning and HE staining on 5 levels in total. When no tumor cells were detected in the HE slides, immunohistochemical staining of the lymph nodes was performed on all 5 levels using the cytokeratin (CK) AE1/AE3 clone antibody (DAKO Agilent, Santa Clara, CA, USA), provided as ready-to-use. Staining was carried out on the fully automated DAKO Omnis immunostainer, using EnVision FLEX Target Retrieval Solution, high pH. Detection was achieved with the EnVision FLEX Horseradish Peroxidase system (DAKO Agilent, Santa Clara, CA, USA). Metastatic disease was categorized as macro-metastasis (a group of tumor cells larger than 2.0 mm), micro-metastasis (a group of tumor cells between 0.2 and 2.0 mm), and isolated tumor cells (ITC, single tumor cells or cell clusters smaller than 0.2 mm).[44]

4.3.5 Statistical Analysis

Data were analyzed using descriptive statistics to summarize patient demographics, tumor characteristics, injection parameters and pathological outcome. The number of patients with lymph node metastases identified only through serial sectioning and/or CK staining through this procedure was determined by two specialized pulmonary pathologists (SV and ML). Difficult cases were discussed together to reach consensus. To eliminate bias in determining whether metastases were found only by additional efforts (serial sectioning and cytokeratin staining) or could also have been detected by conventional methods (one HE stained slide), we defined that the middle section (level 3 out of 5) should contain metastases visible by HE staining. The number needed to detect (NND) more metastasis than through one conventional HE slide and the NND one patient with clinically relevant upstaging was calculated using available formulas.[101]

4.4 Results

A total of fifty patients were included in this feasibility study. Two patients were excluded from analysis. One due to the lung being adherent to the thoracic wall resulting in the loss of anatomical reference after detachment, which precluded accurate ICG injection. A second patient was excluded because ICG was intendedly injected intravenously to visualize segmental borders before transection, leading to ICG accumulation in all lymph nodes which compromised assessment of drainage. Patient, tumor, and surgical characteristics of the forty-eight analyzed patients are summarized in Table 1. Median follow-up time was 288 days (range, 14–805).

Table 1: Patients, lesion, and surgical characteristics.

	Characteristics		Frequency
Patient characteristics	Age, median (\pm IQR)		67 (62–72)
	Gender, <i>n</i> (%)	Male	28 (58.3%)
		Female	20 (41.7%)
	Smoking, <i>n</i> (%)	Never	5 (10.4%)
		Former	31 (64.6%)
		Current	12 (25.0%)
	BMI, median (\pm IQR)		26 (23–28)
	FEV1, median (\pm IQR)		91 (81–105)
	DLCO, median (\pm IQR)		89 (71–102)
Lesion characteristics	Lesion size on CT, median (\pm IQR)		26 (23–28)
	Lobe, <i>n</i> (%)	Upper	32 (66.7%)
		Middle	0 (0.0%)
		Lower	16 (33.3%)
	Lesion type, <i>n</i> (%)	Solid	26 (54.2%)
		Part-solid	4 (8.3%)
		GGO	9 (18.8%)
		Cystic	9 (18.8%)
	Pre-procedural N-stage (post-EBUS), <i>n</i> (%)	cN0	48 (100.0%)
Surgery	Surgery type, <i>n</i> (%)	VATS	31 (64.6%)
		Robotic-VATS	11 (22.9%)
		Thoracotomy	6 (12.5%)
	Extent of resection, <i>n</i> (%)	Lobectomy	47 (97.9%)
		Segmentectomy	1 (2.1%)
	Surgery duration, hh:mm, median (\pm IQR)		03:16 (02:44–03:43)

BMI, body mass index; CT, computed tomography; DLCO, diffusing capacity of the lungs for carbon monoxide; EBUS, endobronchial ultrasound; FEV1, forced expiratory volume in the first second; GGO, ground glass opacity; IQR, interquartile range; VATS, video-assisted thoracoscopic surgery.

4.4.1 ICG injection and SLN procedure

Three patients received transbronchial ICG injection(s) (median, 1 depot; range, 1–3) of 1.0 mL (range, 0.8–1.0 mL). The other 45 patients received transpleural ICG injection during surgery with a median of four depots (range, 3–5) totaling 1.0 mL (range, 1.0–1.2 mL). Successful injection localization was achieved in all patients injected by navigation bronchoscopy (by rEBUS or UTB visualization) and in 42 out of 45 patients that underwent transpleural injections by fluorescent imaging directly after resection (Figure 2). In the three cases where the tumor was not

visible or palpable, injection success could only be determined after resection by visualization of the tumor or palpation in combination with fluorescent imaging.

SLN were found in all patients (100%) following ICG injection. The median number of removed lymph nodes per patient was 7 (range, 4–12) and a median of 3 SLN were allocated per patient (range, 1–6). Intensity measurement of the fluorescence signal was not possible using the equipment available, and therefore comparison of inter-patient variability in NIR signal was not feasible. See Table 2 for all ICG injection and SLN characteristics.

4.4.2 Monochromatic and overlay setting of NIR imaging

Visualization of ICG in the lymph nodes revealed not only uptake by the lymph node itself, but also in the surrounding fatty or connective tissue that is frequently resected with the lymph node. Lymph nodes were initially only assessed by NIR imaging in the overlay setting, which is a combined image of the green pseudocolor fluorescent signal on top of the color image produced by white light.[102] Since the green pseudocolor is projected on top of the normal color image it can be difficult to determine if the fluorescent signal is present in the lymph node or in the surrounding fatty tissue. This may hamper the identification of ICG in nodes as illustrated in Figure 3. Fortunately, we noticed that this could be partly solved by using the monochromatic image setting that only displays the NIR signal, see Figure 4.

4.4.3 Clinical consequences of pathological analysis in SLN

All patients included had a clinical N0 status after guideline concordant workup and staging. After surgery 40 out of 48 patients were diagnosed with pN0-disease (83.3%) of which two patients were found to have isolated tumor cells (pN0(i+), Table 3). Eight patients were diagnosed with pN1- or pN2-disease post-operatively (16.7%, Table 3). The ICG injection was inaccurate in two out of the eight pN+ patients. See Figure 2 for an example of (in)accurate injections.

In one of the remaining six pN+ patients with accurate ICG injection, both the SLN and a lymph node downstream were involved (Patient 2, Table 3). In the remaining five patients, no metastases were found in lymph nodes downstream from the identified positive SLN. In three out of these five patients, metastases were also found upstream, in the peribronchial lymph nodes (region 12–14), which were located deep in the lobectomy specimen and therefore not assessable by NIR imaging during surgery and not classified as SLN. Details on detected metastases in SLN or other lymph nodes can be found in Table 3.

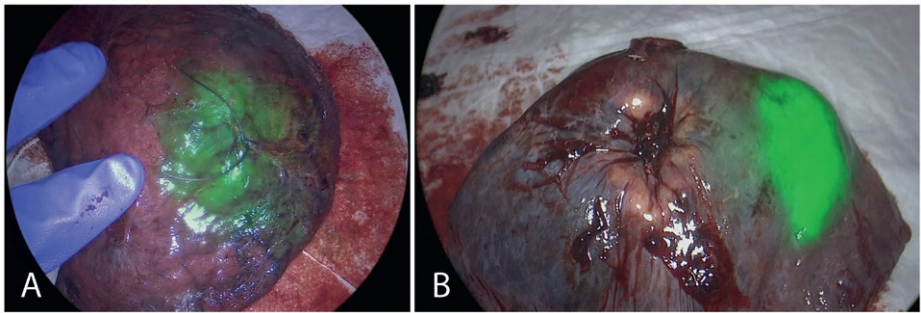


Figure 2: Two examples of transpleurally injected ICG visible on the lung surface directly after resection. (A) In the correct location, as the lesion is located at the suture. (B) In the incorrect location, too far away from the tumor (which is located at the area of pleural retraction).

4

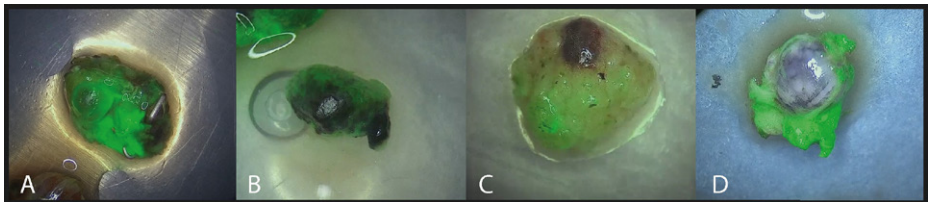


Figure 3: Two examples of ICG fluorescence within lymph nodes (A-B) and two examples of fluorescent signal found in the fatty tissue surrounding the lymph node (C-D).

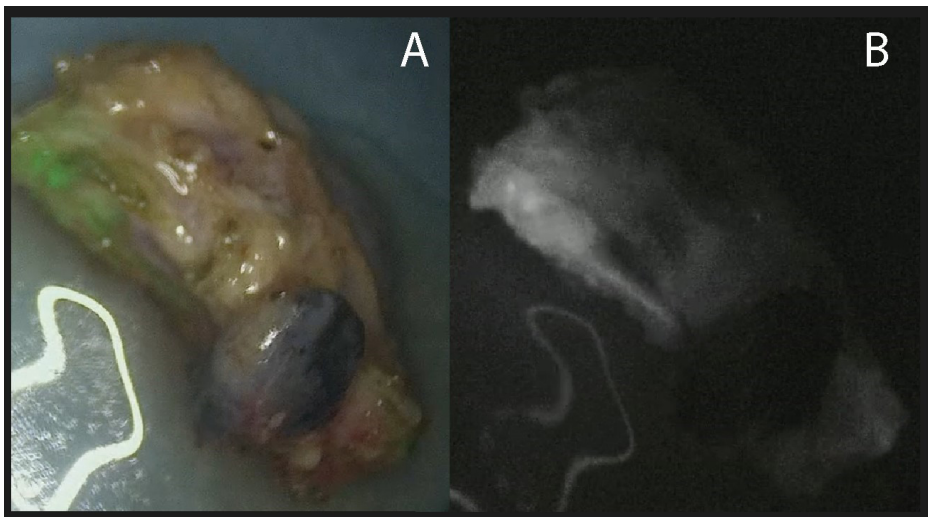


Figure 4: An example of a lymph node where monochromatic view with only fluorescent signal (B) revealed a complete lack of fluorescence signal in the lymph node itself, where this was not possible in only the image with pseudocolor overlay of the fluorescent signal (A).

Table 2: Surgical and injection characteristics. ¹ only scored in patients who underwent a transpleural ICG injection.

Characteristics			Frequency
Surgery	Type of procedure for injection, <i>n</i> (%)	Transbronchial (by navigation bronchoscopy)	3 (6.2%)
		Transpleural	45 (93.8%)
	Lesion locatable for transpleural injection, <i>n</i> (%) ¹		35 (77.8%)
ICG injection	Trans-bronchial	Number of depots, median (\pm IQR)	1 (1–1)
		Total injected volume, mL, median (\pm IQR)	1.0 (0.75–1.0)
		Endobronchial leakage of ICG, <i>n</i> (%)	1 (33.3%)
		Injection success, <i>n</i> (%)	3 (100%)
	Transpleural	Needle used for injection, <i>n</i> (%)	Butterfly needle 23G 14 (31.1%)
			DeFlux needle 23G 29 (64.5%)
			Conventional needle 21G 2 (4.4%)
		Number of depots, median (\pm IQR)	4 (4–4)
		Total injected volume, mL, median (\pm IQR)	1.0 (1.0–1.0)
		Transpleural ICG leakage, <i>n</i> (%)	21 (46.7%)
		Injection success, <i>n</i> (%)	42 (93.3%)
SLN procedure	Number of removed lymph nodes per patient, median (\pm IQR)		7 (6–9)
	Number of fluorescent lymph nodes per patient, median (\pm IQR)		3 (2–5)
	SLN identification, <i>n</i> (%)		48 (100%)
	Number of SLN per patient, median (\pm IQR)		3 (2–3)
	NIR-optics for fluorescence detection, <i>n</i> (%)	Da Vinci Firefly	2 (4.2%)
		Karl Storz NIR	46 (95.8%)
Pathology outcome	Histology type, <i>n</i> (%)	AC	37 (77.1%)
		SCC	10 (20.8%)
		AC-NEC	1 (2.1%)
	N-stage, <i>n</i> (%)	pN0	38 (79.2%)
		pN0(i+), ITC	2 (4.2%)
		pN1	5 (10.4%)
		pN2	3 (6.2%)

AC, adenocarcinoma; ICG, indocyanine green; IQR, interquartile range; ITC, isolated tumor cells; NEC, neuroendocrine carcinoma; NIR, near-infra red; SCC, squamous cell carcinoma; SLN, sentinel lymph node.

In all patients with a pathology-negative SLN and an accurate ICG injection, no metastatic disease was detected in any of the lymph nodes located downstream. No correlations were found between metastatic disease found after surgery and pre- or intraoperative patients or lesion characteristics.

4.4.4 Value of serial sectioning and CK staining for detection of metastatic disease

Serial sectioning and CK staining of the SLN identified no micro- or macro-metastases that would not likely have been found using the conventional work-up with a single level HE-staining. These additional efforts did however identify ITC in the SLN of three patients of which two received a N0(i+) stage and one was already diagnosed with pN1 disease. Clinical interpretation was complicated because the ITC were mostly found on the edges of the lymph node, see also Figure 5. As ITC are currently not a reason for upstaging, the NND to upstage one patient by this technique could not be calculated. The number needed to detect one patient with ITC (N0(i+) stage) was 24 patients.

4.4.5 Safety and adverse events

No adverse events related to the study procedure were observed apart from one patient who had a small parenchymal bleeding caused by the trocar still in situ during the ventilation after ICG injection. However, no intervention was needed since this lobe was to be removed anyway. Transbronchial ICG injection per navigation bronchoscopy prolonged surgery duration by approximately 25 minutes, and approximately 5 minutes were added to perform transpleural injection.

Table 3: Detailed information on all ten patients where tumor cells were ultimately found in the lymph nodes. Some lymph node regions contained multiple lymph nodes, with and without (sufficient) ICG uptake, and were therefore classified as both SLN and other lymph nodes based on NIR signal. Macrometastases were classified as metastases > 2.0 mm, micrometastases are metastases that measured between 0.2 and 2.0 mm and ITC are groups of cells < 0.2 mm. ¹ Peribronchial lymph nodes were not assessed by NIR imaging. ² Station 7 was fluorescent, but less so compared to two lymph nodes from station 10 and one station 11 and was therefore not classified as SLN. ³ A total of five lymph nodes region 10 were removed of which two SLN. Micro-metastases were found in the SLN only.

Nr.	Tumor location	Accurate injection	SLN stations based on ICG uptake		Other nodal regions sampled and evaluated by NIR-imaging		Classification of metastatic disease		
			With metastatic disease	Without metastatic disease	With metastatic disease	Without metastatic disease	Macro-metastasis	Micro-metastases	ITC
1	RLL	Yes		9 + 10 + 11		2 + 4 + 7 + 9 + 10 + 11	Peribronchial ¹		
2	RUL	Yes	10 + 11		7	2 + 4 + 11	7 ² + 10 + 11		
3	LLL	Yes	10	7		5 + 9 + 10 + 11	10 + peribronchial ¹		
4	RUL	Yes	4 + 10	7		2 + 4 + 10 + 11	10	4	
5	RUL	Yes	10	4		2 + 4 + 7 + 10 + 11		10 ³	
6	RUL	Yes	11 + 10 + 7			2 + 4 + 10	11 + peribronchial ¹	10	7
7	RUL	Yes	11	7 + 10		2 + 4 + 10 + 11 + 12			11
8	LLL	Yes	11	10		5 + 7 + 9 + 10			11
9	LUL	No		10 + 11	3 + 5	7 + 10 + 11	3 + 5		
10	RLL	No	11		11	4 + 10	11		

ICG, indocyanine green; ITC, isolated tumor cells; LLL, left lower lobe; LUL, left upper lobe; NIR, near-infra red; RLL, right lower lobe; RUL, right upper lobe; SLN, sentinel lymph node.

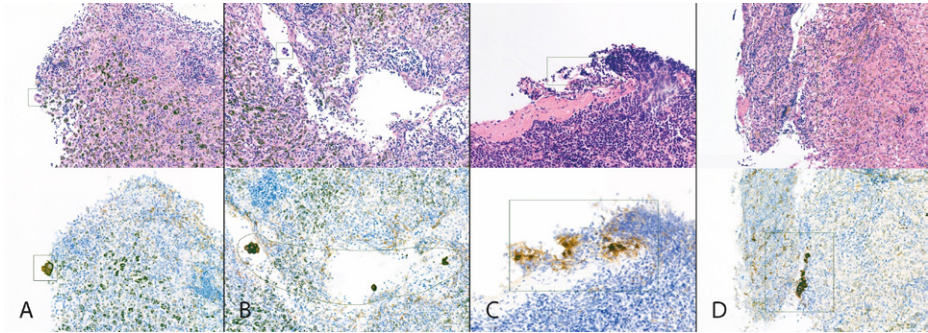


Figure 5: Annotated images of the HE and CK stained slides of lymph nodes where ITC were found. A-B Patient with ITCs on the border and in lymph node station 11. C Patient with ITC on the border of station 11. D Patient with pN1 disease in station 10 and 11, and ITC in station 7 (depicted).

4.5 Discussion

This study demonstrates that SLN identification by ICG injection and NIR imaging during surgery in patients with early-stage NSCLC is feasible and allows for targeted evaluation by pathology. A total of 48 cN0 patients were included, of which 8 were diagnosed with pN+ disease. Of these eight patients, two had inaccurately placed ICG injections. In patients with a successful peritumoral ICG injection and pathology negative SLN, no downstream metastatic spread was found. Regarding to pathological workup, serial section and CK staining did reveal three cases of ITC but did not reveal any macro- or micrometastatic disease that would not have been found by routine histopathological evaluation and thus did not affect staging outcome. Based on these results, the NND one patient with ITC to receive a pN0(i+) instead of pN0 stage is 24 patients. But as per current guidelines and the new ninth edition of the TNM staging manual, ITC do not affect pathological staging nor the eligibility of adjuvant treatments in these patients.[103]

In contrast to lung cancer, the identification of SLN and detailed analysis thereof in the workup of other cancer types has become a routine clinical procedure. This widely accepted SLN methodology has shown to improve staging accuracy and decrease recurrence through eligibility to tailored treatments.[104, 105] The accuracy of SLN detection in lung cancer is however still unknown. One key factor is whether the injection of ICG can always be accurately placed within the target area. We have found that when an accurate injection is not possible, there is no value in finding the lymph node with the most ICG uptake. It is recommended to select cases where ICG injection will be possible based on pre-operative imaging and this could aid in the standardization of the technique. A second limiting factor

is the lack of quantitative measurement of fluorescence to determine which lymph node contains the highest concentration of ICG and if this node truly represents the first site of metastasis in all cases. A complete lymphadenectomy remains necessary to determine the three most fluorescent lymph nodes, which is inherently a subjective manner. Compared to other cancers, the procedure performed during lung surgery cannot determine which lymph nodes should be resected, and which can remain in situ when no metastases are found. The presented technique to find the SLN is therefore only applicable to improve staging of lymph nodes by focused pathological and IHC techniques.

4.5.1 Finding micrometastases or ITC by IHC

A systematic review by Sun et al (2022) reported that more micro-metastases are found when IHC and PCR techniques are used on top of conventional HE-staining.[97] These techniques are however time consuming and in our hands serial sectioning and CK staining of identified SLN did not lead to clinically relevant changes in staging outcome as only ITC were (likely additionally) detected. Furthermore, as illustrated in Figure 5, ITC were mostly found on the edges of the lymph node instead of inside the lymph node and CK-AE1/AE3 generally shows background staining in for instance interstitial reticulum cells which could also be interpreted as contamination.[106, 107] It is however important to accurately diagnose these metastases, as studies show that patients with either micrometastases and/or ITC may have poorer survival than patients without metastases.[44, 53, 108] Unfortunately, most meta-analysis or systematic reviews group patients with micrometastases and ITC, making it impossible to determine the influence of diagnosing only ITC on the prognosis of a patient. With the current guidelines, the presence of ITC (< 0.2 mm, pN0(i+)) does not change nodal stage, while the identification of micro-metastases ($0.2 - 2.0$ mm, pN+) does translate into upstaging, making patients potentially eligible for additional treatment.[1] Future studies will need to determine whether patients diagnosed with ITC have a poorer prognosis compared to micro- or macrometastases or patients without metastases and whether or not they should also be eligible for adjuvant treatment, potentially contributing to more personalized treatment.

4.5.2 SLN identification rate

Using the presented study protocol, SLN were identified in 100% of patients when depots were accurately placed. Most other studies report identification rates of 75–82%.[42, 58, 109, 110] Digesu et al. even reported a 100% identification rate in selected cases.[111] As Phillips et al. and Gilmore et al. both show in their dose escalation studies, several parameters and protocol variations may be of

influence in achieving adequate SLN identification. It can be concluded by their and our results that ventilation of the lung after injection and an ICG dose of at least 1 mg are essential for SLN identification.[56, 58, 109, 110] A very recent study by Stasiak et al. (2025) reported an identification rate of 90.6% in 06 patients after injection of 2.5 mg ICG in 1 ml. In line with our findings, they also found that when the SLN is clean, all lymph nodes downstream are free of tumor cells as well. They also performed injections transpleurally as well as endobronchially and noticed a slightly lower SLN identification rate with the transpleural approach compared to the endobronchial approach.[112] Unfortunately, our endobronchial cohort is too small ($n = 3$) to compare NIR uptake in the lymph nodes.

While we have only investigated the injection of ICG, tracers with radioactive or magnetic properties or even visible dye have also been explored in the past. These agents have generally been studied more extensively but have not demonstrated consistent effectiveness or require complex logistics. ICG remains relatively underexplored in this context.[66, 113] However, the heterogeneity in study outcomes by us and others show that more work is still needed to better understand which methodology would provide for a universally successful approach.

4.5.3 Finding the lymph nodes most at risk

Some surgeons have explored and implemented lobe-specific lymph node dissection in an attempt to find the lymph nodes most at risk.[114] We however noticed in our cohorts of both pN0 and pN+ patients, that when multiple lymph nodes from a single region were resected, some lymph nodes contained ICG while others contained no ICG at all. This suggests that not all lymph nodes in a region are draining lymph fluid from the lung tumor similarly. While the identification of lobe-specific lymph nodes could minimize extra pathological efforts somewhat, SLN identification would theoretically have more potential to identify the lymph nodes most at risk. And while we found a 100% SLN identification rate in correctly placed injections, additional pathological efforts by CK staining and additional sectioning did not seem to detect more metastases. Based on this observation we expect that lobe-specific lymph node dissection would also not have revealed more metastases in this cohort.

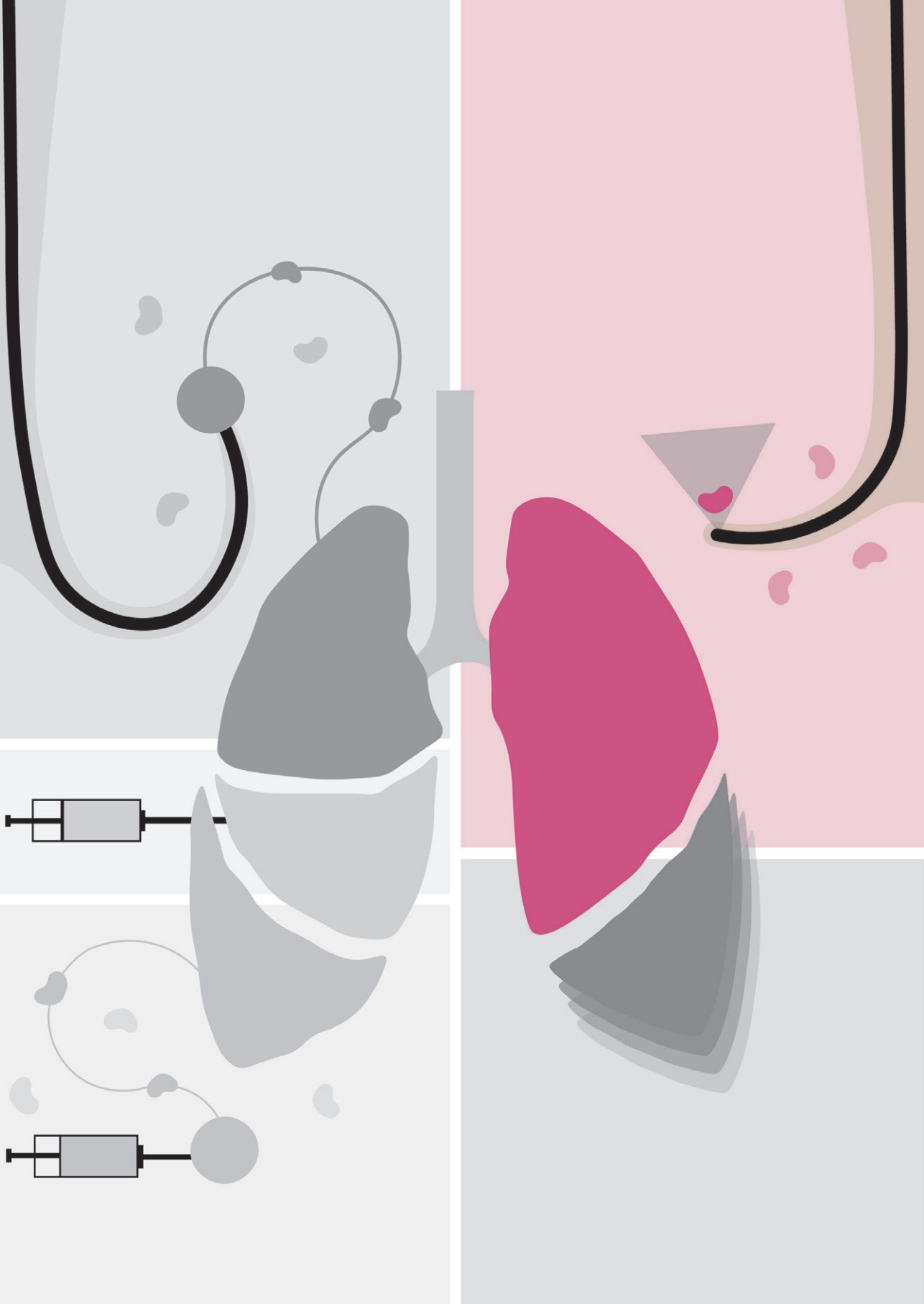
4.5.4 Strengths, limitations, and future considerations

A prominent limitation of our ICG-based SLN procedure is the risk of spillage into the thoracic space after injection, which could possibly result in more fluorescence appearing in the fat surrounding the lymph nodes than in the lymph node itself. This can make differentiation between true nodal uptake and adjacent background

signal challenging. As we illustrated, the overlay images were occasionally misleading, as the 'over' effect caused ICG to appear as originating from the node when it was in fact located in the fatty tissue surrounding the lymph node. The monochromatic view could partly alleviate the problem, as it provided more depth to the NIR signal, but it was not helpful enough when the lymph node was fully embedded in the fatty tissue. This is largely attributed to the subjective nature of the technique and could lead to false-positive or false-negative findings. A second limitation of this technique is the inability to evaluate intrapulmonary lymph nodes by NIR imaging, as these are only found after fixation of the removed lung tissue and are not available at the time of NIR evaluation. These lymph nodes are also embedded close to the fluorescent lung tumor, which makes evaluation without resection difficult due to the overshine of the ICG depots in the resected lung. The presented technique is therefore only applicable to improve staging of lymph nodes that are separately removed by the surgeon. While not performed by us, removal techniques of the more peripheral lymph nodes in station 12 to 14, as demonstrated by Raymond et al. (2022), could perhaps be utilized in future to be able to evaluate all lymph nodes with NIR imaging.[115]

This study was performed in a single center, which might have affected the reproducibility of surgical techniques as well as pathological analysis. Additionally, the sample size of the study was small and does not allow for statistical analysis regarding metastatic disease. Moreover, this study only included cN0-staged patients and it is unclear if treatment of lymph node metastases would impact the drainage of lymph fluid to the lymph nodes and whether a patient could still benefit from additional staging efforts. Considering the rise of neoadjuvant treatment,[116, 117] we believe these patients should be included in future studies on intraoperative SLN procedures to find possible limitations or advantages and define clear inclusion criteria to maximize procedure outcomes.

Finally, at the time of writing, the longest follow-up period in our cohort is 1.5 years. This is insufficient to draw final conclusions about the added accuracy of staging, specifically with respect to disease recurrence. A longer follow-up period and larger population will be needed and will be collected to determine if the recurrence rate in the group of patients with pN0 is different from other pN0 patients in our center and whether implementation of this technique would add value to patient outcome.



Chapter 5

Endobronchial Ultrasound Staging During Navigation Bronchoscopy for Peripheral Pulmonary Nodules in the Real World: Which Patients Will Benefit?

Desi K.M. ter Woerds, Roel L.J. Verhoeven, Ad F.T.M. Verhagen, Erik H.J.G. Aarntzen
and Erik H.F.M. van der Heijden

Published in *Cancers* (2025)

5.1 Abstract

Background: The prevalence of lung cancer in patients with a peripheral pulmonary nodule referred for navigation bronchoscopy (NB) is high. Combining NB with a systematic EBUS for staging is common practice. We investigated the added value of performing EBUS in the population referred for NB in relation to the available pre-procedural [^{18}F]FDG-PET and CT imaging information.

Methods: This single-center study evaluated all consecutive patients who underwent an NB in an academic referral center. [^{18}F]FDG-PET and CT scoring of lymphadenopathy was based on routine [^{18}F]FDG-PET and/or contrast-enhanced chest (ce)CT imaging reports and were correlated to outcome of systematic EBUS and sub-sequent surgery (when available).

Results: In total, 403 patients were included for analysis of which 327 underwent EBUS (81.1%). In 138/403 patients (35%) who had positive lymph nodes on [^{18}F]FDG-PET (86.5%) or ceCT (13.5%), 12 lung cancer patients were diagnosed with N+ disease by EBUS (8.4%). An additional nine EBUS-negative patients were diagnosed with N+ disease after surgery (5.4%). In the group of patients with imaging-negative lymph nodes (65.8%), no metastatic lymph nodes were found by EBUS, and surgery revealed occult nodal metastasis in eight patients (3.1%).

Conclusions: In patients with peripheral pulmonary nodules referred for NB, EBUS may be safely omitted when [^{18}F]FDG-PET or ceCT imaging does not indicate presence of nodal involvement.

5.2 Introduction

As lung cancer screening programs are more widely implemented, there has also been an increase in the detection of incidental pulmonary nodules.[6] These nodules are initially evaluated using lung cancer risk prediction scores based on clinical assessment, radiological features, and nodule growth.[10] The increase in pulmonary nodules detected also translates into more nodules being classified as high-risk and this has led to a rise in referrals for minimally invasive diagnostic navigation bronchoscopy (NB) procedures.[10] In this population, the reported prevalence of lung cancer in patients referred for NB is high with 76% in our own center and others.[17, 118]

NB allows for minimally invasive tissue sampling of peripheral pulmonary nodules that are beyond the reach of conventional bronchoscopy, and it offers a favorable safety profile with a lower risk of complications such as pneumothorax.[11, 59, 119] A frequently cited advantage of NB is the possibility of combining the procedure with immediate staging by endobronchial ultrasound (EBUS) since lymph node staging is equally crucial to determine lung cancer treatment and prognosis. This has become even more important with the recent approval of neoadjuvant (chemo) immunotherapy for patients with stage II and resectable stage IIIa.[117, 120] However, the vast majority of patients referred for NB have small (less than 3 cm), peripherally located nodules (ACCP, group D) for which guidelines state that staging is not routinely needed in absence of suspected lymph nodes based on 2'-[¹⁸F]fluoro-2'-deoxyglucose positron emission tomography ([¹⁸F]FDG-PET) or computed tomography (CT) imaging.[21, 23, 121, 122] Moreover, patients with a high risk of mediastinal metastases are usually scheduled for upfront EBUS and are not referred for NB.

Systematic EBUS has emerged as the preferred technique for locoregional lymph node staging, replacing more invasive surgical staging procedures.[23] Although guidelines on the performance of EBUS do not typically apply to patients referred for NB, the importance of thorough staging and the fact that NB requires general anesthesia have led to the increased practice of combining EBUS with NB in patients with suspected lung cancer.[25, 72, 74]

However, despite guideline-concordant staging, studies show that a significant number of patients staged as clinical N0 based on CT and/or [¹⁸F]FDG-PET imaging or EBUS, are upstaged to pN1 or pN2 after surgery.[23] The rate of occult N1 disease can reach up to 16.6% and upstaging to N2 disease occurs in up to 9.9% highlighting the limitations of current staging techniques.[21, 23, 25, 69, 123]

In this study, we aim to assess the added value of performing systematic EBUS during NB in patients with peripheral nodules. By calculating the number needed to treat (NNT) and evaluating whether certain imaging features, such as [^{18}F]FDG-PET and CT findings, can reliably select patients in whom EBUS staging may be omitted, we hope to personalize and refine the diagnostic and staging workflow for this patient population.

5.3 Methods

This study analyzes clinical and procedural data as prospectively acquired during routine clinical practice in patients who underwent a diagnostic NB between December 2017 and January 2023 in the Radboud University Medical Center, Nijmegen, the Netherlands. During the inclusion period, the Radboud University Medical Center was the only center in the Netherlands performing navigation bronchoscopies and, therefore, evaluated patients from multiple referring centers across the Netherlands. A systematic EBUS was routinely performed in patients scheduled for NB. All patients provided written informed consent to use their data (Reference No. 2017-3706, 2017-3707 and 2019-5148). Patients who underwent an EBUS procedure prior to referral for NB, were excluded. Patients were further excluded from analysis when no NB had been performed based on new clinical findings like an unanticipated central lesion, resorption of the target nodule, or when NB was performed for local treatment purposes. In patients who received a second NB, only the first procedure was analyzed. Patients with a nodule that had an uncertain benign outcome with insufficient or incomplete clinical follow-up of less than 12 months were excluded from analysis, since they could not be categorized correctly, as per international consensus.[14, 73] In our center, the NB procedure is based on cone-beam CT-based 3D-image guidance as has been described in detail by Beyaz et al. (2025).[79]

5.3.1 Data Collection and Case Selection Criteria

Patient demographics and nodule characteristics were collected through investigation of electronic medical records, including size, lobe, radiographic characteristics of the nodule, whether the nodule was < 2 cm from the pleura and pre-procedural and post-operative TNM-stage (8th edition [124]). Follow-up data from 32 referring hospitals were collected. When data about the specific histology or type of treatment a patient received for lung cancer were inconclusive, lacked detail, or were not available during follow-up from referring hospitals, this was categorized as unknown.

5.3.2 Patient Selection and Imaging Criteria for EBUS Performance Analysis

When an [^{18}F]FDG-PET scan was performed up to 6 weeks prior to the NB, [^{18}F]FDG-PET outcome of the lymph nodes was scored imaging positive (iN+) when the report of the Nuclear Physician mentioned any uptake of [^{18}F]FDG in one or multiple (even bilateral) lymph nodes. When no recent [^{18}F]FDG-PET scan was available, lymph nodes were scored on the pre-procedural contrast-enhanced chest CT scan (ceCT) if performed within 6 weeks prior to the NB. The CT outcome was scored iN+ when ipsilateral or mediastinal lymph node(s) with a short axis ≥ 10 mm were found.[125] If despite a negative [^{18}F]FDG-PET-outcome the lymph nodes were still suspected to be cN+ based on size on the ceCT scan, the positive CT outcome overruled the negative [^{18}F]FDG-PET outcome, and the patient was categorized as iN+. No central review of [^{18}F]FDG-PET or ceCT scans was performed, and daily clinical reports were used to categorize nodal status.

5.3.3 Diagnostic Procedures

All patients underwent a cone beam CT (CBCT)-guided NB under general anesthesia as described previously.[79] The choice to combine the procedure with a systematic EBUS was at the discretion of the endoscopist. This decision was not strictly defined and, in general, guided by the available clinical information (i.e., suspected lung cancer versus suspected metastatic pulmonary lesions of non-primary lung cancers), imaging information (i.e., suspected lymph node involvement based on imaging), and/or per-procedural feedback of primary lesion by rapid on-site cytopathology evaluation (ROSE), which was available in all cases.[17]

All EBUS procedures were conducted with a flexible ultrasound bronchoscope (EB-1970UK, Pentax Medical, Tokyo, Japan) using a 22G needle (EchoTip, Cook Medical, Bloomington, IN, USA) for transbronchial needle aspiration (TBNA). Following local and international guidelines, EBUS was systemically performed; stations 4L, 4R, 7, 10L, 10R, 11L, 11Ri, and 11Rs were routinely measured along the short axis. We routinely sample every imaging negative LN > 8 mm, and when PET shows any level of avidity, we aspirate > 5 mm, with clear PET avidity. Also, LN < 5 mm are aspirated when technically feasible, and when there is an applicable EUSb approach it was additionally used routinely and sampled when size > 5 mm and the lymph node characteristics along with clinical indication recommended sampling.[25, 69, 121] Sampling consisted of at least three TBNA passes or until ROSE established that an adequate sample was obtained. Intraprocedural specimen adequacy was defined based on a sufficient presence of lymphocytes in the smears.[126]

5.3.4 Data Analysis

Categorical variables were expressed as absolute and relative frequencies, continuous variables were expressed as means and standard deviations, and non-normally distributed data as median and interquartile range (IQR).

The sensitivity, specificity, negative predictive value (NPV), positive predictive value (PPV), overall accuracy, and number needed to treat (NNT) of nodal imaging to detect N-disease with EBUS were calculated using the standard formulas.[127] The NNT was defined as the number of patients that needed to undergo EBUS to avoid one case of N-disease after surgical resection (pN+), irrespective of the involved location (N1, N2, or N3). The NNT was calculated for all patients, and subgroup analyses were performed for lung cancer patients and/or iN+/iN- patients (Supplementary data).

5.4 Results

After exclusion of patients based on the defined criteria, 403 patients were included for study analysis (Figure 1). In these patients, 504 nodules with a median diameter of 17 mm were biopsied (85.9% with a nodule sized < 30 mm and 14% had a mass sized ≥ 30 mm); 72% of the patients had their lesions located at less than 2 cm from the pleura (Table 1). Of these 403 patients, 138 were defined as having any imaging-positive lymph node involvement (iN+) and 265 as imaging negative (iN-), see also Figure 1. Detailed demographic and lesion data are summarized in Table 1. Lung cancer prevalence in this patient cohort was 67.5%.

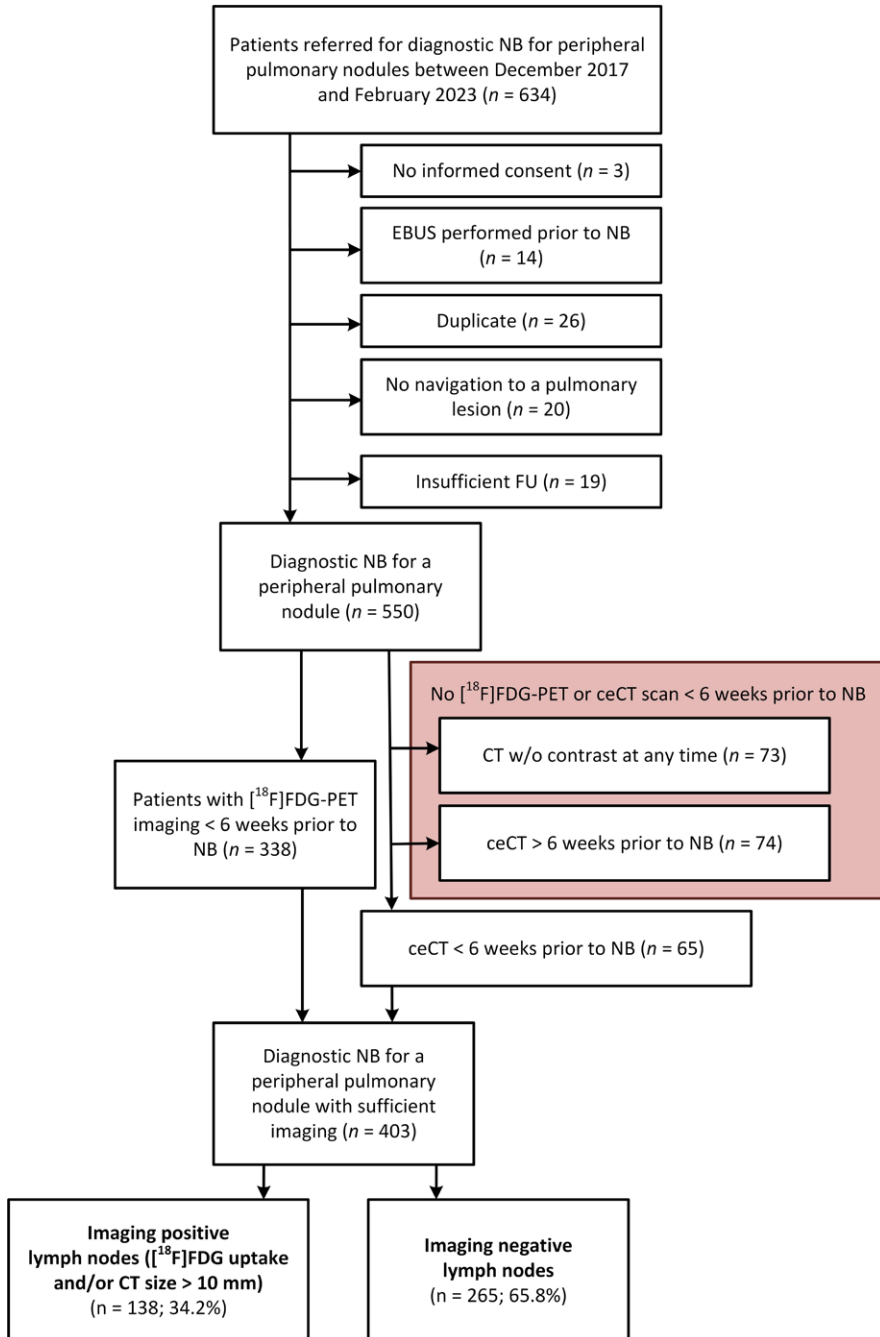


Figure 1: Flowchart of patients receiving a navigation bronchoscopy between December 2017 and February 2023. ceCT, contrast-enhanced computed tomography; EBUS, endobronchial ultrasound; FU, follow-up; NB, navigation bronchoscopy; [¹⁸F]FDG, 2'-[¹⁸F]fluoro-2'-deoxyglucose; PET, positron emission tomography.

Table 1: Demographic data of all included patients ($n = 403$) and nodule characteristics and pathological outcome for the sub-selection of patients with a diagnosis of lung cancer ($n = 272$).

* The [^{18}F]FDG-PET-outcome was scored as positive when any uptake of FDG in one or multiple (even bilateral) lymph nodes was reported in the clinical PET/CT report.

	Patient baseline characteristics, all included patients (n = 403)		Frequency
Patient characteristics	Age, years, median (±IQR)		67 (±11)
	Sex, n (%)	Male	205 (50.9%)
		Female	198 (49.1%)
	BMI, median (±IQR)		24.61 (±5.98)
	Lesion < 2 cm from pleura, n (%)	Yes	298 (72.2%)
		No	105 (27.8%)
	Radiologic nodule characteristics, n (%)	Solid	317 (78.6%)
		Part-solid	47 (11.7%)
		GGO	19 (4.7%)
		Cystic	20 (5.0%)
	Nodule size, mm on CT, median (±IQR)		17 (±12)
	Total number of nodules navigated to, n		504
	Number of nodules evaluated per patient, n (%)	One nodule	308 (76.4%)
	Two nodules	89 (22.1%)	
	Three nodules	6 (1.5%)	
Imaging data	[18F]FDG PET availability < 6 weeks prior to NB, n (%)		338 (83.9%)
	Time between [18F]FDG-PET and NB, days, median (±IQR)		22 days (±14)
	[18F]FDG-uptake in lymph nodes, n (%)	Positive *	122 (36.1%)
		Negative	216 (63.9%)
	In patients without PET or with PET > 6 weeks prior to NB: CT with contrast only < 6 weeks prior to NB, n (%)		65 (16.1%)
	Time between CT contrast and NB, days, median (±IQR)		24 days (±15)
	CT outcome of lymph nodes, n (%)	Positive	19 (29.2%)
		Negative	46 (70.8%)
EBUS	EBUS performed, n (%)	Yes	327 (81.1%)
		No	76 (18.9%)
	TBNA performed, n (%)	Yes	179 (54.7%)
		No	148 (45.3%)
	Number of lymph nodes sampled, median (±IQR)	Imaging-positive group	2 (±2)
		Imaging-negative group	1 (±1)

Table 1: Continued

Subgroup analysis in patients with a final diagnosis of lung cancer (n = 272)			Frequency
	CT stage, n (%)	Tis	5 (1.8%)
		T1a	39 (14.3%)
		T1b	100 (36.8%)
		T1c	46 (16.9%)
		T2a	18 (6.6%)
		T2b	12 (4.4%)
		Pre-procedural characteristics	CT stage, n (%)
T4	4 (1.5%)		
Multiple lesions (all T)	33 (12.1%)		
iN-stage (based on PET and or contrast CT imaging), n (%)	iN–		178 (65.4%)
	iN+		94 (34.6%)
Pre-NB/-EBUS imaging-based cN-stage of all iN+ patients, n (%)	cN0		56 (59.6%)
	cN1		18 (19.1%)
	cN2		15 (16.0%)
	cN3		5 (5.3%)
Lesion location, n (%)	Right upper lobe		98 (36.0%)
	Right middle lobe		10 (3.7%)
	Right lower lobe		38 (14.0%)
	Left upper lobe		60 (22.1%)
	Left lower lobe		29 (10.7%)
Post-procedural characteristics	Post-NB+/-EBUS cN-stage, n (%)	cN0	259 (95.2%)
		cN1	4 (1.5%)
		cN2	5 (1.8%)
		cN3	4 (1.5%)
	Treatment, n (%)	Surgery	115 (42.3%)
		SABR and/or cyberknife	105 (38.6%)
		Combination of treatments	29 (10.7%)
		Best supportive care	15 (5.5%)
		Immunotherapy	4 (1.4%)
		Chemotherapy	3 (1.1%)
		Unknown	1 (0.4%)

Table 1: Continued

Subgroup analysis in patients with a final diagnosis of lung cancer (n = 272)			Frequency
Post-procedural characteristics	Neo-adjuvant treatment, n (%)	Yes	10 (8.7%)
		No	105 (91.3%)
	pN-stage after surgery, n (%)	pN0	97 (84.3%)
		pN1	10 (10.3%)
		pN2	8 (8.2%)
	Tumor histology, n (%)	AC (incl. AAH, ACIS, and MIA)	138 (50.7%)
		SCC	38 (14.0%)
		Unknown (no tissue)	21 (7.7%)
		Carcinoid	8 (2.9%)
		NSCLC(-NOS)	4 (1.5%)
		SCLC	8 (2.9%)
		Mixed AC-SCC	2 (0.7%)
		Multiple (synchronous) histologically different lung cancers	53 (19.5%)

AAH, atypical adenomatous hyperplasia; AC, adenocarcinoma; AIS, adenocarcinoma in situ; BMI, body mass index; CT, computed tomography; EBUS, endobronchial ultrasound; [¹⁸F]FDG, 2'-[¹⁸F]fluoro-2'-deoxyglucose positron emission tomography; IQR, interquartile range; MIA, minimally invasive adenocarcinoma; NB, navigation bronchoscopy; NEC, neuroendocrine carcinomas; NSCLC, non-small cell lung cancer; NOS, not otherwise specified; SABR, stereotactic ablative radiotherapy; SCC, squamous cell carcinoma; TBNA, transbronchial needle aspiration.

5.4.1 EBUS, Imaging and Pathological Outcomes in All Patients

Nodal involvement was scored on [^{18}F]FDG-PET imaging in 83.9% of patients, while ceCT was used in the remaining 16.1% of patients. Based on current guidelines, a staging EBUS was not indicated in 64.7% of the cases. In our cohort however, systematic EBUS was performed in 327 patients (81.1%) and diagnosed metastatic lymph node disease in 13 patients with lung cancer and 1 patient with metastatic disease from colon cancer. EBUS was not performed in some cases where malignant origin of the nodule was judged unlikely based on ROSE during NB (e.g., granulomatous origin in combination with symmetric PET avidity suggesting inflammation), at the discretion of the endoscopist or due to unanticipated logistical issues. Surgical follow-up was available in 115 out of 272 lung cancer patients (42.3%). In the surgically treated subgroup, follow-up revealed an additional 17 patients with lymph node metastases and 1 patient with pN2 disease with previous EBUS-based cN1 disease. Of these 17 patients, 11 underwent EBUS-TBNA and in 6 patients, TBNA was not performed due to small lymph node sizes (< 7.0 mm) or benign lymph node characteristics. Additionally, 1 of 13 EBUS-diagnosed lymph node metastasis was a false positive finding (cN1 down-staged to pN0). The diagnostic outcome of nodules, EBUS and subsequent performed treatments for both the iN+ and iN– group are summarized in Figures 2 and 3, respectively.

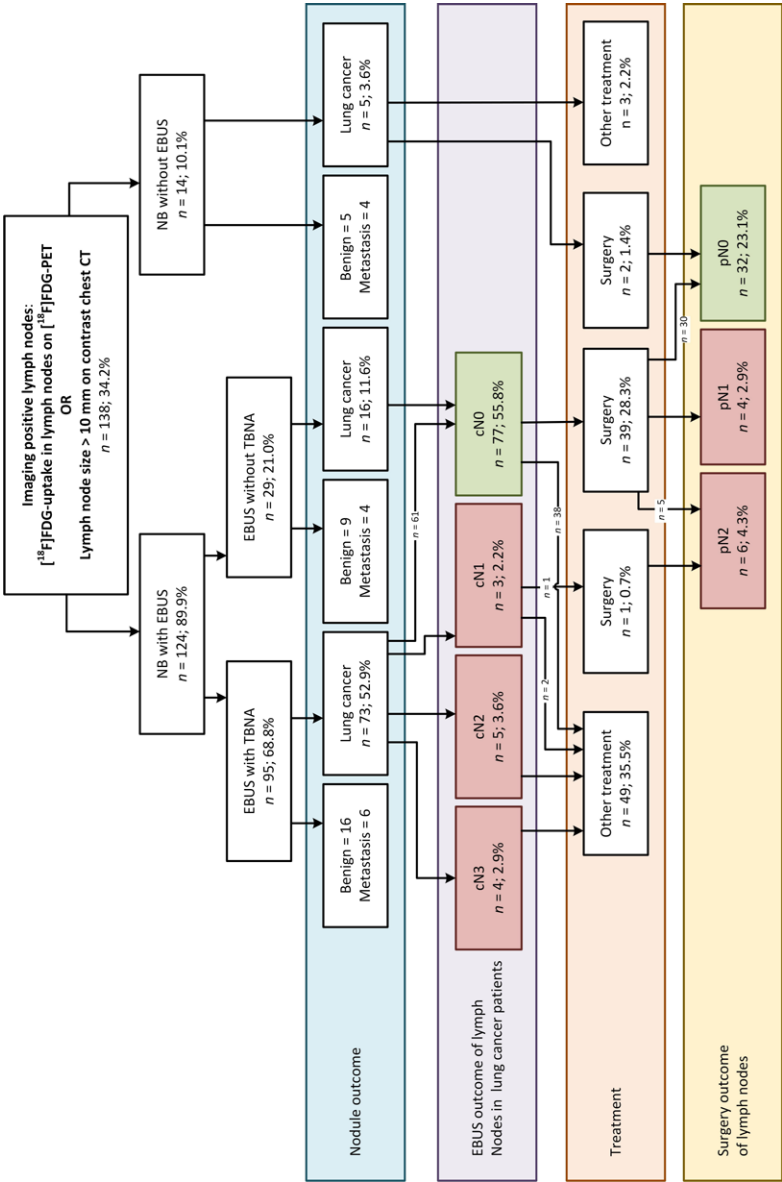


Figure 2: Flowchart of EBUS outcome based on imaging-positive lymph nodes and lesion diagnosis, including N-status after EBUS and/or surgery. CT, computed tomography; EBUS, endobronchial ultrasound; [¹⁸F]FDG, 2-[¹⁸F]fluoro-2-deoxyglucose; FU, follow-up; NB, navigation bronchoscopy; PET, positron emission tomography.

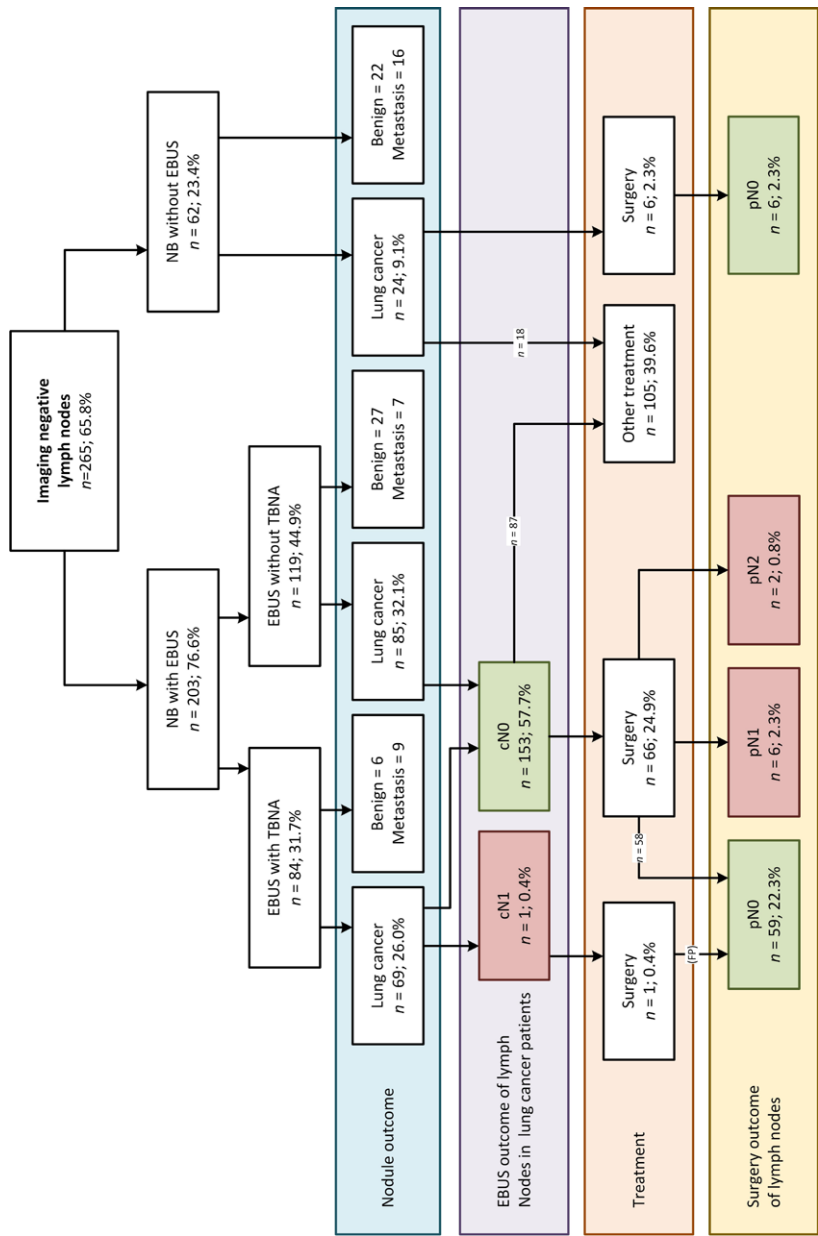


Figure 3: Flowchart of EBUS outcome based on imaging-negative lymph nodes and lesion diagnosis, including N-status after EBUS and/or surgery. EBUS, endobronchial ultrasound; FP, false positive; NB, navigation bronchoscopy; metastasis means pulmonary metastasis of other origin than primary lung cancer.

Following the analysis as summarized in Table 2, the sensitivity, specificity, PPV, NPV, and overall accuracy of [¹⁸F]FDG-PET and CT imaging to predict EBUS outcome are 92.9%, 64.5%, 10.5%, 99.5%, and 65.7%, respectively. The number of EBUS procedures needed to find one patient with metastatic lymph nodes in the overall cohort of 403 patients, the NNT, is 25. When ROSE would provide immediate final diagnosis to prove malignant origin of the target lesion during NB, this would allow selecting only lung cancer patients for EBUS staging in the NB session, the NNT is 10. Details of the NNT calculations can be found in the Supplementary data, Table A1.

Table 2: The sensitivity, specificity, PPV, and NPV of PET/CT imaging in the cohort of patients who received a navigation bronchoscopy and EBUS, irrespective of pathology outcome. ¹ Twelve lung cancer patients and one lymph nodal involvement of metastatic disease from colon cancer. ² One false-positive lymph node.

Accuracy of Nodal Imaging in Navigation Bronchoscopy Patients			
All NB + EBUS patients (n = 327)	EBUS outcome		
	cN+	cN-	Total
iN+	13 ¹	111	124
iN–	1 ²	202	203
Total	14	313	327
Sensitivity	13/(13 + 1)		92.9%
Specificity	202/(111 + 202)		64.5%
PPV	13/(13 + 111)		10.5%
NPV	202/(1 + 202)		99.5%
Overall accuracy	(13 + 202)/327		65.7%
NNT overall			25
NNT iN+ subgroup			10
NNT iN– subgroup			∞

EBUS, endobronchial ultrasound; NB, navigation bronchoscopy; NNT, number needed to treat; NPV, negative predictive value; PPV, Positive Predictive value.

5.4.2 EBUS in the cohort of navigation bronchoscopy Patients with imaging-positive lymph nodes

In total, 138 out of 403 patients were found to have any imaging-positive lymph node finding (34.2%). EBUS was performed in 124 out of these 138 patients (89.9%) and detected lymph node malignancy in 12 lung cancer patients and in 1 patient with colon cancer. Eight out of twelve lung cancer patients had a nodule < 30 mm (66.7%).

In this iN+ subgroup, 42 patients (30.4%) were treated surgically. Upon resection, an additional 9 patients with pN+ disease were found, totaling 21 patients with lymph node metastases (Figure 2). In 6 of these 9 patients, surgery was performed within 6 weeks after NB and none received neoadjuvant treatment (Supplementary data, Table A2). A more detailed analysis of these patients showed that in only one case this nodal involvement was found in a region outside the reach of EBUS.

The NNT for EBUS to find one patient with metastatic lymph nodes in this sub-cohort was 10 patients. If ROSE would provide sufficient evidence to prove malignant cells during NB and this would allow selecting only lung cancer patients for EBUS staging in the NB session, the NNT would become four patients.

5.4.3 EBUS in the cohort of navigation bronchoscopy patients with imaging-negative lymph nodes

A total of 265 out of 403 patients had imaging-negative lymph nodes (65.8%). Herein, EBUS was performed in 203 patients (76.6%) and detected one (false positive) metastatic lymph node. In this case, the pathology report stated that few atypical cells were found, resulting in a multidisciplinary team decision of lymph node metastases (cN1). However, upon surgery no metastatic disease was found (pN0) in this or any other lymph node, thus classifying it as a false positive. No lymph node metastases were found by EBUS in the remainder of the cohort. In a sub-cohort of 73 imaging-negative patients with confirmed lung cancer that also received surgery (27.5%), eight patients were, however, diagnosed with occult metastases after surgery (10.9%, Figure 3). In six of these eight patients, surgery was performed within 6 weeks; none received neoadjuvant treatment and in only one case the nodal involvement was found in a region outside the reach of EBUS (Supplementary data, Table A2).

5.4.4 Surgically verified EBUS performance

Surgery was performed in 115 patients (Figures 2 and 3, Tables 1 and 3). In eight lung cancer patients that proceeded to surgery without having performed EBUS — imaging negative (six patients) as well as imaging positive (two patients) — no lymph node metastases were found.

Of the 107 lung cancer patients who underwent surgery after systematic EBUS upon NB, 18 patients (16.8%) were upstaged. One patient was upstaged from cN1 after EBUS to pN2 after surgery, and 17 patients were upstaged from cN0 to pN+ (15.9%).

The ultrasound-based size of all 1377 lymph nodes evaluated by EBUS and aspirated by TBNA and the pathological outcome of EBUS and surgery are listed in Table 3. In the patients undergoing surgery, a total of 34 lymph nodes were involved, of which 12 were inaccessible by EBUS (35.3%), see Table 3. Final cytology revealed insufficient sampling in 99 out of 360 sampled lymph nodes (27.5%), but none of these lymph nodes were found to contain metastases after surgery. Detailed analysis on nodal imaging per patient as compared to EBUS and surgical findings can be found in Supplementary data, Table A3.

Table 3: EBUS and surgery outcomes: average lymph node size per region, number of times a lymph node was sampled and the pathological outcome per lymph node station after EBUS and after surgery in all patients referred for NB. In multiple patients, more than 1 lymph node was found to contain metastatic cells. * Station 11Ri and 11Rs are separately indicated in EBUS reports, but not separately evaluated in the pathology report of surgically removed tissue.

Lymph Node Station (#)	2L	4L	10L	11L	≥12L	3	5	6	7	8	9	2R	4R	10R	11Ri	11Rs	≥12R	Total
Number of times reported and measured, <i>n</i>	7	239	12	218	0	0	0	0	253	0	0	14	235	53	145	201	0	1377
Average short axis on EBUS (mm)	3.60	4.40	5.05	5.35	-	-	-	-	6.20	-	-	4.90	4.95	4.60	5.30	5.40	-	5.10
Number of times sampled, <i>n</i>	0	41	2	64					83			5	59	6	29	71		360
Benign, <i>n</i>	0	20	2	41					66			3	41	2	22	45		242
Insufficient specimen, <i>n</i>	0	16	0	22					16			2	13	3	6	21		99
Malignant, <i>n</i>	0	5	0	1					1			0	5	1	1	5		19
Malignant after surgery (pN+), <i>n</i>	0	1	0	3	5	0	0	1	3	1	0	1	4	4	5*	6		34

5.5 Discussion

This single-center study evaluated the added value of EBUS in a not further selected, new cohort of patients with peripheral pulmonary nodules, referred for diagnostic navigation bronchoscopy at a tertiary referral center. When following guidelines strictly, a staging EBUS would not have been indicated in 64.7% of the patients based on imaging. Of the 403 included patients who underwent an NB, 327 patients also underwent an EBUS procedure (81.1%) immediately. Only 12 of these patients were diagnosed with lymph node metastases by EBUS, all of whom had positive lymph nodes on [^{18}F]FDG-PET or ceCT imaging (iN+) based on routine clinical reporting. No true metastatic lymph nodes were detected by EBUS in patients with negative imaging (iN-). Surgery however detected another 17 patients (34 lymph nodes) with metastatic disease in both iN+ and iN- patients, of which 35.3% of lymph nodes were inaccessible by EBUS or EUSb.

To assess EBUS effectiveness, the NNT was calculated. In the overall dataset of this study where EBUS had been performed after NB, 25 procedures were required to identify 1 patient with lymph node metastases. A patient stratification scenario where EBUS is limited to only those with positive imaging would have reduced the NNT to 10 patients, without missing any metastases. By performing EBUS only in patients with imaging-positive lymph node findings (based on a [^{18}F]FDG-PET and/or ceCT scan), 65.8% of EBUS procedures could be omitted without missing metastatic disease that would have been found by EBUS in this cohort.

5.5.1 Accuracy of Imaging to Predict Lymph Node Involvement as Found by EBUS and/or Surgery

In this study, lymph nodes were scored imaging positive when any [^{18}F]FDG uptake was reported in the lymph nodes in the thorax in the routine clinical report. Other methods often use central reading by highly specialized radiologists or specified definitions like a signal larger than the background or a maximal standardized uptake value (SUV_{max}) ≥ 2.5 . A large Cochrane meta-analysis by Schmidt-Hansen et al. (2014) found that in normal sized lymph nodes the sensitivity of [^{18}F]FDG-PET based on activity higher than background, $\text{SUV}_{\text{max}} \geq 2.5$ or 'other methods' was 77.4%, 81.3% and 68.0%, respectively, but that the different studies showed a considerable variance hampering interpretation of [^{18}F]FDG-PET accuracy.[128] In our study we relied on the original clinical report only, to maximize the potential of our findings to be generalized to other hospitals. In a meta-analysis by Wu et al. (2013) the diagnostic accuracy for staging by ceCT was investigated, comparing this to [^{18}F]FDG-PET/CT. In a subgroup of six studies of 806 patients where lymph nodes

were assessed by ceCT they report a sensitivity of 74.0%.[129] We found a similar sensitivity of 72.4% in our subgroup of lung cancer patients with a confirmational EBUS and/or surgery (Supplementary data, Table A3). In our study, when we retrospectively selected the subgroup of lung cancer patients, [¹⁸F]FDG-PET and ceCT imaging had an accuracy of 68.9% in detecting nodal involvement, but more importantly, the NPV was 95.0% (Supplementary data, Table A3). We agree with Wu et al. that [¹⁸F]FDG-PET is most likely more sensitive in detecting lymph node metastases than conventional CT alone.

5.5.2 Accuracy of Imaging to Predict if EBUS Will Detect Lymph Node Involvement

A recently published study by Serra Mitja et al. (2024) determined the performance of EBUS-TBNA for mediastinal staging of centrally located T1N0M0 NSCLC.[101] They report an NPV of 98% for EBUS-TBNA and calculated an NNT of 31 patients for the total cohort and 21 patients when only upper lobe tumors are included. They, however, only included T1 patients, and while they took [¹⁸F]FDG-PET imaging into account, their scoring did not account for [¹⁸F]FDG-PET-negative lymph nodes that were enlarged on ceCT imaging. In our cohort, we calculated an NNT of 10 in the cohort of patients with imaging-positive lymph nodes, and in theory even to 4 when primary lung cancer patients can be identified and discriminated malignancy from metastatic disease by ROSE.[130] An important difference to Serra Mitja's study is that our population has peripherally located lesions. However, when hilar node involvement is proven, this may nowadays translate into applying neo-adjuvant chemo-immunotherapy treatment. We, therefore, advocate using both [¹⁸F]FDG-PET and ceCT characteristics to select patients for EBUS staging.

We have found that all patients with metastatic disease diagnosed by EBUS also had imaging-positive lymph nodes as found on [¹⁸F]FDG-PET and/or ceCT imaging (excluding a false positive case). This correlation was also described by Chen et al. (2022), who describe that maximal standardized uptake value (SUV_{max}) of the lymph nodes was an independent predictor of higher diagnostic accuracy of ROSE in EBUS-TBNA in patients with NSCLC with malignant mediastinal lymph nodes.[131] The sensitivity of 92.9% and NPV of 99.5% of imaging as seen in the presented data suggest that [¹⁸F]FDG-PET and ceCT could potentially rule out patients in whom EBUS would not detect metastatic disease. However, as the positive predictive value of imaging in our cohort is relatively low (10.5%), it needs to be emphasized that further (minimally invasive) staging remains required to confirm locoregional metastatic disease.

5.5.3 Strengths and Limitations

While this was a single center cohort study, our center was the only center performing navigation bronchoscopies in the Netherlands during the included time frame. This cohort, therefore, most likely represents a more general, but pre-selected population of patients eligible for navigation procedures. We must emphasize that in the Netherlands we do not (yet) have a lung cancer screening program, so our patients had incidental nodules or were detected during evaluation or follow-up of other primary cancers. This may also explain our finding of almost 20% synchronous malignancies in the nodule pathology.

One of the strengths of our study is that we did not perform a central review of all [^{18}F]FDG-PET and CT scans to assess imaging N-status for all patients but relied on routine imaging reports. By doing so, we believe that our analysis provides a real-world outcome, but this could also have added more variability. However, when assessing [^{18}F]FDG-PET imaging, we focused solely on the [^{18}F]FDG uptake in the lymph nodes without considering or adjusting it based on the uptake in the nodule(s), but the physician performing EBUS did use this information when deciding to proceed or refrain from EBUS immediately following NB. As a result, we cannot investigate a possible correlation between the [^{18}F]FDG uptake in the primary lesion and the lymph nodes in our cohort, so, as de Leyn et al. state in their guideline, this relation should be taken into account when evaluating nodal involvement on imaging.[121]

Another possible bias concerning the performance of EBUS staging is the fact that the endoscopist is not blinded for both the imaging status and the onsite ROSE results of the nodule(s) and/or lymph node aspirations, which may have influenced the decision to perform EBUS or the decision to continue performing EBUS-TBNA or not.[17] There is a possibility that the metastases found during surgery could have been found by EBUS if the endoscopist would not have taken the imaging into account. Nonetheless, performing an EBUS in imaging-negative patients does not seem to provide upstaging and could in our view be omitted in this cohort.

5.5.4 Guidelines and Unexpected Nodal Disease

Current lung cancer staging guidelines do not recommend routine use of EBUS staging for nodules < 30 mm.[121, 126] While EBUS can be easily combined with an NB in one procedure, the added time and resources raise the question if EBUS can be omitted in certain cases without compromising staging accuracy. Our cohort of patients referred for a primary NB is preselected to exclude patients with high risk of mediastinal or clear hilar metastatic disease and have a median lesion size

of 17 mm (85.9% had a lesion of < 30 mm). Apart from one false positive lymph node in the iN– cohort, all 12 patients that were diagnosed with metastatic lung cancer through EBUS had imaging-positive lymph nodes. This implies that [¹⁸F]FDG-PET and ceCT imaging information of lymph node involvement in this cohort of patients can be used for determining the necessity of an EBUS procedure rather than using lesion size alone, in a navigation bronchoscopy cohort. Performing EBUS in patients with [¹⁸F]FDG-avid lymph nodes, regardless of size, as can be concluded from the results of this study as well, is still according to the guidelines by the ACCP and ESTS.[121, 122]

Systematic EBUS and EUSb staging in this preselected group could not detect lymph node involvement in 17 patients diagnosed with lung cancer (7.0%) but were detected upon surgery in both the imaging-positive and image-negative group. This aligns with the reported upstaging rates of 6% to 26.7% as found in other studies.[69, 132-134] Interestingly, in most of these cases (88%), the involved lymph nodes were theoretically accessible for EBUS and/or EUSb (Table 3). Additionally, the sensitivity of EBUS in this cohort of patients is lower than reported in prior EBUS studies and is only 44.4% when looking at these EBUS accessible lymph nodes and 54.5% when these patients had surgery within 6 weeks after NB (Table A2). This difference can, however, be explained by fact that our cohort is selected to have a low prevalence of nodal disease and cannot be compared to prior studies evaluating EBUS performance in a more general population including many more patients with advanced disease.[21, 121]

5.6 Conclusions

This single-center study demonstrates that the decision to add systemic EBUS staging to a navigation bronchoscopy procedure in patients with peripheral nodules (median size, 17 mm) can be based on [¹⁸F]FDG-PET or ceCT imaging of the lymph nodes. In our cohort, 81.1% of patients underwent EBUS, yet lymph node metastases were only detected by EBUS in those with imaging-positive nodes, with no true positive findings in imaging-negative cases. These findings suggest that EBUS could be omitted in patients with recent imaging-negative lymph nodes without missing metastases detectable by EBUS. This would reduce the NNT from 25 to 10 patients.

5.7 Supplementary data

NNT calculation details

$$\text{NNT} = \frac{1}{\text{CER} - \text{EER}} \quad (1)$$

NNT was calculated as 1/absolute risk reduction (ARR), where ARR is control event rate (CER) minus experimental event rate (EER). In our case, CER is the rate of N+ disease after surgical resection when all patients had undergone resection without an EBUS procedure, and EER is the rate of pN+ disease in patients undergoing resection after EBUS. See Table A1 for the NNT calculations of all NNT given in this chapter.

EBUS performance analysis

A supplementary analysis was performed to assess the performance of EBUS as compared to surgical staging in the population with proven lung cancer patients ($n = 118$). Patients with cytologically confirmed lymph nodal involvement by EBUS ($n = 12$) and all patients with surgical staging are included.

Surgical staging revealed lymph nodal involvement in 18 patients and confirmed a pN0-status in 89 patients. One iN+ patient was diagnosed with N1 involvement after EBUS and was revealed to have pN2 after surgery. In the iN+ subgroup, upstaging to pN2 disease was found in five patients with cN0, and upstaging to pN1 disease was found in four patients. In the iN+ subgroup, upstaging to pN2 disease was found in two patients with cN0 and upstaging to pN1 disease was found in six patients. In one case, downstaging was observed from a single case of atypia, which turned out to be a false positive EBUS outcome. Lymph node regions 5, 6, and 12+ were defined as not accessible for EBUS. Details are summarized in Table A2.

Imaging performance analysis for all EBUS and surgery patients

A supplementary analysis was performed where the performance of imaging by PET or CT contrast (within 6 weeks before NB) was determined based on all patients with available EBUS data irrespective of the final diagnosis of the peripheral pulmonary nodule combined with patients that did not undergo EBUS but were staged with surgery ($n = 251$). Details are summarized in Table A3.

Table A1: The NNT calculations of all NNT given in this chapter calculated according to the formula given in (1).

Calculation of Number of EBUS Procedures Needed During NB to Prevent One Unexpected pN+ Disease During Surgery as Stated in Table 3, Numbers Derived from Figures 2 and 3.		
NNT (all patients)	$\frac{1}{\frac{n = cN^+ \text{ or } pN^+}{all\ NB + EBUS} - \frac{n = unexpected\ pN^+}{all\ NB + EBUS}}$	$\frac{1}{\frac{30}{327} - \frac{17}{327}}$
	$\frac{1}{\frac{4+5+3+5+4+6+2+1^\alpha}{124+203} - \frac{5+4+6+2}{124+203}}$ $^\alpha$ one lymph node metastases from a colon cancer metastasis in the lung	$\frac{1}{\frac{22}{126} - \frac{9}{126}} = 9.7$
NNT (iN+ subgroup)	$\frac{1}{\frac{n = iN^+ \text{ with } cN^+ \text{ or } pN^+}{n = iN^+ NB + EBUS} - \frac{n = iN^+ unexpected\ pN^+}{n = iN^+ NB + EBUS}}$	$\frac{1}{\frac{22}{126} - \frac{9}{126}} = 9.7$
	$\frac{1}{\frac{4+5+3+5+4+1^\alpha}{126} - \frac{5+4}{126}}$ $^\alpha$ one lymph node metastases from a colon cancer metastasis in the lung	
NNT (iN+-sub-group)	$\frac{1}{\frac{n = iN^- \text{ with } cN^+ \text{ or } pN^+}{n = iN^- NB + EBUS} - \frac{n = iN^- unexpected\ pN^+}{n = iN^- NB + EBUS}}$	$\frac{1}{\frac{8}{201} - \frac{8}{201}} = \infty$
	$\frac{1}{\frac{0^\beta + 6 + 2}{201} - \frac{6 + 2}{201}}$ $^\beta$ The false negative lymph node is not taken into account	
Calculation of number of EBUS procedures needed during NB to prevent one unexpected pN+ disease during surgery, in the subgroup of proven lung cancer patients only, as stated in online Table A2, numbers derived from Figures 2 and 3.		
NNT after final diagnosis (lung cancer patients)	$\frac{1}{\frac{n = cN^+ \text{ or } pN^+ (LC)}{all\ NB + EBUS (LC)} - \frac{n = unexpected\ pN^+ (LC)}{all\ NB + EBUS (LC)}}$	$\frac{1}{\frac{29}{118} - \frac{17}{118}} = 9.8$
	$\frac{1}{\frac{4+5+3+5+4+6+2}{4+5+3+5+4+30+59+6+2} - \frac{5+4+6+2}{4+5+3+5+4+30+59+6+2}}$	
NNT after final diagnosis (iN+ lung cancer patients)	$\frac{1}{\frac{n = iN^+ \text{ with } cN^+ \text{ or } pN^+ (LC)}{n = iN^+ NB + EBUS (LC)} - \frac{n = iN^+ unexpected\ pN^+ (LC)}{n = iN^+ NB + EBUS (LC)}}$	$\frac{1}{\frac{21}{51} - \frac{9}{51}} = 4.3$
	$\frac{1}{\frac{4+5+3+5+4}{4+5+3+5+4+30} - \frac{5+4}{4+5+3+5+4+30}}$	

EBUS, Endobronchial Ultrasound; NB, Navigation Bronchoscopy; NNT, Number Needed to Treat.

Table A2: The sensitivity, specificity, PPV, and NPV of EBUS in the cohort of lung cancer patients with cytologically confirmed N-status by EBUS or pN-status confirmed by surgery. ^a One false-positive lymph node (atypical cells in pathology, MDT decision cN1). ^b In two patients, only micrometastases were found in station 12, which is inaccessible by EBUS. Additional calculations were performed by excluding patients with nodal involvement in EBUS inaccessible regions. ^c In six patients, surgery was performed after more than 6 weeks due to comorbidities, neo-adjuvant treatment, or treatments of synchronous cancers. In this subgroup, pulmonary surgery was performed 47 to 136 days after the NB + EBUS, and they were, therefore, left out of this secondary analysis.

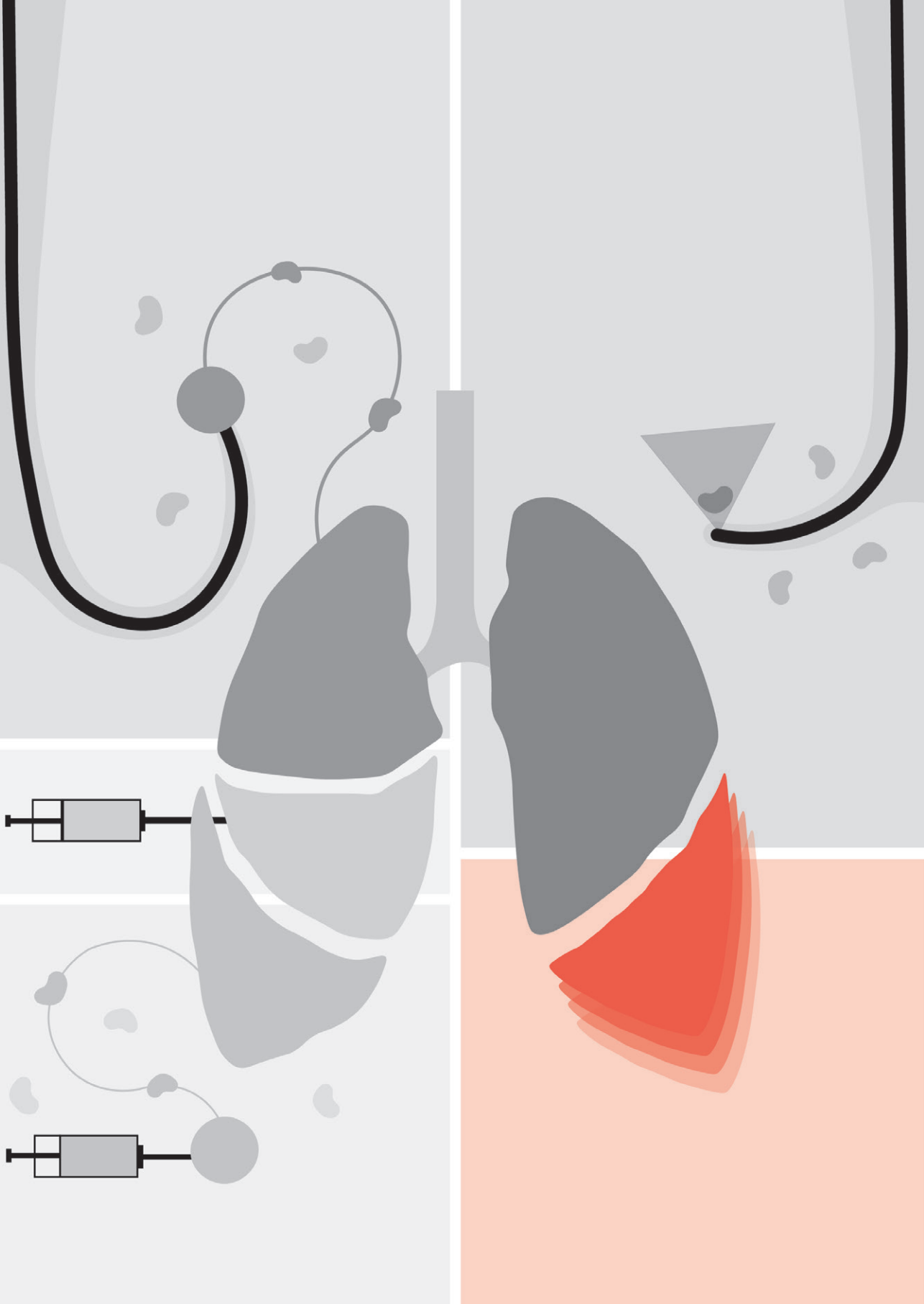
Accuracy of EBUS in Surgically Treated cN0 Lung Cancer Patients			
Lung cancer patient subgroup: NB+EBUS with surgical confirmation (<i>n</i> = 118)	Pathology N-status		
	pN+	pN-	Total
EBUS N+	12	1 ^a	13
EBUS N-, all (accessible ^b)	17 (15)	88	105
EBUS N-, surgery < 6w after NB (accessible ^b) ^c	12 (10)	61	
Total	29	89	118
Sensitivity (all)	12/(12 + 17)		41.4%
Sensitivity (EBUS accessible)	12/(12 + 15)		44.4%
Sensitivity (surgery < 6w after NB)	12/(12 + 12)		50.0%
Sensitivity (surgery < 6w after NB + EBUS accessible)	12/(12 + 10)		54.5%
Specificity (all)	88/(1 + 88)		98.9%
Specificity (surgery < 6w after NB)	61/(1 + 61)		98.4%
PPV	12/(12 + 1)		92.3%
NPV (all)	88/(17 + 88)		83.8%
NPV (EBUS accessible)	88/(15 + 88)		85.4%
NPV (surgery < 6w after NB)	61/(12 + 61)		83.6%
NPV (surgery < 6w after NB + EBUS accessible)	61/(10 + 61)		85.9%
Overall accuracy	(12 + 88)/118		84.7%
NNT overall			10
NNT iN+ subgroup			4
NNT iN- subgroup			∞

EBUS, Endobronchial Ultrasound; NB, Navigation Bronchoscopy; NNT, Number Needed to Treat; NPV, Negative Predictive Value; PPV, Positive Predictive value

Table A3: The sensitivity, specificity, PPV, and NPV of PET/CT imaging in the cohort of lung cancer patients who have a pN status confirmed by either EBUS or surgery.

Accuracy of Nodal Imaging in Patients for Lymph Nodal Involvement; EBUS and Surgical Staging Combined			
Imaging status of all lung cancer patients with EBUS and/or surgery (<i>n</i> = 251)	N-status (EBUS + surgery)		
	N+	N-	Total
iN+	21	70	91
iN-	8	152	160
Total	29	222	251
Sensitivity	21/(21 + 8)		72.4%
Specificity	199/(199 + 107)		68.5%
PPV	21/(21 + 70)		23.1%
NPV	152/(8 + 152)		95.0%
Overall accuracy	(21 + 152)/251		68.9%

EBUS, Endobronchial Ultrasound; NPV, Negative Predictive Value; PPV, Positive Predictive value.



Chapter 6

Diagnostic Challenges in a Cohort of Screen-detected Nodules Referred for Navigation Bronchoscopy: prevalence of second primary disease

Desi K.M. ter Woerds, Roel L.J. Verhoeven, Erik H.J.G. Aarntzen, Shoko Vos,
Ad F.T.M. Verhagen and Erik H.F.M. van der Heijden

Submitted

6.1 Abstract

Background: Currently, in early-stage lung cancer, often multiple nodules are present upon presentation, or a second lung lesion develops during follow-up. The nature of this lesion has profound impact on therapeutic options. We set out to assess the need of repeated (minimally invasive) diagnosis and treatment procedures by determining the incidence of second primary lung cancer (SPLC) and recurrence in our navigation bronchoscopy (NB) program for incidental pulmonary lesions.

Methods: We retrospectively reviewed reports of patients referred for NB and diagnosed with early-stage lung cancer between December 2017 and May 2021. Classification of synchronous, metachronous SPLC, or recurrent disease were based on molecular analysis or pathology-based MDT decisions.

Results: In our population of patients referred for NB, 188 patients were diagnosed as (early-stage) lung cancer. Twenty-four percent had a history of lung cancer upon referral for NB. In total, in 40.4% of the patients a new lung lesion that required additional diagnosis and treatment was found. These could be classified as metachronous SPLC in 26% and recurrence in 19%. In newly diagnosed patients, 22% developed SPLC or recurrent disease during a median follow-up time of only 3.3 years (range, 0.5–5.8 years).

Conclusion: Our findings demonstrate that in a patient cohort undergoing NB for peripheral pulmonary nodules, 40.4% had SPLC or recurrent disease. Most of these patients had metachronous SPLC, underlining the need to obtain adequate tissue that allows for molecular comparison. In newly diagnosed lung cancer patients 22% needed new procedures which impacts the need for health care facilities.

6.2 Introduction

Lung cancer is the leading cause of mortality from cancer worldwide, with non-small cell lung cancer (NSCLC) representing the majority of cases. Early-stage NSCLC is characterized by small lung tumors without extensive nodal involvement or distant metastases. These early stage cancers frequently do not translate into symptoms and are detected as incidental pulmonary nodules on CT-scans or in lung cancer screening programs.[6] Nowadays these nodules can be safely and accurately diagnosed using image guided navigation bronchoscopy (NB) techniques.[14] However, often, multiple nodules are simultaneously detected and second primary lung cancer (SPLC) may occur in 2.5%–20.8% of newly diagnosed lung malignancies.[135] When multiple pulmonary nodules are present, targeted evaluation is required to determine its origin and the relation between the multiple lesions using genomic and molecular characterization to distinguish metastatic disease from SPLC.[135, 136]

Besides the clinical need to analyze multiple lesions during a single diagnostic procedure, often these patients had prior episodes of cancers or are referred anew for the analysis of newly arisen nodules detected during follow-up. This translates into a need for larger volume of diagnostic capacity in a nodule care center then based on the incidence of detected incidental nodules in screening or routine clinical care.

Although modern imaging technologies like high resolution CT and 2'-deoxy-2'-[¹⁸F]fluorodeoxyglucose ([¹⁸F]FDG) positron emission tomography (PET) imaging are useful, pathological confirmation remains the gold standard. It can not only enable analysis of an earlier tumor but can also confirm eligibility for targeted therapies. The primary challenge lies in the ability to obtain tissue samples in all cases and or nodules to determine their relationship between the different tumors, both over time and when detected simultaneously.

While the risk of recurrence diminishes over time, the risk of developing SPLC remains increased.[47-49] A histologically or clonally distinct tumor that develops in an individual with a previous history of lung cancer is called metachronous SPLC.[46] New lesions are frequently detected during follow-up but are then often treated without analysis of their relative (clonal) relation with prior cancer(s). [50] Subsequently, distinguishing between recurrent disease and metachronous SPLC can be difficult, as both can present similarly on imaging but have distinct implications on prognosis, treatment options and patient counselling. With the

implementation of novel diagnostic methods, such as NB, it has become feasible to obtain a pathology-confirmed diagnosis of newly detected and multiple pulmonary lesions suspected for malignancy, which were previously mostly inaccessible for sampling.[14, 15]

The effect of the high incidence of newly detected pulmonary nodules during follow-up on the future need for diagnostic and therapeutic interventions is largely unknown. Therefore, we aimed to identify the incidence of SPLC and recurrent disease in our cohort of patients referred for diagnostic NB. With this exploration we aim to better prepare for the future needs and capacity of health care resources including the newly developing navigation bronchoscopy programs.

6.3 Methods

Since the start of our NB program at Radboud university medical center in Nijmegen, the Netherlands in December 2017 to June 2021, a registry was built to collect data that allowed patient, lesion as well as follow-up analysis. For this study we focused on patients diagnosed with NSCLC stage I to IIIA (T1a-T4, N0-N1, and M0) during NB and excluded patients diagnosed with SCLC or referred for (repeat) biopsy of known metastatic disease. Follow-up data from patients were retrieved from electronic patient files and from thirty-two referring centers. Tumors were staged according to the eighth edition of the International Association for the Study of Lung Cancer (IASLC) TNM classification system.[124]

All patients provided written informed consent to use their data (Reference No. 2017-3706, 2017-3707 and 2019-5148). Patients were excluded when they had indicated to opt-out of all retrospective research or when they received NB for (re-) biopsy for (molecular) analysis of known stage IV disease. Information on all lung cancer diagnoses – in medical history, during NB and in follow-up – was collected. In case of lack of information on family history of lung cancer, surgery type or surgery outcome, this was categorized as unknown.

6.3.1 Pathological analysis

Synchronous SPLC was defined as the detection of multiple lung tumors that are (suspected) different in origin and have been diagnosed either on the same day through imaging or biopsy or were found in one surgical specimen. Recurrence was defined as a new episode of the same tumor after treatment of curative intent. This includes when recurrent tumor involvement is limited to lymph nodes (based

on cytology, histology, or imaging) without a primary lung lesion (cT0 or cTx), this was classified as recurrent disease. To determine if a second lung tumor was metachronous SPLC or recurrent disease, routine morphology (different tumor type or growth pattern), and routine molecular analysis with additional clonal comparison (on indication) were used to confirm similarity. When these were not available, the MDT decision on synchronous or metachronous SPLC and/or recurrence was used. The Martini and Melamed criteria were separately applied to the collected data to compare outcomes in the case of SPLC and recurrence.[137] These criteria state that a metachronous tumor can be identified if the histology is different (A) or if histology is the same but the interval between cancers was at least 2 years (B) or the second tumor is a carcinoma in situ (ACIS, C) or the second tumor is in a different lobe or lung and is staged N0 and M0 (D).

6.3.2 Data analysis

Categorical variables were expressed as absolute and relative frequencies, while continuous variables were expressed as mean and standard deviation. Non-normally distributed data were summarized using medians and interquartile ranges (IQR). Descriptive analysis, including scatter plots, and statistical analysis were performed using SPSS statistics (Version 29.0, IBM SPSS Statistics for Windows, USA). Differences in continuous variables between groups were analyzed using an independent samples t-test for normally distributed data, and the Mann-Whitney U test for non-normally distributed data. Differences in categorical variables between groups were analyzed using a chi-square test or Fisher's exact test where appropriate. A p-value < 0.05 was considered statistically significant.

6.4 Results

Of the 362 included patients that underwent NB between December 2017 and May 2021, a total of 188 NSCLC patients were included for analysis (Figure 1). In the total group of included patients the mean follow-up time was 3.3 years (range, 0.1–6.3 years) since NB. Baseline characteristics are summarized in Table 1. Forty-five patients (23.9%) had a history of lung cancer upon referral for NB for the analysis of a new lung lesion.

Detailed information on demographic data and treatment of the first lung cancer diagnosis of these patients and patients with one lung cancer diagnosis is summarized in Table 2. Patients who received systemic treatment or best supportive care for early-stage disease had comorbidities, for example other cancer diagnoses.

As expected, patients who developed recurrence after surgery for an initial lung cancer ($n = 13$) were more often diagnosed with pN+ disease ($p = 0.002$) or pN+, R+ and/or PL+ disease ($p = 0.002$) than patients who did not develop recurrence after surgery ($n = 91$; Table 2).

Table 1: Patient and tumor characteristics.

Patient baseline characteristics, all lung cancer patients ($n = 188$)		Frequency
Age at first lung cancer diagnosis, years, median (\pm IQR)		66 (± 14)
Gender, n (%)	Male	96 (51.1%)
	Female	92 (48.9%)
Family history of lung cancer, n (%)	Yes	42 (22.3%)
	No	83 (44.1%)
	Unknown	63 (33.5%)
History of (non-lung) cancer, n (%)		71 (37.8%)
History of lung cancer, n (%)		45 (23.9%)
Smoking history, n (%)	Current	64 (34.0%)
	Former	109 (58.0%)
	Never	15 (8.0%)
Total number of nodules navigated to, n		230
Nodules per patient, n		1.22
Nodule size, mm, median (\pm IQR)		17.4 (± 8.9)
Stage at NB, n (%)	IA	144 (76.6%)
	IB	20 (10.6%)
	IIA	6 (3.2%)
	IIB	16 (8.5%)
	IIIA	2 (1.1%)

NB, navigation bronchoscopy, IQR, interquartile range.

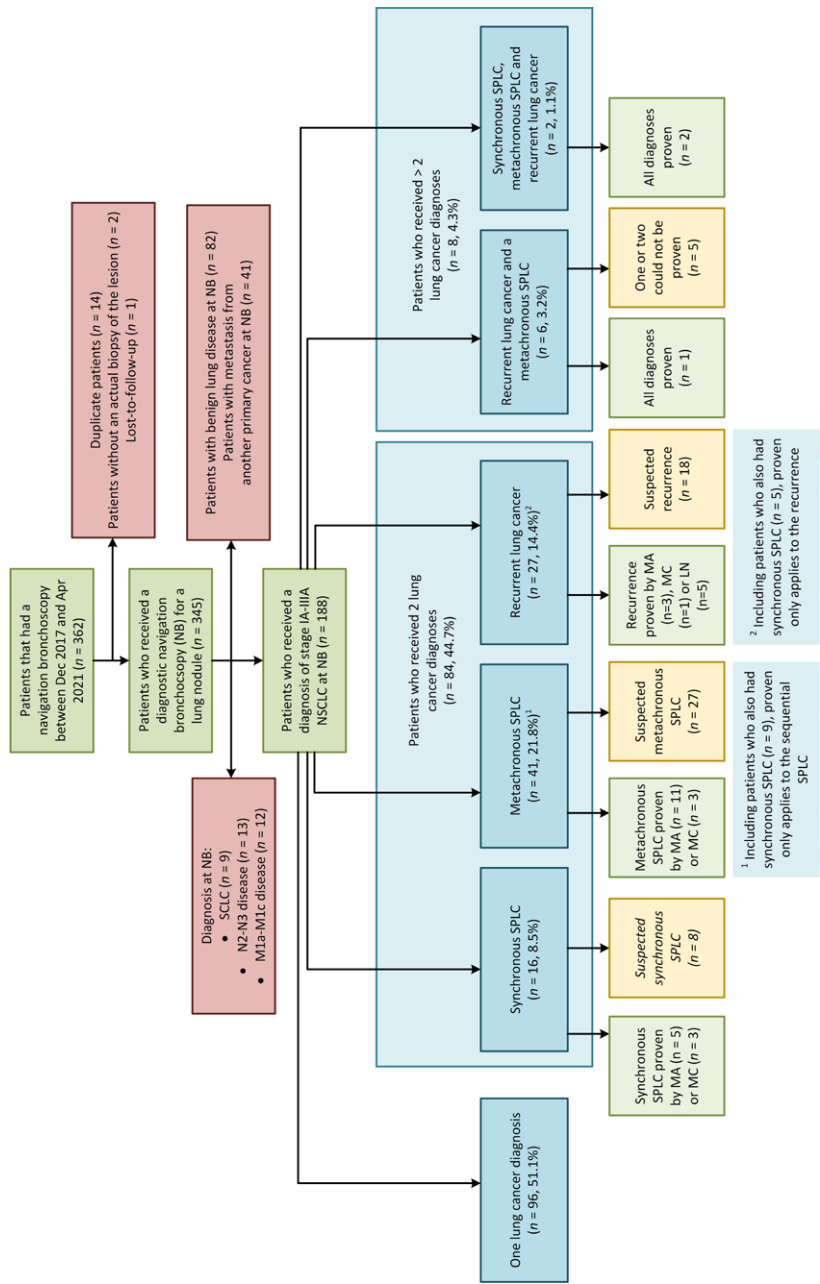


Figure 1: Flowchart of patient inclusion. Frequencies are all relative to patients who received a diagnosis of early-stage lung cancer during NB (n = 188). FU, follow-up, LN, lymph node disease, MA, molecular analysis, MC, morphological characteristics, NB, navigation bronchoscopy, NSCLC, non-small cell lung cancer, SPLC, small cell lung cancer, SPLC, second primary lung cancer.

Table 2: Treatment types of the initial lung tumor when a patient had one diagnosis of lung cancer, synchronous SPLC, metachronous SPLC, or recurrent disease. Patients with multiple episodes (i.e. SPLC and recurrence thereafter) are not included in this table.

Treatment characteristics		Patients with one lung cancer diagnosis (n = 96)	Patients with synchronous SPLC (n = 16)	Patients with metachronous SPLC (n = 32)	Patients with recurrent lung cancer (n = 22)
Age at first diagnosis, years, median (\pm IQR)		67 (\pm 11)	68 (\pm 13)	63 (\pm 12)	65 (\pm 14)
Lung cancer diagnosis before NB, n (%)		0 (0%)	0 (0%)	23 (72%)	8 (36%)
Follow-up available, years, median (\pm IQR)		2.9 (\pm 2.3)	3.8 (\pm 2.5)	6.0 (\pm 4.0)	3.9 (\pm 2.7)
Surgery, n (%)		57 (59%)	10 (63%)	24 (75%)	13 (59%)
Clinical stage distribution of first diagnosis, n (%)	IA	44 (77%)	5 (50%)	15 (63%)	8 (62%)
	IB	5 (9%)	2 (20%)	5 (21%)	4 (31%)
	IIA	2 (4%)	1 (10%)	-	-
	IIB	5 (9%)	2 (20%)	3 (13%)	1 (8%)
	IIIA	1 (2%)	-	1 (4%)	-
Surgery type, n (%)	(R-)VATS	53 (93%)	9 (90%)	18 (75%)	9 (62%)
	Thoracotomy	3 (5%)	1 (10%)	3 (13%)	3 (23%)
	Unknown	1 (2%)	-	3 (13%)	1 (8%)
Extensiveness, n (%)	Segmentectomy	10 (18%)	1 (10%)	-	-
	Lobectomy	46 (81%)	9 (90%)	24 (100%)	13 (100%)
	Bilobectomy	1 (2%)	-	-	-
	pN0	50 (88%)	9 (90%)	21 (88%)	7 (54%)
pN-stage, n (%) [*]	pN1	2 (4%)	1 (10%)	2 (8%)	4 (31%)
	pN2	4 (7%)	-	1 (4%)	2 (15%)
	Unknown	1 (2%)	-	-	-
	pN+, R+ or PL+- stage, n (%) ^{**}	12 (21%)	3 (30%)	4 (17%)	8 (62%)
Adjuvant therapy, n (%)		9 (16%)	4 (40%)	7 (29%)	3 (23%)

Table 2: Continued

Treatment characteristics	Patients with one lung cancer diagnosis (n = 96)	Patients with synchronous SPLC (n = 16)	Patients with metachronous SPLC (n = 32)	Patients with recurrent lung cancer (n = 22)
Radiotherapy, n (%)	33 (34%)	5 (31%)	6 (19%)	9 (41%)
Clinical stage distribution of first diagnosis, n (%)				
IA	30 (91%)	5 (100%)	6 (100%)	6 (67%)
IB	1 (3%)	-	-	2 (22%)
IIA	1 (3%)	-	-	-
IIB	1 (3%)	-	-	1 (11%)
Systemic therapy, n (%)	2 (2%)	1 (6%)	2 (6%)	-
Clinical stage distribution of first diagnosis, n (%)				
IA	-	1 (100%)	1 (50%)	-
IB	1 (50%)	-	-	-
IIA	-	-	-	-
IIB	1 (50%)	-	1 (50%)	-
IIIA	-	-	-	-
Best supportive care, n (%)	4 (4%)	-	-	-
Clinical stage distribution of first diagnosis, n (%)				
IA	3 (75%)	-	-	-
IIA	1 (25%)	-	-	-

* Significant difference in pN+ disease between patients with recurrence (n = 13) and without recurrence (n = 91) who underwent surgery (p = 0.002).

** significant difference in patients with N+, R+ and/or PL+ disease between patients with recurrence (n = 13) and without recurrence (n = 91) who underwent surgery (p = 0.002).

NB, navigation bronchoscopy, IQR, interquartile range, SPLC, second primary lung cancer, (R-)VATS, (robotic) video assisted thorascoscopic surgery.

6.4.1 Incidence of SPLC and recurrence

Of the 188 NSCLC patients, 96 (51.1%) had only one diagnosis of a lung tumor during follow-up (see Figure 1). A total of 32 patients had a diagnosis of two synchronous SPLC (17.0%), 49 patients had a diagnosis of metachronous SPLC (26.1%), and 35 patients had a diagnosis of recurrent disease (18.6%). Some patients received multiple of these diagnoses: nine patients were diagnosed with both synchronous and metachronous SPLC; five patients were diagnosed with synchronous SPLC and recurrent disease; and six patients were diagnosed with metachronous SPLC and recurrent disease of one of the prior lung tumors (3.2%). There were two patients diagnosed with synchronous SPLC, metachronous SPLC and recurrent disease of one of these cancers (1.1%); all proven by molecular analysis. Of the 76% of patients that were diagnosed with lung cancer for the first time during NB, 22% developed metachronous SPLC or recurrence after a median follow-up time of only 3.3 years (range, 0.5–5.8 years) in this subgroup.

6.4.2 Pathological assessment of relationship between multiple diagnoses

Of the 33 diagnoses of synchronous SPLC in 32 patients, a total of 18 diagnoses (54.5%) were based on molecular analysis ($n = 7$, 21.2%) or distinctly different routine morphology ($n = 11$, 33.3%). Of the total 59 diagnoses of metachronous SPLC in 49 patients, 21 diagnoses (35.6%) were based on molecular analysis ($n = 14$, 23.7%) or morphology ($n = 7$, 11.9%). Of the 39 diagnoses of recurrence in 35 patients in this cohort, a total of 15 diagnoses (38.5%) were made based on molecular analysis ($n = 6$, 15.4), morphology assessment ($n = 2$, 5.1%) or based on findings in the lymph nodes without a primary lung lesion ($n = 7$, 17.9%). In the remaining cases without a pathology proven relationship to earlier lung tumors, the relationship of tumors was based on MDT decision who took patient medical history, lung cancer history, presentation, and CT and [^{18}F]FDG-PET imaging features into account in addition to pathology consultation.

6.4.3 Simulation of application of Martini and Melamed criteria in this cohort

When the Martini and Melamed criteria based on time interval and basic-histology would have been applied to distinguish recurrent and second primary lung cancer incidences in this cohort, 14 lung lesions diagnosed as recurrent disease would have been classified as SPLC (from 39 diagnoses to 25 diagnoses) by Martini and Melamed. The other way around, only one lung lesion diagnosed as SPLC was classified as recurrence by the Martini and Melamed criteria (from 33 diagnoses to 32 diagnoses).

6.4.4 Time-interval analysis of patients with proven SPLC versus recurrent disease

For time analysis we excluded patients with more than two lung cancers diagnosed by NB. Thirty-two patients were diagnosed with metachronous SPLC with a mean interval time between first and second primary lung cancer of 3.3 years (range, 0.1–17.1 years, Figure 2). In 22 patients recurrent disease was confirmed after a mean interval time between first diagnosis and recurrence of 1.7 years (range, 0.7–6.1 years, Figure 2). Based on an independent samples T-test ($p = 0.015$), these time intervals are significantly different (Figure 2). When looking at the duration of follow-up between these two groups, the median duration of FU in patients with metachronous SPLC was 6.0 years (range, 1.5–25.5 years) and in patients with recurrence was 3.9 years (range, 1.1–12.0 years) and this was significantly different ($p = 0.045$). However, it should also be noted that 11 out of the 22 patients diagnosed with recurrence died during follow-up and only 8 out of 32 patients with metachronous SPLC, prolonging the follow-up time.

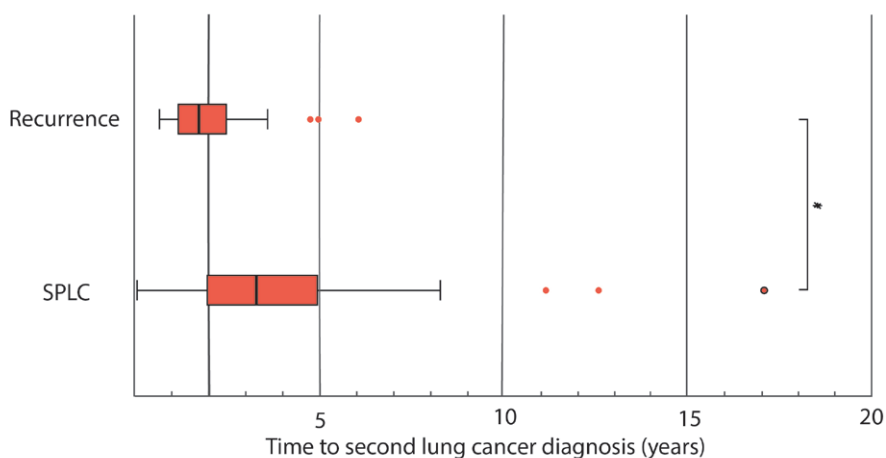


Figure 2: Subgroup analysis of time between initial lung cancer and recurrence ($n = 22$) or metachronous SPLC ($n = 32$). Seven patients with recurrence (31.8%) and twenty-four patients with metachronous SPLC (75%) were diagnosed after 2 years. * $p = 0.015$. SPLC, second primary lung cancer.

6.5 Discussion

In our cohort of patients referred for evaluation of newly detected pulmonary nodules by image-guided NB, we found a high incidence (40.4%) of second lung malignancy, constituting of metachronous SPLC (26%) or recurrent disease (19%). Upon initial presentation 24% of patients had a history of lung cancer. Of the 76% of patients that were diagnosed with lung cancer for the first time during NB, 22% developed new lesions after a median follow-up time of only 3.3 years. These results suggest that this patient cohort has a high need for additional (minimally invasive) diagnostic procedures and subsequent treatments, which has profound implications for the health care capacity and needed volume of NB-programs in the future.

The proportion attributed to recurrent disease of 19% can be considered relatively low compared to literature standards (26% to 45% according to 9th edition of the TNM staging).[1] More of our patients with new nodules were diagnosed as metachronous SPLC (26%). Compared to previous studies that investigated cohorts of patients receiving curative surgical or radiotherapeutic therapy collected between the early 2000's and 2015, our cohort shows a noteworthy increase in this SPLC incidence.[49, 138-144] Chang et al. (2015) reported an incidence in the STARS and ROSEL trial, of only three patients with SPLC (5.2%), either treated with surgery ($n = 2$) or SABR ($n = 1$) and reported a 15.5% recurrence rate after a median follow-up of 3.4 years.[143] Choi et al. (2024) found an incidence of metachronous SPLC of 5.7% amongst a cohort of 8448 patients diagnosed with lung cancer between 1997 and 2006, who were followed through 2018.[49] Fink-Neuboeck et al. (2020) recently reported that among their 342 consecutive surgical patients with NSCLC, 50.3% of patients developed recurrence, while 7.3% was diagnosed with SPLC and 2.3% of patients developed both SPLC and recurrence during 10–16 years follow-up, all proven by immunohistochemical processing.[141] To the best of our knowledge, the highest incidence of metachronous SPLC is documented by Leroy et al. (2019) who saw an incidence of 16.1% in a cohort of 522 surgically treated patients with stage I-III NSCLC with a median follow-up of 4.9 years. All these incidence reports however included patients over 10 years ago. Advanced NB has since become available and implemented in routine practice in many centers around the world, enabling early diagnoses of small peripheral lung nodules. In new referrals, these nodules are found either as incidental findings, or in a screening program, but also, as we show here in 24% of cases, as newly detected lesions during follow-up after initial lung cancer diagnosis and treatment. The incidence found in this study is higher than in earlier reported studies, which may have been influenced by patient

selection, different cohorts, or improved CT-imaging quality and better detection, or changes in type of curative treatment over time. Also, the total number chest CT's and of incidental pulmonary nodules found in these chest CT has been doubled over the last decade, resulting in more stage I lung cancer diagnosis, which changed the overall lung cancer population.[6]

Given the large group of patients that present with multiple or secondary lung lesions, there seems to be an even greater need for extensive tissue acquisition as well as a need for tissue sparing treatments to allow re-intervention. Moreover, the increased incidence of second lung cancer diagnoses, implies that stratification of patient referral is present in this cohort and that the implementation of such a program can have consequences on patient care complexity.

6.5.1 Guidelines on surveillance

International guidelines generally recommended that early-stage lung cancer patients who have undergone curative treatment are followed with regular computed tomography (CT) scans – every 6 months for the first 2 years, and annually for the next 3 years.[145] Our study shows that this specific cohort of patients diagnosed with lung cancer during NB not only has a high incidence of SPLC (of which 25% was diagnosed after 5 years) but also patients diagnosed with recurrent disease even after 5 years. Several other groups have furthermore studied the risk of developing SPLC, revealing that patients with a history of lung cancer seem significantly more prone to developing (new) lung cancer(s) compared to the general population, regardless of smoking history.[49, 139, 142] We would advise to continue CT follow-up in lung cancer survivors after the 5-year-mark, based on our observations. Specifically in countries, like the Netherlands, where no screening program has (yet) been implemented while the chance to develop SPLC does not decrease for these patients.[146] By prolonging surveillance and implementing diagnostic efforts when a lesion is identified, SPLC or recurrence could be diagnosed in an early stage, enabling more (curative) treatment options.

6.5.2 Criteria to identify metachronous SPLC

Recently, van Rossum et al. (2024) reported that in the Netherlands, 66% of patients treated with SABR, did not receive a definitive pathological diagnosis but that diagnosis was based on clinical information only.[50] This lack of pathological confirmation could not only cause overtreatment but also creates challenges in follow-up, as no pathological comparison can be made to determine the relationship between the treated tumor and a newly identified lesion. In our cohort, 54 of 131 multiple lung cancers diagnoses could be confirmed as either

SPLC or recurrence, distinct morphology, or clinical presentation of recurrence in the lymph nodes (41.2%), leaving a considerable proportion of cases reliant on MDT decisions. We have also seen that without molecular information, the relationship of multiple diagnoses of lung cancer differs significantly between MDT decision and the Martini and Melamed criteria, highlighting substantial discrepancies between these methods. Tian et al. (2022) showed that the pooled sensitivity and specificity for distinguishing SPLC and intrapulmonary metastases based on the Martini and Melamed criteria were 78% and 47%.[147] Meanwhile, current guidelines suggest that MDT decisions are a suitable alternative when comparable tumor tissue is unavailable, allowing detailed evaluation of patient and tumor information, [148, 149] tissue confirmation is still the gold standard. Therefore, we strongly recommend obtaining biopsies of all lesions to enable current and future morphological and molecular analysis.

Kaaki et al. (2021) mention that taking biopsies of all lung nodules can be challenging and the quality of the biopsies is of high importance for subsequent pathological and clonal analysis when comparing two lung cancer specimens.[150] Besides a different tumor histology or tumor subtype, all other modalities used to distinguish lung tumors are not necessarily confirmatory but more suggestive and could aid in the MDT decision. However, Chiang et al. (2022) found that histologic interpretation was discordant with next-generation sequencing in 22% of cases.[136] The molecular analyses on small tissue biopsies can be performed but is challenging due to limited amount of DNA.

6.5.3 Strengths and limitations

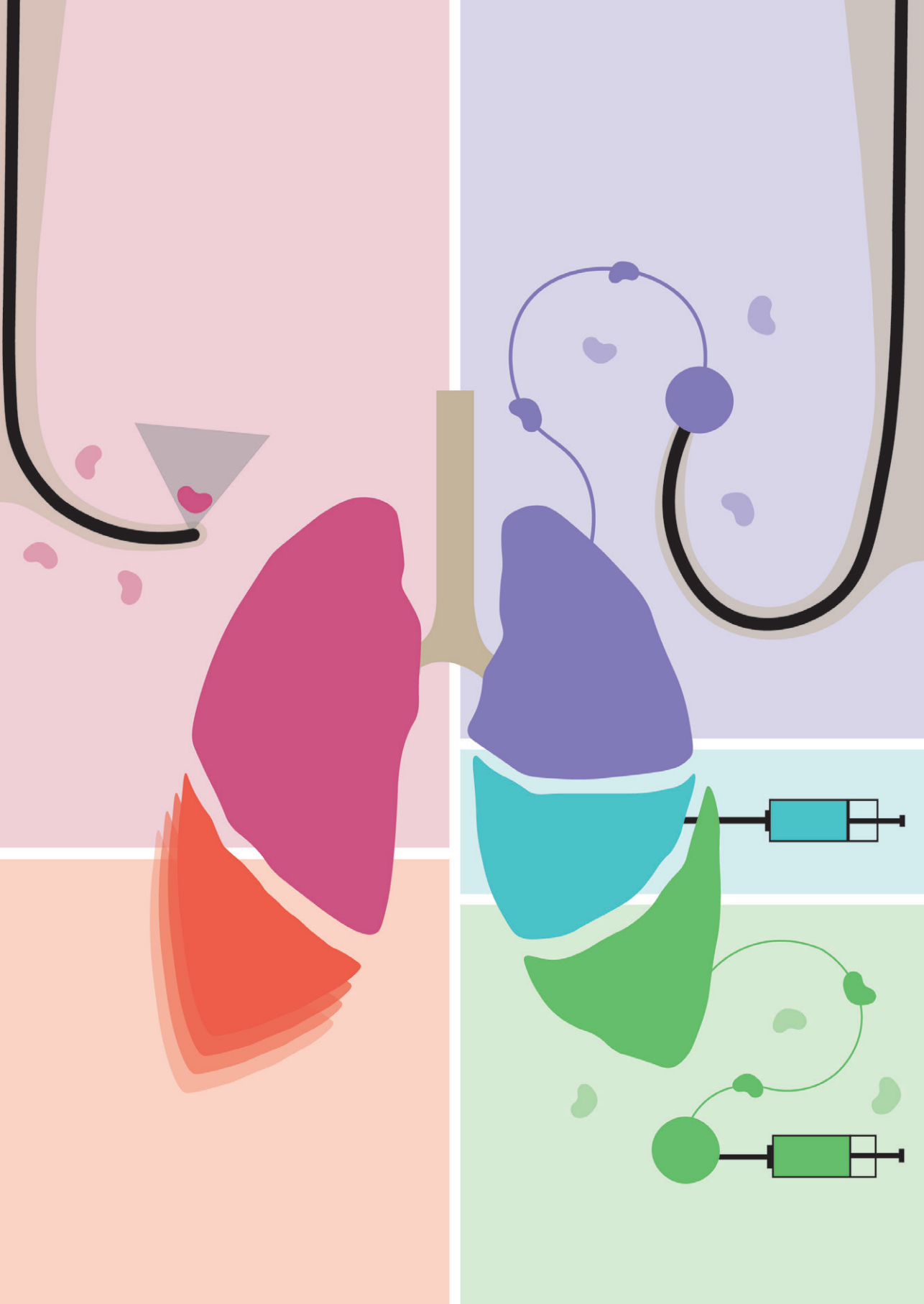
The strength of this study is that we have evaluated all patients referred for analysis of pulmonary nodules and performed a detailed analysis of clinical follow-up in a representative cohort of patients with early-stage lung cancer irrespective of the treatment chosen. This population of patients referred for NB is specific since our (and most) NB program(s) exclude patients with a high suspicion of lymph node involvement thus selecting patients with early-stage lung cancer rather than advanced stage disease.

Patients with a history of lung cancer that develop recurrence could also have tumor manifestations in other organs as the only site of recurrence. These patients will not be referred for NB and this could influence the incidence ratio found here. A potential weakness is that this is a single center cohort from a university reference center, the median follow-up time of 3.3 years for the complete cohort and 3.9 and 6.0 years for the patients with a diagnosis of recurrence and metachronous SPLC,

respectively, is relatively short. Additionally, not all diagnoses were proven by molecular or morphological analysis. Additional metachronous SPLC or recurrent lung cancers, could potentially be identified with a longer follow-up period, further increasing the incidence of SPLC and recurrent disease and defining additional care needs of these patients.

6.6 Conclusions

In this cohort of patients referred for NB, 188 patients were diagnosed with early-stage lung cancer. Of those patients, 40.4% were diagnosed with a second lung lesion, either during NB or after NB. We observed a high incidence of synchronous SPLC ($n = 32$, 17%), metachronous SPLC ($n = 49$, 26%) and a considerable group of patients with recurrent disease ($n = 35$, 19%). A history of lung cancer was present in 24% of patients and of the 76% of patients that were diagnosed with lung cancer for the first time with NB, 22% developed SPLC or recurrence after a median follow-up time of only 3.3 years. This volume of patients has significant implications for healthcare resources including the capacity of emerging navigation programs and comes on top of the volume of newly detected peripheral pulmonary nodules (as incidental findings or in screening programs) and the volume of patients that need a diagnostic NB for benign nodules or repeated biopsy during metastatic disease treatments. Our findings also underline the importance of obtaining extensive tissue sampling to facilitate molecular or morphological analysis to differentiate between SPLC and recurrence. And lastly, since 25% of patients with metachronous SPLC were diagnosed later than 5 years after initial treatment, a continued follow-up beyond the routine 5-year term may be considered to detect recurrent disease and metachronous SPLC in time.



Chapter 7

Summary, general discussion
and future perspectives

7.1 Summary

Early detection of lung cancer is essential to enable curative treatment and improve survival outcomes. The stage of disease is determined by tumor size, dissemination to the lymph nodes and the presence of distant metastases. In early-stage disease, dissemination to the lymph nodes is more detrimental for the prognosis of the patient than tumor size. The lymph nodes are primarily evaluated based on size on CT imaging and [^{18}F]FDG-uptake on PET imaging. Tissue based staging by EBUS-TBNA or cervical mediastinoscopy is performed when guidelines recommend pathological assessment based on imaging features. Despite these extensive staging efforts, 1 in 4 patients is upstaged from clinical N0 (cN0) to pN+ after surgery. Additionally, 1 in 3 stage IB-IIIB lung cancer patients develop second primary lung cancers or are diagnosed with recurrent disease within 3.5 years after treatment with curative intent, which may suggest that disease dissemination remains undetected after surgery. In this thesis, new methodologies and techniques are introduced to improve staging in early-stage lung cancer by focusing on sentinel lymph node analysis (part I). In part II the population of an image-guided navigation bronchoscopy program is analyzed in detail focusing on diagnostic and staging procedures with the aim to further optimize the care of these patients, while making optimal use of our available healthcare resources.

Part I - Feasibility and added value of a sentinel lymph node procedure in lung cancer

The sentinel lymph node (SLN) procedure is a methodology to improve staging and thus optimize recurrence prediction in other cancers by identifying the lymph nodes most at risk of metastases. However, despite initial positive results from other trials, the technical feasibility and added value have not been proven and the SLN procedure has therefore not been adopted in clinical practice in lung cancer care. The SLN procedure can be done by injecting tracers with different characteristics and in Part I of this thesis, several methods are explored.

In **Chapter 2** we performed an *ex vivo* study to investigate a novel method to inject $^{99\text{m}}\text{Tc}$ -ICG-nanocolloid endobronchially and test feasibility of this method in lung cancer specimen using an ultrasound guided device (IVUS Pioneer Plus), originally developed for endovascular use. The aim was to verify this method while allowing us to learn as much as possible to use this approach in an *in vivo* study at a later phase. We were able to successfully inject the tracer using this approach, which allowed us to both visualize the tumor as well as injection in US imaging in real-time. Subsequent SPECT/CT-imaging identified 76.7% of the placed injection

depots individually. The injection with this methodology was assessed to be feasible, allowing us to continue into an *in vivo* study.

Subsequently, in **Chapter 3** this method using the IVUS catheter was investigated in an *in vivo* feasibility study. The primary aim was to identify the SLN using SPECT/CT imaging following endobronchial ^{99m}Tc -nanocolloid injection during a navigation bronchoscopy procedure. We varied the injection location (peri- or intratumorally), injection volume, injection speed and timing and settings of SPECT imaging to increase the identification of SLN. While the procedure proved to be feasible and the methodology allowed us to inject 96.7% of tumors under real-time ultrasound guidance, SLN could only be detected by subsequent SPECT/CT imaging in 32.3% of patients. Additionally, injecting an iodinated contrast agent preceding to ^{99m}Tc -nanocolloid injections visualized that tracer leakage was present in multiple cases. Based on these results we conclude that a ^{99m}Tc -nanocolloid-based SLN procedure is feasible to perform but does not allow for sufficient SLN identification. Future research should investigate alternative imaging methods and tracers.

In **Chapter 4**, we shift focus to evaluate feasibility of an alternative method to identify the SLN during surgery. Here the SLN procedure is investigated using an injection of ICG and NIR imaging for identification. After transpleural or endobronchial injection of ICG, the lung was ventilated, and the lung and lymph nodes were removed according to standard surgical practice. The most fluorescent lymph nodes were subjected to more detailed additional pathological evaluation. The intraoperative SLN procedure proved feasible and SLN were identified in 100% of patients. However, this did not translate in the detection of micro- or macrometastases that would not have been found by conventional pathological analysis.

Part II - Evaluating current diagnostic and staging practices

In Part II of this thesis, a detailed evaluation of diagnostic and staging procedures already embedded in clinical practice was performed. This part aims to identify methods to optimize healthcare utilization, quality, and cost-effectiveness.

When a small peripheral lung nodule is diagnosed by navigation bronchoscopy, a systematic EBUS procedure can easily be performed during the same anesthesia session. The lesion is then not only diagnosed, but in the case of lung cancer, lymph node involvement and therewith staging can be completed in a single visit. When following guidelines, it is however not always mandatory to perform an EBUS in all patients, since most patients referred for a navigation bronchoscopy

are suspected to only have small nodule(s) and no lymph node involvement based on imaging. In **Chapter 5**, we investigated the added value of systematic EBUS in these patients in order to identify patients who would (or specifically would not) benefit from an EBUS during navigation bronchoscopy. Our results suggest that EBUS during navigation bronchoscopy can be safely omitted in all patients when lymph node involvement is absent on (recent) [^{18}F]FDG-PET/CT or ceCT imaging. In our cohort, this would mean that in 65.8% of patients an EBUS procedure could be safely omitted, as no lymph node metastases would not be found by EBUS. The use of imaging to support better selection of patients for a systematic EBUS during navigation bronchoscopy, could enable improved use of (limited) OR-time without compromising staging accuracy reducing the number of EBUS procedures to be performed from 1 in every 25 cases in the unselected cohort to 1 in 10 EBUS procedures in the selected population, without missing a single relevant metastatic case in this population.

In **Chapter 6**, we set out to investigate the incidence of recurrent disease in the population of patients referred for a navigation bronchoscopy procedure. The origin of secondary lung cancer findings in patients referred was analyzed to better estimate the disease burden and need for future diagnostic and therapeutic procedures in this cohort. We therefore aimed to identify the incidence of synchronous SPLC, metachronous SPLC and recurrent disease in this cohort. In this chapter, we report that 40.4% of the patients diagnosed with early-stage lung cancer during navigation bronchoscopy were (also) diagnosed with either metachronous SPLC, recurrent disease or both. Most of our patients with new nodules were diagnosed as metachronous SPLC (26%). We found that a substantial proportion of patients referred for a navigation bronchoscopy (for a new lung lesion), presented with a history of lung cancer (24%). This analysis showed that patients in this cohort often require additional (minimally invasive) diagnostic procedures and subsequent treatment with a mean follow-up period of only 3.3 years. This study also underlines the importance of obtaining extensive histological tissue samples to facilitate clonal analysis and improve differentiation between recurrence and SPLC. Lastly, we recommend continuing follow-up after the currently recommended 5 years, since 25% of patients with metachronous SPLC were diagnosed after 5 years.

7.2 General discussion and future perspectives

The work in this thesis aimed to improve the diagnosis and staging of early-stage lung cancer. Central in part I were the development and assessment of the SLN procedure, by integration of innovative radial ultrasound guided injection and SPECT/CT, NIR and CBCT imaging. Both minimally invasive endobronchial and surgical approaches were evaluated in a real-world clinical setting. Additionally, current practices were evaluated to identify methods to improve healthcare utilization. In this discussion, these findings are placed in the context of current diagnostic and staging approaches, with a glimpse into future directions in lung cancer care.

7.2.1 SLN methodology

Although SLN procedures have shown to be of added value for several cancer types, much work is still needed to decide on the role of the SLN procedure in lung cancer. In the past decades, several groups studied SLN procedures for lung cancer. Many different protocols were reported, but none have been implemented into guidelines or change of daily clinical care. In this thesis we focused on technical feasibility of such procedures with the intent to generate a scientific basis for a standard SLN procedure in lung cancer.

From previous literature on the SLN procedure in breast cancer and melanoma it is known, that there is a discrepancy in the SLN identification rate of these cancers and in the accumulation of radiotracer in the lymph nodes.[70] The lymph nodes have shown to accumulate less than 1% of the injected radioactive dose in breast cancer patients, even after tissue massaging, while in melanoma around 2.1% accumulates.[33] This has not specifically been quantified in lung cancer and could potentially be too little to distinguish the accumulation in the lymph nodes from the injection depots and their dissemination throughout the lung, at the time of imaging. However, the imaging window is limited by the radioactive decay of ^{99m}Tc , which has a half-life of approximately 6 hours. Figure 1 captures the inability to see the lymph nodes where ^{99m}Tc -nanocolloid drains to (in most patients) while we have seen in **Chapter 4** that the SLN was found by ICG in 100% of patients, even at the mediastinal level. It is moreover possible that SPECT imaging resolution was not sufficient to detect the accumulation in the lymph nodes in the middle of the thorax in **Chapter 3**. Compared to *the ex vivo* lung in **Chapter 2**, the complete thorax causes greater attenuation and scatter of gamma radiation, thereby increasing background noise when scanning patients.[151] Imaging the SLN in breast cancer and melanoma is therefore inherently different from lung cancer,

as the lung is a less superficial organ. The intraoperative injection, as performed in **Chapter 4**, allows for direct visualization of the tracer in the lymph nodes at a superficial level. Some limitations are still present in this method, like the leakage of tracer throughout the thorax and the limited penetration depth of NIR but the imaging resolution is high enough to detect the (small) migrated volumes of tracer.

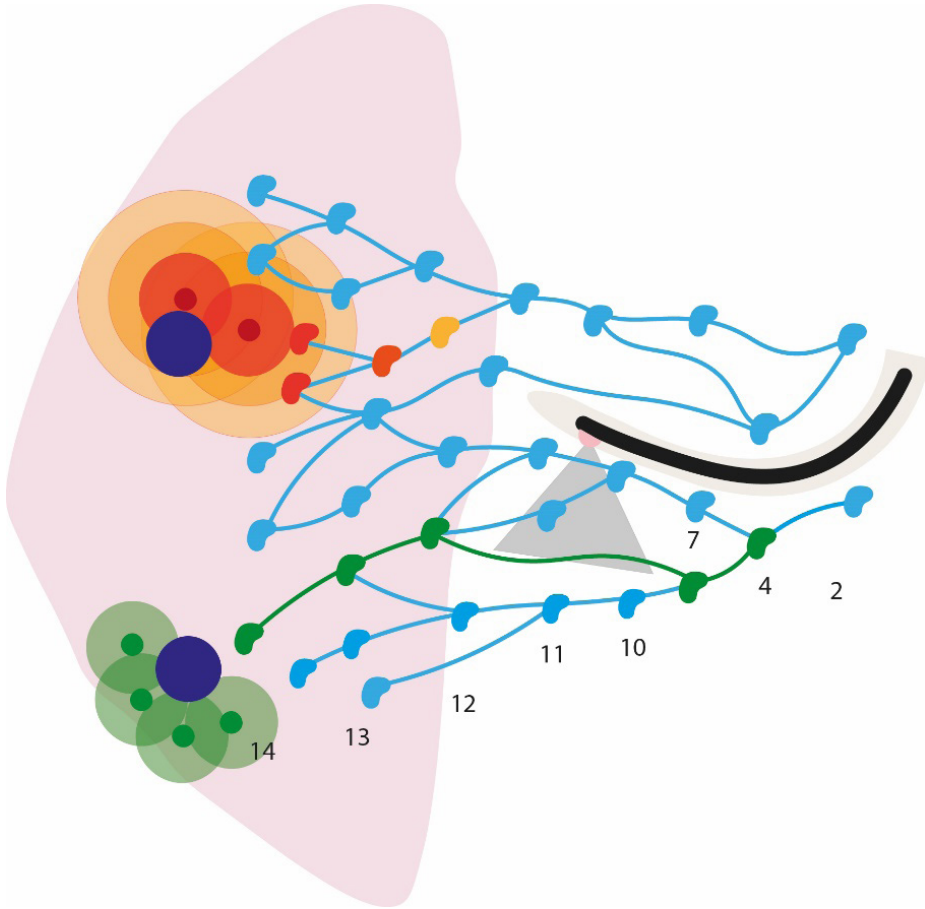


Figure 1: A visualization of a lung lobe with endobronchial injections with ^{99m}Tc -nanocolloid (the upper red dots), pleural injections of ICG (the lower green dots) and the EBUS scope in the bronchus visualizing the lymph nodes on ultrasound. While the image is not anatomically correct, this depiction shows a possible explanation for the phenomenon of 'skip metastases', by the manner in which lymph node(s) (regions) are connected by lymphatic ducts, as depicted by the green flow from the injection.

7.2.2 Anatomical, pathological, and immunological dimensions of SLN evaluation

Patient specific lymphatic drainage patterns

The term skip metastases has been used to refer to a phenomenon in which regional (N1, station 10–12) nodes are spared while distant (N2, station 2–9) nodes are involved. Riquet et al. (1989) were the first to introduce the diverging nature of lymphatic connections, which could take on a different shape compared to the known tree-shape of the bronchi and vessels and can therefore bypass stations.[152] Moreover, apart from a centrally directed lymphatic drainage pattern, a sub pleural drainage route exists, what makes final dissemination unpredictable. A visual representation of skip metastases, albeit not anatomically correct, can be found in Figure 1. While there is no evidence on the exact drainage or formation of metastases, it is likely that the lymphatic ducts are structured in a way that facilitate the phenomenon of skip metastases. Moreover, not only the anatomy of the lymphatic system in the patient, but also the (tumor) microenvironment plays a large role in the drainage or formation of metastases and therewith tracer dissemination.[42, 153] Because this lymphatic drainage pattern differs per patient it is hard to predict the location of the SLN based on high resolution or contrast enhanced CT or even [^{18}F]FDG-PET imaging.[152, 154] If we look at all patients with an accurate injection in Table 3 of **Chapter 4**, we can see that there were multiple lymph nodes from either station 10 and/or 11 of which some were fluorescent (SLN) and some were not fluorescent (enough) and therefore classified as ‘other lymph nodes’. Lymph node metastases were always found in the SLN in this group of patients and this proves that the metastatic cells follow a predictable path that can be recreated by an accurately injected tracer.[155]

Intraoperative SLN procedure to increase detection of metastatic disease

With the rising interest in sublobar resections like segmentectomies an intraoperative SLN procedure to perform a limited lymphadenectomy, has also gained interest. Determining the lymph node(s) where metastases would reside and being able to process the lymph node alongside the removed lung segment could prove essential in minimizing the extent of surgery while ensuring oncological safety.[156, 157] However, the method as described in **Chapter 4** shows that all lymph nodes still have to be removed to determine the hottest lymph node(s) and also shows that usually multiple SLN are detected. This technique offers a relative assessment, not a quantitative measurement. However, **Chapter 4** also shows that, when the hottest lymph nodes were free of tumor cells, all lymph nodes downstream were also free of tumor cells when a complete lymphadenectomy was performed. A very recent study performed by Stasiak et al. (2025) corroborated our observation

in their study involving 106 patients with an identified SLN. Interestingly, in one patient, a single lymph node from station 5 was removed and analyzed, while residual fluorescence in the same region suggested that additional nodes may have been present. No further dissection was performed at that time. This patient later developed a recurrence in station 5, leading researchers to suspect that a lymph node may have been wrongfully left in situ.[112] Our study, along with the findings of Stasiak et al. (2025) suggests that determining which lymph nodes to focus on during pathological evaluation could be a more favorable and potentially time-efficient approach.

The emerging role of lymph nodes for immune therapy

If the SLN procedure can be improved to a point where SLN detection can be done *in vivo* or tracer-uptake can otherwise be quantified, it might also eventually serve as a tool to perform a less extensive lymphadenectomy, specifically in segmentectomies. When a minimal lymphadenectomy can be performed without minimizing staging accuracy, the risks associated with lymph node dissection (bleeding, chylothorax or nerve damage) decrease.[112] Yet, a potentially even more important aspect of minimal lymphadenectomy would be the preservation of immune cells in the lymph nodes in the lung. Several animal studies have demonstrated that the primary site for generation of tumor-specific T lymphocytes are the lymph nodes that drain lymphatic fluid from the tumor. A pre-clinical study performed by Fear et al. (2021) showed that mice with lung cancer and micrometastases survived longer after surgery when their tumor-draining lymph nodes were preserved, compared to those who underwent complete lymphadenectomy.[158] This suggests that lymph node removal impairs anti-tumor response, which could hamper the efficacy of adjuvant immunotherapy, which needs these lymph nodes and the immune cells present there to treat (possibly systemic) disease. This was corroborated by a more recent study in which Deng et al. (2023) found in 144 patients that removal of ≥ 16 lymph nodes significantly decreased the efficacy of immunotherapy. Removal of < 16 lymph nodes was associated with better retention of immunological potential[112, 159] Yet, with these pilot studies having been reported, more research is warranted to further assess if this topic is of value, specifically in the discussion on whether or not to implement the SLN procedure in clinical practice.

7.2.3 Biopsy quality and volume: implications for histopathological evaluation

Added value of pathological evaluation of the lung tumor

In **Chapter 6** we show that the incidence of metachronous SPLC in our navigation bronchoscopy cohort is relatively high compared to other groups. However, only 35.6% was proven based on molecular or detailed morphology analysis. With the rise of neo-adjuvant treatments, more patients might be presented at surgery with a tumor that have already responded to treatment preceding surgery, ideally with a complete pathological response. The original histologic type might not be retrievable from the resected tissue in such cases. When a biopsy of sufficient quality is collected of all suspected lesions before treatment, molecular or morphological analysis becomes available in the future, if patients are diagnosed with a second lung lesion. Subsequently, the incidences of metachronous SPLC or recurrence could be better determined, even in broader populations, better estimating the healthcare resources needed to diagnose and treat these patients. Lastly, sufficient biopsies also enable analysis for criteria to receive immunotherapy, whether that is at the moment of diagnosis or later when the disease has been able to progress under treatment.

Added value of extensive pathological evaluation of lymph nodes

In **Chapter 4** we identified the SLN in all patients (100%) but the additional pathological evaluation of the SLN did not reveal upstaging that would otherwise have been missed, only 2 cases with isolated tumor cells (ITC) were found, no new micro- or macrometastatic disease affecting the final pN-stage. This fortunately means the procedure as performed per clinical practice in the Radboudumc delivers sufficient staging of the lymph nodes after surgery and we found no evidence on possible improvement of pathological assessment by implementation of the SLN procedure. However, in the study performed by Stasiak et al. (2025) several additional micrometastases were found in their cohort of 106 patients by use of cytokeratin AE1/AE3 staining, similar to our protocol in **Chapter 4**. Also other studies have reported upstaging due to micrometastatic disease in as much as 27–45% of lung cancer patients but did not report separately on ITC.[44, 160] There is no conclusive research available on the influence of ITC on the prognosis of lung cancer patients and ITC are therefore not a factor for upstaging in the current guidelines.[44, 53, 108] When future research would reveal that ITC do or do not significantly impact overall or disease free survival, the SLN procedure as performed in **Chapter 4** could be proven to be valuable in predicting recurrence. However, costs and efforts should be taken into account, as the ICG injection and

NIR evaluation do not require much effort, but the additional pathological analysis is labor-intensive and therefore expensive. Defining a patient group most likely to develop (micro-)metastases, would be an interesting aspect of future research on improving lung cancer staging.

7.2.4 Towards local treatment for early-stage NSCLC

If future developments would allow for successful preoperative identification of the SLN, as attempted in **Chapter 3**, this procedure could not only guide targeted pathological evaluation but also aid in optimal (local) treatment strategies. Nowadays curative treatment can be offered by surgery or stereotactic ablative radiotherapy (SABR), but new local treatments like microwave ablation, cryotherapy or pulsed electric field treatment are under investigation in many ongoing studies. Detailed knowledge on the lymph nodes most likely to harbor metastases in patients with specific tumor sizes, stages or other characteristics that warrant additional treatment, could allow for adjustment of radiation planning in these patients.[161] Additionally, the ability to precisely inject an agent could open new avenues for selectively intensifying local treatment potentially alongside systemic (neo)adjuvant therapy.

Intratumoral treatment

In the Netherlands, neoadjuvant immunotherapy has been approved for patients with stage II-III disease and a PD-L1 expression of $> 1\%$.[162] The added value of neoadjuvant chemoimmunotherapy is also becoming more evident and is even highly recommended for patients with resectable stage III.[162, 163] The systemic delivery of chemo- and immunotherapy results in the treatment of the primary tumor as well as (distant) metastasis but can also cause adverse reactions in healthy tissue (i.e., pneumonitis, hepatitis and thyroiditis) with up to 20% of patients experiencing grade 3–4 toxicities.[164, 165] Alternatively, to increase survival while minimizing these immune-related adverse events in the future, neoadjuvant therapy could be delivered locally, into or surrounding the tumor.[166–171] A navigation bronchoscopy procedure, where a catheter is positioned directly at the tumor site, provides an opportunity to not only diagnose the lesion but also directly treat the lung cancer. Apart from imaging and detection of SLN, another important goal of the trial performed in **Chapter 3** was to evaluate the possibility to perform real-time image guided injections. To enable implementation of local treatment in clinical practice, it is important to further study this technique and be able to (better) predict how intratumoral injections behave in the lung. In recent years, several experimental approaches have investigated the local delivery of cytotoxic or immunotherapeutic agents directly into solid tumors, including early-stage lung cancer.[75, 76, 167, 172]

The focus in many of these studies is on the pharmacodynamics of slow and prolonged release of the agent, for which nanoparticles or biodegradable gels have been researched in pre-clinical and clinical settings. Biodegradable gels and nanoparticle carriers have been developed to allow for sustained release of agents over time.[173] For example, cisplatin embedded in thermosensitive hydrogels and paclitaxel bound to polymer-based particles have been tested in early-phase clinical trials and preclinical models, showing good local tolerability and preliminary signs of efficacy.[172, 174-176] These formulations are designed to retain the drug at the injection site and slowly release it, thereby maximizing tumor exposure and limiting systemic toxicity.[166] Although still in a research phase, these techniques offer a highly targeted and minimally invasive treatment strategy.

Image-guided navigation bronchoscopy as a platform to diagnose and treat (one-stop-shop)

Beyond the pharmacological and clinical aspects of local treatment, knowledge on image guidance and precise positioning of injection systems is lacking. In this thesis we investigated a novel device for real-time ultrasound guided endobronchial injection using the Pioneer Plus IVUS catheter and describe its use both *ex vivo* and *in vivo* in **Chapters 2 and 3**, respectively. CBCT-guided navigation bronchoscopy uses 3D-imaging and augmented fluoroscopy for navigation to the lesion and biopsy through pre-curved extended working channels. Augmented fluoroscopy cannot compensate for breathing motion and passive deformation of extended working channels. We illustrate that the addition of ultrasound guidance offers the opportunity of real-time guidance, minute repositioning when needed and image-guided control of injection, which is a key factor for any form of local injection.

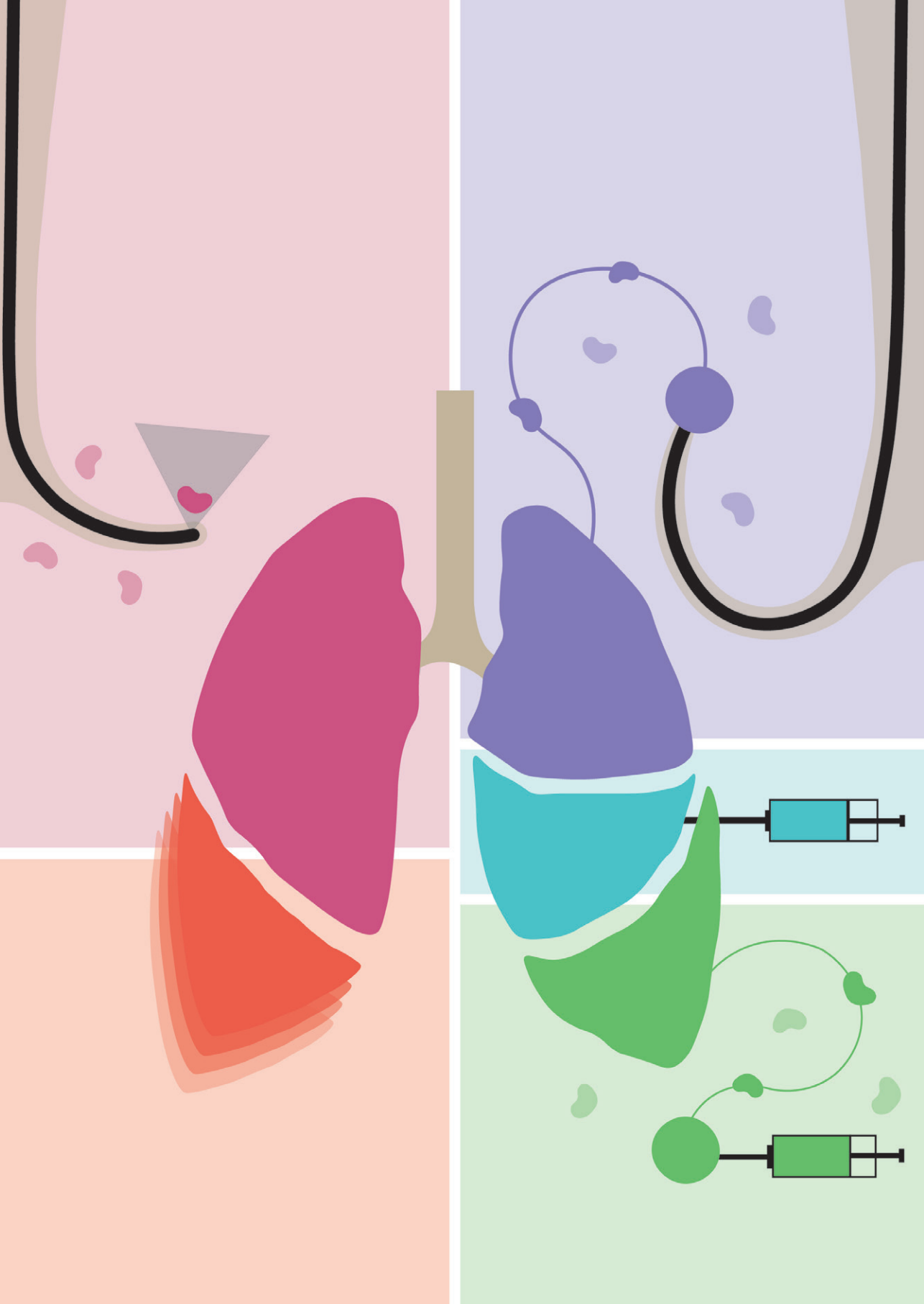
While a navigation bronchoscopy creates an ideal setting to perform intratumoral injection(s), the combination of taking biopsies and injecting a liquid substance in the same procedure could also create some challenges. A small bleeding could for example negatively affect visibility of the target lesion (for both CBCT and ultrasound) and may also affect the ability of the tumor and its environment to retain the injected agent at the desired injection location. We have seen in **Chapter 3** that 38.7% of patients developed a minor (intraparenchymal) bleeding after diagnostic sampling.

Another topic of concern in offering a one-stop-shop for diagnosis and treatment in a single visit is our observation that in our cohort of patients referred for CBCT-NB the number of nodules navigated to is 1.25 per patient (**Chapter 5**) and are often diagnosed with synchronous SPLC that need detailed molecular analysis

which cannot be offered onsite. Very often, not only the treatment of these patients becomes more complex, also the navigation procedure and staging of these patients is more difficult. The growing complexity of navigation procedures and the growing shortage in healthcare personnel warrants exploration of new technological advancements, a more efficient use of time and resources and better selection of patients who are most likely to benefit most from each option. Intratumoral therapies are currently too little explored to be used outside research settings in (early-stage) lung cancer. The combination of diagnosis, staging and treatment as offered in a navigation bronchoscopy setting holds large potential, but requires more research.

Considering the substantial number of patients with SPLC as seen in **Chapter 6**, local treatment will specifically be preferable in patients who underwent multiple surgeries or radiotherapy treatments and for whom further invasive interventions have become technically challenging or clinically undesirable.

In conclusion, this thesis underscores the importance of technological innovations in image guidance, exploring the potential of ultrasound guided real-time injection in small peripheral lesions and investigating sentinel lymph node detection using different tracers and imaging techniques such as SPECT and NIR imaging. It also underlines the importance of multidisciplinary collaboration in the diagnostic work-up of early-stage lung cancer. By addressing key elements in the development of the SLN procedure, lymph node staging and the diagnosis of SPLC, we aimed to enhance diagnostic and staging accuracy and facilitate more personalized staging and treatment strategies for future patients.



References

1. Rami-Porta, R., et al., *The International Association for the Study of Lung Cancer Lung Cancer Staging Project: Proposals for Revision of the TNM Stage Groups in the Forthcoming (Ninth) Edition of the TNM Classification for Lung Cancer*. J Thorac Oncol, 2024. **19**(7): p. 1007-1027.
2. Bray, F., et al., *Global cancer statistics 2022: GLOBOCAN estimates of incidence and mortality worldwide for 36 cancers in 185 countries*. CA Cancer J Clin, 2024. **74**(3): p. 229-263.
3. de Nijs, K., et al., *Medical costs of lung cancer by stage, histology and first-line treatment modality in the Netherlands (2012-2021)*. Eur J Cancer, 2024. **208**: p. 114231.
4. Goldstraw, P., et al., *The IASLC Lung Cancer Staging Project: Proposals for Revision of the TNM Stage Groupings in the Forthcoming (Eighth) Edition of the TNM Classification for Lung Cancer*. Journal of Thoracic Oncology, 2016. **11**(1): p. 39-51.
5. Ferlay, J., et al., *Cancer statistics for the year 2020: An overview*. International Journal of Cancer, 2021. **149**(4): p. 778-789.
6. Hendrix, W., et al., *Trends in the incidence of pulmonary nodules in chest computed tomography: 10-year results from two Dutch hospitals*. Eur Radiol, 2023. **33**(11): p. 8279-8288.
7. Blandin Knight, S., et al., *Progress and prospects of early detection in lung cancer*. Open Biol, 2017. **7**.
8. Herder, G.J., et al., *Clinical Prediction Model To Characterize Pulmonary Nodules: Validation and Added Value of 18 F-Fluorodeoxyglucose Positron Emission Tomography*. Chest, 2005. **128**(4): p. 2490-2496.
9. Sadaghiani, M.S., S.P. Rowe, and S. Sheikhbahaei, *Applications of artificial intelligence in oncologic (18)F-FDG PET/CT imaging: a systematic review*. Ann Transl Med, 2021. **9**(9): p. 823.
10. Callister, M.E.J., et al., *British Thoracic Society guidelines for the investigation and management of pulmonary nodules: accredited by NICE*. Thorax, 2015. **70**.
11. Folch, E.E., et al., *Electromagnetic Navigation Bronchoscopy for Peripheral Pulmonary Lesions: One-Year Results of the Prospective, Multicenter NAVIGATE Study*. Journal of Thoracic Oncology, 2019. **14**(3): p. 445-458.
12. Lentz, R.J., et al., *Navigational Bronchoscopy or Transthoracic Needle Biopsy for Lung Nodules*. N Engl J Med, 2025.
13. Kops, S.E.P., et al., *Cone beam CT-guided navigation bronchoscopy: a cost-effective alternative to CT-guided transthoracic biopsy for diagnosis of peripheral pulmonary nodules*. BMJ Open Respiratory Research, 2022. **9**(1).
14. Kops, S.E.P., et al., *Diagnostic yield and safety of navigation bronchoscopy: A systematic review and meta-analysis*. Lung Cancer, 2023. **180**: p. 107196.
15. Verhoeven, R.L.J., et al., *Cone-beam CT in lung biopsy: a clinical practice review on lessons learned and future perspectives*. Annals of Translational Medicine, 2022. **11**(10): p. 361.
16. Verhoeven, R.L.J., et al., *Cone-beam CT and Augmented Fluoroscopy-guided Navigation Bronchoscopy: Radiation Exposure and Diagnostic Accuracy Learning Curves*. J Bronchology Interv Pulmonol, 2021. **28**(4): p. 262-271.
17. Verhoeven, R.L.J., S. Vos, and E. van der Heijden, *Multi-modal tissue sampling in cone beam CT guided navigation bronchoscopy: comparative accuracy of different sampling tools and rapid on-site evaluation of cytopathology*. Journal of Thoracic Disease, 2021. **13**(7): p. 4396-4406.
18. Leong, S.P., et al., *The lymphatic system and sentinel lymph nodes: conduit for cancer metastasis*. Clin Exp Metastasis, 2022. **39**(1): p. 139-157.
19. Olympus, *15th Anniversary of Scientific Study on EBUS-TBNA — a Review*. 2019. p. 14.
20. Mountain, C.F. and C.M. Dresler, *Regional lymph node classification for lung cancer staging*. Chest, 1997. **111**(6): p. 1718-23.

21. Vilmann, P., et al., *Combined endobronchial and esophageal endosonography for the diagnosis and staging of lung cancer: European Society of Gastrointestinal Endoscopy (ESGE) Guideline, in cooperation with the European Respiratory Society (ERS) and the European Society of Thoracic Surgeons (ESTS)*. Endoscopy, 2015. **47**(6): p. 545-559.
22. Xia, Y., et al., *Evaluation of lymph node metastasis in lung cancer: who is the chief justice?* J Thorac Dis, 2015. **7**: p. 5231-237.
23. Bousema, J.E., et al., *Endosonography With or Without Confirmatory Mediastinoscopy for Resectable Lung Cancer: A Randomized Clinical Trial*. J Clin Oncol, 2023. **41**(22): p. 3805-3815.
24. White, A. and S.J. Swanson, *Surgery versus stereotactic ablative radiotherapy (SABR) for early-stage non-small cell lung cancer: less is not more*. J Thorac Dis, 2016. **8**: p. S399-S405.
25. Beyaz, F., et al., *Occult lymph node metastases in clinical N0/N1 NSCLC; A single center in-depth analysis*. Lung Cancer, 2020. **150**: p. 186-194.
26. Ong, P., et al., *Endobronchial ultrasound-guided transbronchial needle aspiration for systematic nodal staging of lung cancer in patients with N0 disease by computed tomography and integrated positron emission tomography-computed tomography*. Ann Am Thorac Soc, 2015. **12**(3): p. 415-9.
27. Shingyoji, M., et al., *Endobronchial ultrasonography for positron emission tomography and computed tomography-negative lymph node staging in non-small cell lung cancer*. Ann Thorac Surg, 2014. **98**(5): p. 1762-7.
28. International Atomic Energy Agency, *Radiopharmaceuticals for sentinel lymph node detection: status and trends*. 2015, Vienna: IAEA Headquarters.
29. Sun, W.Y.L., et al., *Diagnostic accuracy of sentinel lymph node biopsy using indocyanine green in lung cancer: a systematic review and meta-analysis*. Gen Thorac Cardiovasc Surg, 2020. **68**(9): p. 905-913.
30. Fortuin, A.S., et al., *Ultra-small superparamagnetic iron oxides for metastatic lymph node detection: back on the block*. Wiley Interdiscip Rev Nanomed Nanobiotechnol, 2018. **10**(1).
31. Hasan, S. and M.A. Prelas, *Molybdenum-99 production pathways and the sorbents for 99Mo/99mTc generator systems using (n, γ) 99Mo: a review*. SN Applied Sciences, 2020. **2**: p. 1782.
32. Liu, Y., et al., *Palladium-based nanomaterials for cancer imaging and therapy*. Theranostics, 2020. **10**(22): p. 10057-10074.
33. Gommans, G.M.M., *Radiopharmaceutical and clinical aspects of sentinel lymph node procedures in breast cancer patients*. 2009, Vrije Universiteit Amsterdam. p. 160.
34. Liptay, M.J., et al., *Intraoperative radioisotope sentinel lymph node mapping in non-small cell lung cancer*. The Annals of Thoracic Surgery, 2000. **70**(2): p. 384-389.
35. Michenfelder, M.M., et al., *Particle-size and radiochemical purity evaluations of filtered 99mTc-sulfur colloid prepared with different heating times*. J Nucl Med Technol, 2014. **42**(4): p. 283-288.
36. Taghizadeh Kermani, A., et al., *Accuracy of sentinel node biopsy in the staging of non-small cell lung carcinomas: systematic review and meta-analysis of the literature*. Lung Cancer, 2013. **80**(1): p. 5-14.
37. Deken, M.M., et al., *Near-infrared fluorescence imaging compared to standard sentinel lymph node detection with blue dye in patients with vulvar cancer - a randomized controlled trial*. Gynecologic Oncology, 2020. **159**(3): p. 672-680.
38. Russell, P.S., et al., *Fluorescent Tracers for In Vivo Imaging of Lymphatic Targets*. Front Pharmacol, 2022. **13**.
39. KleinJan, G.H., et al., *The best of both worlds: a hybrid approach for optimal pre- and intraoperative identification of sentinel lymph nodes*. Eur J Nucl Med Mol Imaging, 2018. **45**(11): p. 1915-1925.
40. Chiyoda, T., et al., *Sentinel node navigation surgery in cervical cancer: a systematic review and metaanalysis*. Int J Clin Oncol, 2022. **27**(8): p. 1247-1255.

41. Thongvitokomarn, S. and N. Polchai, *Indocyanine Green Fluorescence Versus Blue Dye or Radioisotope Regarding Detection Rate of Sentinel Lymph Node Biopsy and Nodes Removed in Breast Cancer: A Systematic Review and Meta-Analysis*. Asian Pac J Cancer Prev, 2020. **21**(5): p. 1187-1195.
42. Hachey, K.J. and Y.L. Colson, *Current innovations in sentinel lymph node mapping for the staging and treatment of resectable lung cancer*. Semin Thorac Cardiovasc Surg, 2014. **26**(3): p. 201-209.
43. NVALT. *Richtlijn Niet-kleincellig longcarcinoom*. 2020; Available from: https://richtlijndatabase.nl/richtlijn/niet_kleincellig_longcarcinoom/startpagina_-_niet-kleincellig_longcarcinoom.html.
44. Huyuk, M., et al., *A systematic review and meta-analysis of the prognostic impact of lymph node micrometastasis and isolated tumor cells in patients with stage I-IIIa non-small cell lung cancer*. Histopathology, 2023. **82**: p. 650-663.
45. Lafuente-Sanchis, A., et al., *Clinical Significance of Molecular Micrometastasis in the Sentinel Lymph Node of Early-stage Non-Small Cell Lung Cancer Patients*. Am J Clin Oncol, 2018. **41**(11): p. 1106-1112.
46. Østrup Jensen, S., et al., *Second Primary Lung Cancer - An Emerging Issue in Lung Cancer Survivors*. J Thorac Oncol, 2024. **19**(10): p. 1415-1426.
47. Muraoka, Y., et al., *Dynamics of recurrence after curative resection of nonsmall cell lung cancer*. J Surg Oncol, 2023. **128**(7): p. 1205-1212.
48. Demicheli, R., et al., *Recurrence dynamics for non-small-cell lung cancer: effect of surgery on the development of metastases*. J Thorac Oncol, 2012. **7**(4): p. 723-730.
49. Choi, E., et al., *Risk model-based management for second primary lung cancer among lung cancer survivors through a validated risk prediction model*. Cancer, 2024. **130**(5): p. 770-780.
50. van Rossum, P.S.N., et al., *Real-World Acute Toxicity and 90-Day Mortality in Patients With Stage I NSCLC Treated With Stereotactic Body Radiotherapy*. J Thorac Oncol, 2024. **19**(11): p. 1550-1563.
51. Isaka, M., et al., *Risk factors for local recurrence after lobectomy and lymph node dissection in patients with non-small cell lung cancer: Implications for adjuvant therapy*. Lung Cancer, 2018. **115**: p. 28-33.
52. van den Berg, L.L., et al., *Patterns of Recurrence and Survival after Surgery or Stereotactic Radiotherapy for Early Stage NSCLC*. Journal of Thoracic Oncology, 2015. **10**(5): p. 826-831.
53. He, Z., et al., *Detection of occult tumor cells in regional lymph nodes is associated with poor survival in pN0 non-small cell lung cancer: a meta-analysis*. J Thorac Dis, 2016. **8**(3): p. 375-385.
54. Karamustafaoglu, Y.A., et al., *Sentinel lymph node mapping in patients with operable non-small cell lung cancer*. Journal of Thoracic Disease, 2013. **5**(3): p. 317-320.
55. Chao, Y.K., *Deciding to trust, coming to believe: sentinel lymph node assessment in lung cancer*. Journal of Thoracic Disease, 2018. **10**: p. S3978-S3980.
56. Gilmore, D.M., O.V. Khullar, and Y.L. Colson, *Developing intrathoracic sentinel lymph node mapping with near-infrared fluorescent imaging in non-small cell lung cancer*. J Thorac Cardiovasc Surg, 2012. **144**(3): p. S80-S84.
57. Caso, R., G.D. Jones, and D.R. Jones, *Sentinel lymph node mapping in lung cancer: a step forward?* Journal of Thoracic Disease, 2018. **10**: p. S3254-S3256.
58. Gilmore, D.M., et al., *Identification of metastatic nodal disease in a phase 1 dose-escalation trial of intraoperative sentinel lymph node mapping in non-small cell lung cancer using near-infrared imaging*. J Thorac Cardiovasc Surg, 2013. **146**(3): p. 562-570.
59. Pritchett, M.A., et al., *Cone-Beam CT With Augmented Fluoroscopy Combined With Electromagnetic Navigation Bronchoscopy for Biopsy of Pulmonary Nodules*. J Bronchology Interv Pulmonol, 2018. **25**(4): p. 274-282.

60. Verhoeven, R., et al., *Real-time 3D cone beam CT imaging guidance for advanced navigation bronchoscopy to centimeter sized lesions*, in *European Respiratory Journal*. 2019.
61. Verhoeven, R.L.J., et al., *Cone-Beam CT Image Guidance With and Without Electromagnetic Navigation Bronchoscopy for Biopsy of Peripheral Pulmonary Lesions*. *J Bronchology Interv Pulmonol*, 2021. **28**(1): p. 60-69.
62. Cicensia, J., S.K. Avasarala, and T.R. Gildea, *Navigational bronchoscopy: a guide through history, current use, and developing technology*. *Journal of Thoracic Disease*, 2020. **12**(6): p. 3263-3271.
63. Abele, J.T., et al., *Lymphoscintigraphy in early-stage non-small cell lung cancer with technetium-99m nanocolloids and hybrid SPECT/CT: a pilot project*. *Ann Nucl Med*, 2014. **28**(5): p. 477-83.
64. Philips. *Pioneer Plus IVUS-guided re-entry catheter*. Devices 2018 [cited 12-12-2021]; Available from: <https://www.usa.philips.com/healthcare/product/HICIGTDPPLUS/pioneer-plus-ivus-guided-re-entry-catheter>.
65. Celikoglu, F., S.I. Celikoglu, and E.P. Goldberg, *Intratumoural chemotherapy of lung cancer for diagnosis and treatment of draining lymph node metastasis*. *Journal of Pharmacy and Pharmacology*, 2010. **62**(3): p. 287-295.
66. Gregor, A., H. Ujiie, and K. Yasufuku, *Sentinel lymph node biopsy for lung cancer*. *Gen Thorac Cardiovasc Surg*, 2020. **68**(10): p. 1061-1078.
67. Uribe-Etxebarria Lugariza-Aresti, N., et al., *Biopsy of the sentinel node in lung cancer*. *Medicina Clínica (English Edition)*, 2017. **148**(6): p. 257-259.
68. Postmus, P.E., et al., *Early and locally advanced non-small-cell lung cancer (NSCLC): ESMO Clinical Practice Guidelines for diagnosis, treatment and follow-up*. *Ann Oncol*, 2017. **28**: p. iv1-iv21.
69. Steinfort, D.P., *Systematic mediastinal staging in non-small cell lung cancer: Filling in the guideline evidence gap*. *Respirology*, 2023: p. 1-3.
70. Niebling, M.G., et al., *A systematic review and meta-analyses of sentinel lymph node identification in breast cancer and melanoma, a plea for tracer mapping*. *Eur J Surg Oncol*, 2016. **42**(4): p. 466-473.
71. Persico, M.G., et al., *(99m)Tc-human serum albumin nanocolloids: particle sizing and radioactivity distribution*. *J Labelled Comp Radiopharm*, 2015. **58**(9): p. 376-382.
72. Khandhar, S.J., et al., *Electromagnetic navigation bronchoscopy to access lung lesions in 1,000 subjects: first results of the prospective, multicenter NAVIGATE study*. *BMC Pulm Med*, 2017. **17**: p. 59.
73. Gonzalez, A.V., et al., *Assessment of Advanced Diagnostic Bronchoscopy Outcomes for Peripheral Lung Lesions: A Delphi Consensus Definition of Diagnostic Yield and Recommendations for Patient-centered Study Designs. An Official American Thoracic Society/American College of Chest Physicians Research Statement*. *Am J Respir Crit Care Med*, 2024. **209**(6): p. 634-646.
74. Yu Lee-Mateus, A., et al., *Robotic-assisted bronchoscopy versus CT-guided transthoracic biopsy for diagnosis of pulmonary nodules*. *Respirology*, 2023. **28**(1): p. 66-73.
75. Mori, V., et al., *Visualizing intratumoral injections in lung tumors by endobronchial ultrasound*. *J Cancer*, 2023. **14**(4): p. 544-553.
76. DuComb, E.A., et al., *Endobronchial ultrasound-guided transbronchial needle injection of cisplatin results in dynamic changes in the tumor immune microenvironment*. *Respir Med Res*, 2023. **84**: p. 100994.
77. DeMaio, A. and D. Sterman, *Bronchoscopic intratumoural therapies for non-small cell lung cancer*. *Eur Respir Rev*, 2020. **29**.
78. Association, W.M., *World Medical Association Declaration of Helsinki: Ethical Principles for Medical Research Involving Human Subjects*. *JAMA*, 2013. **310**(20): p. 2191-2194.

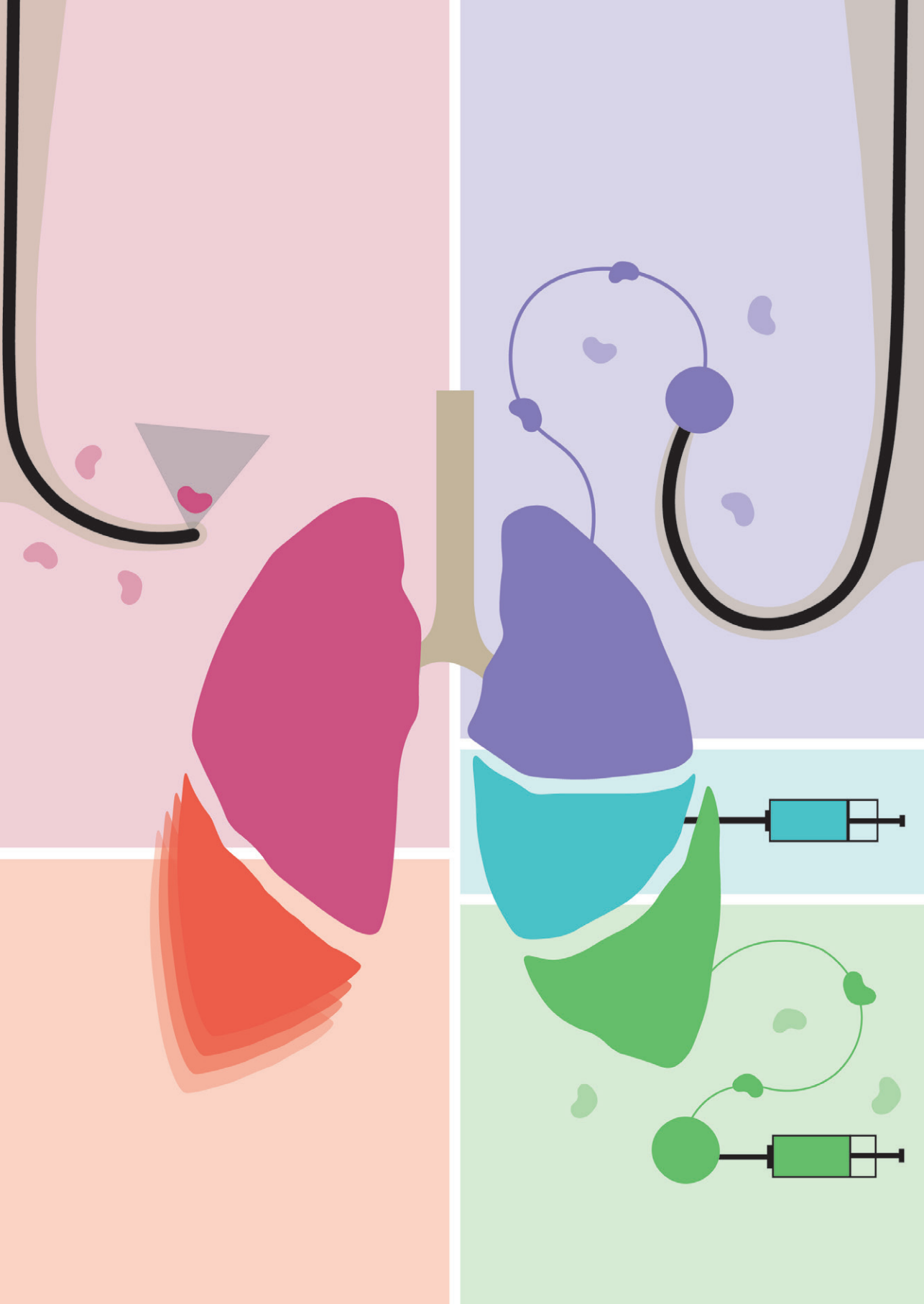
79. Beyaz, F., et al., *Cone Beam Computed Tomography-guided Navigation Bronchoscopy with Augmented Fluoroscopy for the Diagnosis of Peripheral Pulmonary Nodules: a step-by-step guide*. Respiration, 2025. **104**(3): p. 216-228.
80. ter Woerds, D.K.M., et al., *Ex-vivo exploration of an endobronchial sentinel lymph node procedure in lung cancer for optimizing workflow and evaluating feasibility of novel imaging tools*. Journal of Thoracic Disease, 2023. **15**(2): p. 291-299.
81. Park, J., et al., *Endobronchial Ultrasound Using Guide Sheath-Guided Transbronchial Lung Biopsy in Ground-Glass Opacity Pulmonary Lesions without Fluoroscopic Guidance*. Cancers (Basel), 2024. **16**(6): p. 1203.
82. Wijma, I.N., et al., *Radiation Principles, Protection and Reporting for Interventional Pulmonology*. Respiration, 2024. **103**(11): p. 707-722.
83. Folch, E.E., et al., *Standardized Definitions of Bleeding After Transbronchial Lung Biopsy: A Delphi Consensus Statement From the Nashville Working Group*. Chest, 2020. **158**(1): p. 393-400.
84. Boston Scientific. *iNod™ | Ultrasound Guided System*. 2024 [cited 2023 09-11-2023]; Available from: <https://www.bostonscientific.com/en-US/products/ultrasound-guidance-system/inod-ultrasound-guided-biopsy-needle.html>.
85. Mlosek, R.K., B. Migda, and M. Migda, *High-frequency ultrasound in the 21(st) century*. J Ultrason, 2021. **20**(83): p. e233-e241.
86. Liptay, M.J., et al., *Intraoperative Sentinel Lymph Node Mapping in Non-Small-Cell Lung Cancer Improves Detection of Micrometastases*. Journal of Clinical Oncology, 2002. **20**(8): p. 1984-1988.
87. Sugi, K., et al., *Effect of radioisotope sentinel node mapping in patients with cT1 N0 M0 lung cancer*. J Thorac Cardiovasc Surg, 2003. **126**(2): p. 568-573.
88. Nomori, H., et al., *In vivo identification of sentinel lymph nodes for clinical stage I non-small cell lung cancer for abbreviation of mediastinal lymph node dissection*. Lung Cancer, 2004. **46**(1): p. 49-55.
89. Nomori, H., et al., *Sentinel node navigation segmentectomy for clinical stage IA non-small cell lung cancer*. J Thorac Cardiovasc Surg, 2007. **133**(3): p. 780-785.
90. Nomori, H., et al., *Sentinel node identification in clinical stage Ia non-small cell lung cancer by a combined single photon emission computed tomography/computed tomography system*. J Thorac Cardiovasc Surg, 2007. **134**(1): p. 182-187.
91. Sugi, K., et al., *Usefulness of sentinel lymph node biopsy for the detection of lymph node micrometastasis in early lung cancer*. Interact Cardiovasc Thorac Surg, 2008. **7**(5): p. 913-915.
92. Liptay, M.J., et al., *Intraoperative sentinel node mapping with technitium-99 in lung cancer: results of CALGB 140203 multicenter phase II trial*. J Thorac Oncol, 2009. **4**(2): p. 198-202.
93. Kim, E.M., et al., *Size Control of (99m)Tc-tin Colloid Using PVP and Buffer Solution for Sentinel Lymph Node Detection*. J Korean Med Sci, 2015. **30**(6): p. 816-822.
94. Kjellman, P., et al., *Optimizing retention of multimodal imaging nanostructures in sentinel lymph nodes by nanoscale size tailoring*. Nanomedicine, 2014. **10**(5): p. 1089-1095.
95. Romano, G., et al., *Sentinel Lymph Node Mapping in Lung Cancer: A Pilot Study for the Detection of Micrometastases in Stage I Non-Small Cell Lung Cancer*. Tomography, 2024. **10**(5): p. 761-772.
96. Shah, A., et al., *Real-world study of disease-free survival & patient characteristics associated with disease-free survival in early-stage non-small cell lung cancer: A retrospective observational study*. Cancer Treat Res Commun, 2023. **36**.
97. Sun, J., et al., *Lymph node micrometastasis in non-small cell lung cancer*. Biomed Pharmacother, 2022. **149**.
98. Wada, H., et al., *Minimally invasive electro-magnetic navigational bronchoscopy-integrated near-infrared-guided sentinel lymph node mapping in the porcine lung*. PLoS One, 2015. **10**(5): p. 1-13.

99. Lardinois, D., et al., *ESTS guidelines for intraoperative lymph node staging in non-small cell lung cancer*. Eur J Cardiothorac Surg, 2006. **30**(5): p. 787-792.
100. van der Woude, L., et al., *Completeness of lymph node dissection in patients undergoing minimally invasive- or open surgery for non-small cell lung cancer: A nationwide study*. Eur J Surg Oncol, 2021. **47**(7): p. 1784-1790.
101. Serra Mitja, P., et al., *EBUS-TBNA for mediastinal staging of centrally located T1N0M0 non-small cell lung cancer clinically staged with PET/CT*. Respirology, 2024. **29**: p. 158-165.
102. Gregor, A., et al., *Preclinical feasibility of bronchoscopic fluorescence-guided lung sentinel lymph node mapping*. J Thorac Cardiovasc Surg, 2023. **165**(1): p. 337-350.
103. IASLC, *Staging Manual in Thoracic Oncology*. Third ed. Vol. 3. 2024, IASLC: IASLC. 1-194.
104. Farrow, N.E., et al., *Adjuvant Therapy is Effective for Melanoma Patients with a Positive Sentinel Lymph Node Biopsy Who Forego Completion Lymphadenectomy*. Ann Surg Oncol, 2020. **27**(13): p. 5121-5125.
105. Li, B., et al., *Evaluation of adjuvant therapy for T1-2N1miM0 breast cancer without further axillary lymph node dissection*. Front Surg, 2022. **9**: p. 1-13.
106. Doglioni, C., et al., *Cytokeratin-immunoreactive cells of human lymph nodes and spleen in normal and pathological conditions*. Virchows Archiv A Pathol Anat 1990. **416**: p. 479-490.
107. Tajima, Y., et al., *Immunohistochemical Demonstration of Cytokeratin is Useful for Detecting Micrometastatic Foci from Gallbladder Carcinoma in Regional Lymph Nodes*. Japanese Journal of Clinical Oncology, 1999. **29**(9): p. 425-428.
108. Carretta, A., *Clinical value of nodal micrometastases in patients with non-small cell lung cancer: time for reconsideration?* Journal of Thoracic Disease, 2016. **8**(12): p. E1755-E1758.
109. Stasiak, F., et al., *Sentinel Lymph Node in Non-Small Cell Lung Cancer: Assessment of Feasibility and Safety by Near-Infrared Fluorescence Imaging and Clinical Consequences*. J Pers Med, 2022. **13**: p. 90.
110. Phillips, W.W., et al., *Finding the "True" N0 Cohort: Technical Aspects of Near-infrared Sentinel Lymph Node Mapping in Non-small Cell Lung Cancer*. Ann Surg, 2020. **272**(4): p. 583-588.
111. Digesu, C.S., et al., *Long-term outcomes after near-infrared sentinel lymph node mapping in non-small cell lung cancer*. J Thorac Cardiovasc Surg, 2018. **155**(3): p. 1280-1291.
112. Stasiak, F., et al., *Sentinel lymph node detection for lung cancer surgery: a possible pathological surrogate of overall lymph node dissection*. Front Oncol, 2025. **15**.
113. Ter Woerds, D.K.M., et al., *Feasibility of Non-Invasive Sentinel Lymph Node Identification in Early-Stage NSCLC Through Ultrasound Guided Intra-Tumoral Injection of (99m)Tc-Nanocolloid and Iodinated Contrast Agent During Navigation Bronchoscopy*. Cancers (Basel), 2024. **16**(22): p. 3863.
114. Ding, N., et al., *Predictors of lymph node metastasis and possible selective lymph node dissection in clinical stage IA non-small cell lung cancer*. J Thorac Dis, 2018. **10**(7): p. 4061-4068.
115. Raymond, C., et al., *Maximizing lymph node dissection from fresh lung cancer specimens*. Eur J Cardiothorac Surg, 2022. **63**(1): p. ezac554.
116. Spicer, J.D., et al., *Neoadjuvant and Adjuvant Treatments for Early Stage Resectable NSCLC: Consensus Recommendations From the International Association for the Study of Lung Cancer*. J Thorac Oncol, 2024. **19**(10): p. 1373-1414.
117. Forde, P.M., et al., *Neoadjuvant Nivolumab plus Chemotherapy in Resectable Lung Cancer*. N Engl J Med, 2022. **386**(21): p. 1973-1985.
118. Giri, M., et al., *Advancements in navigational bronchoscopy for peripheral pulmonary lesions: A review with special focus on virtual bronchoscopic navigation*. Front Med (Lausanne), 2022. **9**: p. 989184.

119. Lentz, R.J., et al., *Navigational Bronchoscopy Versus Computed Tomography-guided Transthoracic Needle Biopsy for the Diagnosis of Indeterminate Lung Nodules: Initial Results From the VERITAS Multicenter Randomized Trial*. American Journal of Respiratory and Critical Care Medicine 2024. **209**(Online Abstracts Issue).
120. Bott, M.J., et al., *Initial results of pulmonary resection after neoadjuvant nivolumab in patients with resectable non-small cell lung cancer*. J Thorac Cardiovasc Surg, 2019. **158**(1): p. 269-276.
121. De Leyn, P., et al., *Revised ESTS guidelines for preoperative mediastinal lymph node staging for non-small-cell lung cancer*. Eur J Cardiothorac Surg, 2014. **45**(5): p. 787-798.
122. Silvestri, G.A., et al., *Noninvasive staging of non-small cell lung cancer: ACCP evidenced-based clinical practice guidelines (2nd edition)*. Chest, 2007. **132**: p. 178S-201S.
123. Hoeijmakers, F., et al., *Mediastinoscopy for Staging of Non-Small Cell Lung Cancer: Surgical Performance in The Netherlands*. Ann Thorac Surg, 2019. **107**(4): p. 1024-1031.
124. Detterbeck, F.C., et al., *The Eighth Edition Lung Cancer Stage Classification*. Chest, 2017. **151**(1): p. 193-203.
125. Lim, E., et al., *Guidelines on the radical management of patients with lung cancer*. Thorax, 2010. **65**: p. iii1-27.
126. Steinfort, D.P., et al., *Proposed quality indicators and recommended standard reporting items in performance of EBUS bronchoscopy: An official World Association for Bronchology and Interventional Pulmonology Expert Panel consensus statement*. Respirology, 2023. **28**(8): p. 722-743.
127. Trevethan, R., *Sensitivity, Specificity, and Predictive Values: Foundations, Plabilities, and Pitfalls in Research and Practice*. Front Public Health, 2017. **5**(307).
128. Schmidt-Hansen, M., et al., *PET-CT for assessing mediastinal lymph node involvement in patients with suspected resectable non-small cell lung cancer*. Cochrane Database Syst Rev, 2014. **2014**(11).
129. Wu, Y., et al., *Diagnostic value of fluorine 18 fluorodeoxyglucose positron emission tomography/computed tomography for the detection of metastases in non-small-cell lung cancer patients*. Int J Cancer, 2013. **132**(2): p. E37-47.
130. Cardoso, A.V., et al., *The value of rapid on-site evaluation during EBUS-TBNA*. Rev Port Pneumol (2006), 2015. **21**(5): p. 253-258.
131. Chen, Y.Y., et al., *High SUVmax Is an Independent Predictor of Higher Diagnostic Accuracy of ROSE in EBUS-TBNA for Patients with NSCLC*. J Pers Med, 2022. **12**: p. 451.
132. Miao, H., et al., *Occult mediastinal lymph node metastasis in FDG-PET/CT node-negative lung adenocarcinoma patients: Risk factors and histopathological study*. Thorac Cancer, 2019. **10**(6): p. 1453-1460.
133. Marziali, V., et al., *Prognostic significance of uncertain resection for metastasis in the highest mediastinal lymph node after surgery for clinical N0 non-small cell lung cancer*. Front Surg, 2023. **10**: p. 1115696.
134. DuComb, E.A., et al., *Evidence for Expanding Invasive Mediastinal Staging for Peripheral T1 Lung Tumors*. Chest, 2020. **158**(5): p. 2192-2199.
135. Wang, Z., et al., *Multiple primary lung cancer: Updates and perspectives*. Int J Cancer, 2024. **155**(5): p. 785-799.
136. Chiang, C.L., et al., *Recent Advances in the Diagnosis and Management of Multiple Primary Lung Cancer*. Cancers (Basel), 2022. **14**(1): p. 242.
137. Martini, N. and M.R. Melamed, *Multiple primary lung cancers*. The Journal of Thoracic and Cardiovascular Surgery, 1975. **70**(4): p. 606-612.
138. Morellato, J.B.F., et al., *Routine follow-up after surgical treatment of lung cancer: is chest CT useful?* J Bras Pneumol, 2021. **47**(4): p. e20210025.

139. Mo, Y., et al., *Postoperative radiotherapy might be a risk factor for second primary lung cancer: A population-based study*. *Front Oncol*, 2022. **12**: p. 918137.
140. Leroy, T., et al., *Let us not underestimate the long-term risk of SPLC after surgical resection of NSCLC*. *Lung Cancer*, 2019. **137**: p. 23-30.
141. Fink-Neuboeck, N., et al., *Hazards of Recurrence, Second Primary, or Other Tumor at Ten Years After Surgery for Non-Small-Cell Lung Cancer*. *Clin Lung Cancer*, 2020. **21**(4): p. 333-340.
142. Choi, E., et al., *Second Primary Lung Cancer Among Lung Cancer Survivors Who Never Smoked*. *JAMA Netw Open*, 2023. **6**(11): p. e2343278.
143. Chang, J.Y., et al., *Stereotactic ablative radiotherapy versus lobectomy for operable stage I non-small-cell lung cancer: a pooled analysis of two randomised trials*. *The Lancet Oncology*, 2015. **16**(6): p. 630-637.
144. Lou, F., et al., *Patterns of recurrence and second primary lung cancer in early-stage lung cancer survivors followed with routine computed tomography surveillance*. *J Thorac Cardiovasc Surg*, 2013. **145**(1): p. 75-82.
145. Eberhardt, W.E., et al., *2nd ESMO Consensus Conference in Lung Cancer: locally advanced stage III non-small-cell lung cancer*. *Ann Oncol*, 2015. **26**(8): p. 1573-1588.
146. Hardavella, G., et al., *Lung cancer screening: where do we stand? Breathe (Sheff)*, 2024. **20**(2): p. 230190.
147. Tian, S., et al., *Differential Diagnostic Value of Histology in MPLC and IPM: A Systematic Review and Meta-Analysis*. *Front Oncol*, 2022. **12**: p. 871827.
148. Kamigaichi, A., et al., *Postoperative Recurrence and Survival After Segmentectomy for Clinical Stage 0 or IA Lung Cancer*. *Clin Lung Cancer*, 2019. **20**(5): p. 397-403.
149. Nakamichi, S., et al., *Comparison of Radiotherapy and Chemoradiotherapy for Locoregional Recurrence of Non-small-cell Lung Cancer Developing After Surgery*. *Clin Lung Cancer*, 2017. **18**(6): p. e441-e448.
150. Kaaki, S.K. and T.A. D'Amico, *Multiple pulmonary nodules: a management dilemma*. *Current Challenges in Thoracic Surgery*, 2022. **4**: p. 38.
151. Oddstig, J., et al., *The radiation dose to overweighted patients undergoing myocardial perfusion SPECT can be significantly reduced: validation of a linear weight-adjusted activity administration protocol*. *J Nucl Cardiol*, 2017. **24**(6): p. 1912-1921.
152. Riquet, M., G. Hidden, and B. Debesse, *Direct lymphatic drainage of lung segments to the mediastinal nodes*. *The Journal of Thoracic and Cardiovascular Surgery*, 1989. **97**(4): p. 623-632.
153. Di, J., et al., *Size, shape, charge and "stealthy" surface: Carrier properties affect the drug circulation time in vivo*. *Asian J Pharm Sci*, 2021. **16**(4): p. 444-458.
154. Riquet, M., et al., *Skip mediastinal lymph node metastasis and lung cancer: a particular N2 subgroup with a better prognosis*. *Ann Thorac Surg*, 2005. **79**(1): p. 225-233.
155. Yoshida, Y., et al., *Visualization of patterns of lymph node metastases in non-small cell lung cancer using network analysis*. *JTCVS Open*, 2022. **12**: p. 410-425.
156. Altorki, N., et al., *Lobar or Sublobar Resection for Peripheral Stage IA Non-Small-Cell Lung Cancer*. *N Engl J Med*, 2023. **388**(6): p. 489-498.
157. Seitlinger, J., et al., *What is the appropriate "first lymph node" in the era of segmentectomy for non-small cell lung cancer?* *Front Oncol*, 2022. **12**: p. 1078606.
158. Fear, V.S., et al., *Tumour draining lymph node-generated CD8 T cells play a role in controlling lung metastases after a primary tumour is removed but not when adjuvant immunotherapy is used*. *Cancer Immunol Immunother*, 2021. **70**(11): p. 3249-3258.

159. Deng, H., et al., *Impact of lymphadenectomy extent on immunotherapy efficacy in post-resectional recurrent non-small cell lung cancer: a multi-institutional retrospective cohort study*. *Int J Surg*, 2024. **110**(1): p. 238-252.
160. Izbicki, J.R., et al., *Mode of spread in the early phase of lymphatic metastasis in non-small-cell lung cancer: significance of nodal micrometastasis*. *The Journal of Thoracic and Cardiovascular Surgery*, 1996. **112**(3): p. 623-630.
161. Ah-Thiane, L., et al., *The Sentinel Lymph Node in Treatment Planning: A Narrative Review of Lymph-Flow-Guided Radiotherapy*. *Cancers (Basel)*, 2023. **15**(10): p. 2736.
162. Federatie Medisch Specialisten, *Richtlijn niet-kleincellig longcarcinoom*. 2025.
163. Houda, I., et al., *Challenges and controversies in resectable non-small cell lung cancer: a clinician's perspective*. *Lancet Reg Health Eur*, 2024. **38**: p. 100841.
164. Lipson, E.J., et al., *Antagonists of PD-1 and PD-L1 in Cancer Treatment*. *Semin Oncol*, 2015. **42**(4): p. 587-600.
165. Topalian, S.L., et al., *Safety, activity, and immune correlates of anti-PD-1 antibody in cancer*. *N Engl J Med*, 2012. **366**(26): p. 2443-54.
166. Warner, J.S., et al., *Intratumoral Chemotherapy: The Effects of Drug Concentration and Dose Apportioning on Tumor Cell Injury*. *Bioengineering (Basel)*, 2024. **11**(8).
167. Khan, F.B., et al., *Initial Safety and Feasibility Results From a Phase 1, Diagnose-and-Treat Trial of Neoadjuvant Intratumoral Cisplatin for Stage IV NSCLC*. *JTO Clin Res Rep*, 2024. **5**(3): p. 100634.
168. Mori, V., et al., *Cisplatin Pharmacodynamics Following Endobronchial Ultrasound-Guided Transbronchial Needle Injection into Lung Tumors*. *Sci Rep*, 2019. **9**(1): p. 6819.
169. Mori, V., et al., *A computational modeling approach for dosing endoscopic intratumoral chemotherapy for advanced non-small cell lung cancer*. *Sci Rep*, 2022. **12**(1): p. 44.
170. Melero, I., et al., *Intratumoural administration and tumour tissue targeting of cancer immunotherapies*. *Nature Reviews Clinical Oncology*, 2021. **18**(9): p. 558-576.
171. Champiat, S.A.-O., et al., *Intratumoral Immunotherapy: From Trial Design to Clinical Practice*. *Clinical Cancer Research*, 2021. **27**(3): p. 665-679.
172. Jimenez-Labaig, P., et al., *Intratumoral therapies in head and neck squamous cell carcinoma: A systematic review and future perspectives*. *Cancer Treat Rev*, 2024. **127**: p. 102746.
173. Ke, X., et al., *Physical and chemical profiles of nanoparticles for lymphatic targeting*. *Adv Drug Deliv Rev*, 2019. **151-152**: p. 72-93.
174. Volovat, S.R., et al., *A multicenter, single-arm, basket design, phase II study of NC6004 plus gemcitabine in patients with advanced unresectable lung, biliary tract, or bladder cancer*. *OncoTarget*, 2020. **11**(33): p. 3105-3117.
175. DuVall, G.A., et al., *Phase 2: a dose-escalation study of OncoGel (ReGel/paclitaxel), a controlled-release formulation of paclitaxel, as adjunctive local therapy to external-beam radiation in patients with inoperable esophageal cancer*. *Anticancer Drugs*, 2009. **20**(2): p. 89-95.
176. Piha-Paul, S.A., et al., *First-in-human, phase I/IIa study of CRLX301, a nanoparticle drug conjugate containing docetaxel, in patients with advanced or metastatic solid malignancies*. *Invest New Drugs*, 2021. **39**(4): p. 1047-1056.



Appendices

Nederlandse samenvatting
Research Data Management
List of publications
PhD Portfolio
Curriculum Vitae
Dankwoord

Nederlandse samenvatting

Longkanker is wereldwijd de belangrijkste oorzaak van sterfte door kanker. Jaarlijks krijgen meer dan anderhalf miljoen mensen de diagnose, en hoewel de behandelopties de laatste jaren zijn verbeterd, is de ziekte vaak al in een vergevorderd stadium bij ontdekking. Dit maakt vroege opsporing en precieze stadiëring van levensbelang. In **hoofdstuk 1** laten we zien dat verspreiding van longkanker naar de lymfeklieren is een kritieke factor voor de prognose en voor het kiezen van de juiste behandeling. Bij vroege stadia van longkanker heeft uitzaaiing naar lymfeklieren vaak grotere invloed op de overleving dan de tumorgrootte zelf. Op dit moment worden CT- en PET-scan gebruikt om zowel de longafwijking als de (verdachte) lymfeklieren in beeld te brengen. Bij verdenking op verspreiding van de kanker naar de lymfeklieren, kan een EBUS of cervicale mediastinoscopie worden verricht om bipten af te nemen. Toch blijkt in ongeveer 1 op de 4 patiënten waarbij deze lymfeklieren schoon worden verklaard en die daarna een operatie ondergaan, dat er toch verspreiding naar de lymfeklieren aanwezig was. Dat betekent dat ondanks alle diagnostiek vooraf, toch uitzaaiingen gemist worden. Daarnaast komt bij ongeveer 1 op de 3 patiënten met stadium IB-IIA binnen 3,5 jaar na curatieve behandeling een recidief voor. Het doel van dit proefschrift is om zowel nieuwe technieken te onderzoeken voor nauwkeurigere stadiëring van longkanker, als om de bestaande diagnostiek efficiënter en doelmatiger in te zetten in de klinische praktijk.

In andere vormen van kanker, zoals borstkanker en melanoom, wordt gebruik gemaakt van een poortwachter klier procedure. Dit is een techniek waarbij er injecties met een tracer worden gezet rondom de tumor, die vervolgens met de lymfevloeistof mee afvloeien richting de lymfeklieren en daar ophopen. De tracer wordt vervolgens in beeld gebracht en de lymfeklieren waar deze stof wordt gevonden, zijn ook de lymfeklieren waarheen tumorcellen zich als eerste zullen verspreiden. Deze klieren worden vervolgens zeer gedetailleerd onderzocht. Bij longkanker is deze techniek nog niet onderdeel van de standaard diagnostiek en behandeling. **Deel I** van dit proefschrift richt zich op het ontwikkelen en testen van technieken die een poortwachter klier procedure mogelijk kunnen maken voor patiënten met longkanker.

In **hoofdstuk 2** onderzochten we een nieuwe injectietechniek waarbij met behulp van een katheter met een echokop een radioactieve tracer onder begeleiding van echo geïnjecteerd kan worden in het longweefsel vanaf buiten het lichaam. Door na de injectie(s) een SPECT-scan te maken van het weefsel, konden 76,7% van de

naast elkaar geplaatste injecties individueel teruggevonden worden. Alle injecties die rondom de tumor geplaatst werden waren succesvol, maar als injecties in de tumor geplaatst werden waren deze alleen succesvol als ze in een niet-solide tumor geplaatst werden. Wanneer injecties in een solide tumor geplaatst werden, vond er in 35,7% van de injecties een lekkage plaats. Omdat er in *ex vivo* longen geen bloedstroom of lymfedrainage is, kon verspreiding naar lymfeklieren niet worden onderzocht. Toch was dit een belangrijke eerste stap in het ontwikkelen van een veilige en effectieve injectiemethode.

Vervolgens onderzochten we in **hoofdstuk 3** of we deze methode konden toepassen bij patiënten met een verdenking op vroeg-stadium longkanker. Tijdens een navigatiebronchoscopie werd met behulp van de katheter met een echokop een radioactieve tracer geïnjecteerd. Verschillende parameters, zoals de injectieplaats, het injectievolume en de injectiesnelheid werden gevarieerd om de optimale condities te bepalen om de poortwachter klier(en) te vinden. De tumoren konden in 30 van de 31 patiënten met behulp van de echokop in beeld gebracht worden, maar in 10 van de 31 patiënten kon de poortwachter klier gevonden worden op de SPECT-scan. Na het uitvoeren van de procedure bij een aantal patiënten bleek dat een deel van de geïnjecteerde stof niet op de juiste plaats terecht was gekomen. In de tweede helft van het onderzoek werd er daarom voorafgaand aan de injectie van de radioactieve stof een contrastmiddel geïnjecteerd die direct zichtbaar werd op de beeldvorming tijdens de navigatiebronchoscopie. Hiermee kon de naaldpositie van de katheter veranderd worden, zodat lekkage richting de bloed- of lymfevaten vermeden kon worden en de radioactieve tracer daarna op de juiste plek kon worden geïnjecteerd. Deze studie toont aan dat de techniek veilig en uitvoerbaar is, maar dat de identificatie van de poortwachter klier op SPECT-beeldvorming mogelijk tekortschiet. We hypothetiseren dat beeldvorming met behulp van PET en alternatieve tracers mogelijk een hogere resolutie bieden en daarmee uitkomst kan bieden om deze procedure te verbeteren in de toekomst.

In **hoofdstuk 4** beschrijven we een andere benadering, namelijk het uitvoeren van de poortwachter klier procedure tijdens een longoperatie. Hierbij hebben we gebruik gemaakt van een fluorescente kleurstof, indocianine groen, die met infrarood beeldvorming in kaart kan worden gebracht. De kleurstof werd tijdens de operatie geïnjecteerd rondom en in de tumor, waarna de lymfeklieren werden verwijderd zoals gebruikelijk bij deze operatie en deze werden vervolgens beoordeeld op hun hoeveelheid kleurstof. De lymfeklieren met de meeste kleurstof werden vervolgens bij de pathologie nauwkeuriger en met meerdere kleuringen bekeken om uitzaaiingen beter te kunnen opsporen. Deze procedure

bleek technisch haalbaar en er kon bij alle patiënten één of meer poortwachter klier(en) worden aangemerkt. Hoewel er geen uitzaaiingen zijn gevonden in deze lymfeklieren die met de standaard diagnostiek over het hoofd zouden zijn gezien, bleek wel dat een tumor-vrije poortwachter klier een goede voorspeller is van de afwezigheid van verdere uitzaaiingen stroomafwaarts. Bij twee patiënten waren er geïsoleerde tumorcellen gevonden in één lymfeklier. De invloed van deze geïsoleerde tumorcellen op de prognose van deze patiënten zijn nog onzeker. Uit de literatuur blijkt dat deze procedure in andere ziekenhuizen wel kan leiden tot het vinden van meer uitzaaiingen die anders gemist waren. Dit onderzoek zet daarom een goede stap richting een standaardprocedure die op grotere schaal toegepast moet worden om de toegevoegde waarde te bepalen.

In **deel II** van dit proefschrift staat de toepassing van bestaande diagnostische technieken in de kliniek centraal. In **hoofdstuk 5** onderzochten we of het routinematig uitvoeren van een EBUS tijdens een navigatiebronchoscopie procedure bij patiënten met kleine, perifere longafwijkingen wel altijd zinvol is. Onze resultaten tonen aan dat wanneer er bij 2 van de 3 patiënten geen verdenking is op uitzaaiingen in de lymfeklieren op basis van een PET-scan of op basis van een CT-scan met contrast en er bij deze patiënten ook geen uitzaaiingen gevonden waren met de EBUS-procedure. Dit betekent dat de EBUS-procedure veilig achterwege gelaten kan worden op basis van beeldvorming. Dit kan kostbare tijd en capaciteit van de operatiekamer besparen, zonder de nauwkeurigheid van de diagnostische procedure te beperken.

In **hoofdstuk 6** onderzochten we de incidentie van patiënten met een recidief of tweede primaire longtumor bij patiënten die via een navigatiebronchoscopie met longkanker waren gediagnosticeerd. We vonden dat in onze patiëntengroep 26% gediagnosticeerd werd met een tweede primaire longkanker, zowel tijdens als na de navigatiebronchoscopie, en dat 19% met een recidief gediagnosticeerd werd. Opvallend was dat een kwart van de patiënten die deze procedure ondergingen al eens gediagnosticeerd waren met (en behandeld waren voor) longkanker. Helaas kon maar in iets meer dan 1 op de 3 tumoren het onderscheid tussen of vergelijk met een eerdere longtumor bewezen worden. Deze bevindingen onderstrepen de noodzaak om altijd een biopsie te nemen, zodat de relatie van een nieuwe tumor met een eerdere tumor met behulp van moleculaire diagnostiek onderzocht kan worden. Ook adviseren we om langdurige follow-up te doen, ook na de standaard 5 jaar, zodat nieuwe tumoren vroegtijdig kunnen worden ontdekt.

Tot slot wordt in de discussie in **hoofdstuk 7** besproken hoe de resultaten van onze studies de basis leggen om in de (nabije) toekomst de diagnostiek en therapie van patiënten met vroeg-stadium longkanker te kunnen verbeteren. We discussiëren de beperkingen van onze populatie en studieopzet en welke mogelijkheden onderzocht kunnen worden om de condities voor patiënten die deze procedures te ondergaan verbeterd kan worden. Wij hebben echter niet kunnen laten zien dat patiënten die deze procedure ondergingen beter gediagnosticeerd konden worden, maar we benadrukken het belang van andere literatuur en de kleine studiepopulatie die gebruikt is. We laten zien hoe naast diagnostiek, de navigatiebronchoscopie procedure ook mogelijkheden biedt om lokale therapie toe te passen en op welke manier hier barrières verwacht kunnen worden, maar ook waar de kansen liggen. Daarnaast laten we zien dat het lymfesysteem per patiënt en per tumorlocatie verschillend is en welke bijdrage de poortwachter klier procedure in de toekomst zou kunnen leveren aan gepersonaliseerde behandelingen. Tegelijkertijd benadrukken we dat de resultaten uit deel II helpt om ons zorgsysteem zo efficiënt mogelijk in te zetten en patiënten in een zo vroeg mogelijk stadium te diagnosticeren om de beste behandeling te bieden voor hun longkanker of recidief.

De resultaten van dit onderzoek dragen bij aan het verbeteren van diagnostiek en behandeling van longkanker, met uiteindelijk als doel een betere prognose en kwaliteit van leven voor patiënten.



Research Data Management

Ethics and privacy

All studies described in this thesis were conducted in accordance with the Declaration of Helsinki and relevant national and international regulations. The institutional ethics review committee CMO Radboudumc (dossier numbers: 2020-6946, 2017-3706, 2017-3707 and 2019-5148) and the recognized Medical Ethics Review Committee METC Oost-Nederland (file number: NL81008.091.22) have given approval to conduct these studies.

The privacy of all study participants was safeguarded by the use of pseudonymization. The pseudonymization key was stored separately from the research data, on a secured network drive accessible only to selected members of the research team. Data collection from electronic medical records (EMR) was performed by personnel with a treatment relationship and/or based on informed consent. Informed consent was obtained from all participants for the collection and processing of their data for this research. Consent was also obtained for sharing and reuse of the (pseudonymized) data for future research.

Data collection and storage

For the CAELC trial (chapter 2), data were collected in Microsoft Excel and processed using SPSS. For the INITIATE trial (chapters 3 and 4), data collection occurred via electronic Case Report Forms (eCRF) in CastorEDC. All Castor databases are securely stored and accessible only to project members. Hardcopy data (CDs, documents) are stored in locked cabinets at the Radboudumc of which the digital data is stored securely on the internal server of the Department of Pulmonary Diseases.

Clinical data for Chapters 5 and 6 were extracted from EMR (EPIC) at the Radboudumc and stored securely on internal servers of the Department of Pulmonary Diseases. Digital source files and analysis data were archived on the department's research server with continuous back-ups. Metadata and documentation (protocols and readme files) are included to support reuse. Data will be archived for 15 years in accordance with Radboudumc policy.

Data sharing according to the FAIR principles

All studies are or will be published open access. datasets from the published chapters 2, 3, 4 and 5 in this thesis are published in Research Documentation Collections (RDCs) in the Radboud Data Repository with closed access*. The data underlying chapter 6 will be archived with closed access in an RDC of the Radboud

Data Repository after termination of the study. All data are or will be archived as an RDC remain available for at least 15 years after termination of the studies.

*The table below details where the data and research documentation for each chapter can be found on the Radboud Data Repository (RDR). All data archived as a Data Sharing Collection remain available for at least 15 years after termination of the studies.

Chapter	RDR - RDC	Name Data Repository
2, 3 & 4	DOI: 10.34973/m62m-st29	Injection of 99mTc-Nanocolloid and ICG To Identify, retrieve and quAlify Tumor draining lymph nodes in Early-stage lung cancer
5	DOI: 10.34973/j73q-t907	Added value of EBUS during navigation bronchoscopy

RDC = Research Documentation Collection

List of publications

In this thesis

Ter Woerds DKM, Verhoeven RLJ, van der Heide SM, Verhagen AFTM, Aarntzen EHJG, van der Heijden EHFM. *Ex-vivo* exploration of an endobronchial sentinel lymph node procedure in lung cancer for optimizing workflow and evaluating feasibility of novel imaging tools. *Journal of Thoracic Disease*. 2023 Feb 28;15(2):291–299. doi: 10.21037/jtd-22-984

Ter Woerds DKM, Verhoeven RLJ, Aarntzen EHJG, van der Heijden EHFM. Feasibility of non-invasive sentinel lymph node identification in early-stage NSCLC through ultrasound guided intra-tumoral injection of ^{99m}Tc-nanocolloid and iodinated contrast agent during navigation bronchoscopy. *Cancers (Basel)*. 2024 Nov 19;16(22):3868. doi: 10.3390/cancers16223868

Ter Woerds DKM, Verhoeven RLJ, van der Heide SM, Looijen-Salamon MG, Vos S, Aarntzen EHJG, Verhagen AFTM, van der Heijden EHFM. Feasibility of intraoperative indocyanine green injection to identify lymph nodes at risk of metastatic disease for early-stage lung cancer. *JTCVS Techniques*. 2025 May 21;32:172-181. doi: 10.1016/j.xjtc.2025.05.003

Ter Woerds DKM, Verhoeven RLJ, Verhagen AFTM, Aarntzen EHJG, van der Heijden EHFM. Endobronchial ultrasound staging during navigation bronchoscopy for peripheral pulmonary nodules in the real world: which patients will benefit? *Cancers (Basel)*. 2025;17(10):1700. doi: 10.3390/cancers17101700

Other publications

Ter Woerds DKM, Verhoeven RLJ, van der Heide SM, Verhagen AFTM, Aarntzen EHJG, van der Heijden EHFM. MA04.08 Navigation bronchoscopy mediated sentinel lymph node procedure: an explorative study in ex-vivo lung cancer specimens. *Journal of Thoracic Oncology*. 2022;17(9 Suppl):S57. doi: 10.1016/j.jtho.2022.07.098

Verhoeven RLJ, Kops SEP, Wijma IN, Ter Woerds DKM, van der Heijden EHFM. Cone-beam CT in lung biopsy: a clinical practice review on lessons learned and future perspectives. *Annals of Translational Medicine*. 2023 Aug 30;11(10):361. doi: 10.21037/atm-22-2845



PhD Portfolio

Department: Pulmonary Diseases

PhD period: 01-04-2021 – 31-01-2025

PhD Supervisor(s): Prof. Dr. H.F.M. van der Heijden and Prof. Dr. A.F.T.M. Verhagen

PhD Co-supervisor(s): Dr. R.L.J. Verhoeven and Dr. E.H.J.G. Aarntzen

Training activities	Hours
Courses	
Radboudumc - eBROK Course (2020)	42.00
RU - Workshops Research Grant Proposal (2020–2021)	21.00
Radboudumc - Introduction day (2021)	6.00
RIHS - Introduction course for PhD candidates (2021)	15.00
RU - Project management for PhD Candidates (2021)	56.00
RU - Effective Writing Strategies (2021)	84.00
Cancer development and immune defense - Master Biomedical Sciences (2021)	84.00
RU - Workshops Research Grant Proposal (2021–2022)	21.00
Radboudumc - Scientific integrity (2022)	20.00
Radboudumc - Basistraining Monitoring (2022)	42.00
RU - Statistiek voor promovendi met SPSS (2023)	60.00
Radboudumc - Re-registration BROK (2023)	5.00
RU - The Art of finishing up (2024)	10.00
RU - Zelfinzicht: de sleutel voor je loopbaan (2024)	7.00
Seminars	
Symposium: One day on Small Nodules in Lung Cancer (2021)	7.00
Symposium Interventional Pulmonology (2023)	8.00
NVvTG - Terugkomdag TG in de Nucleaire Geneeskunde (2023)	3.50
Radboud Research Integrity Rounds (2023–2024)	3.00
Conferences	
CaRe days, virtual meeting (2021)	28.00
6th European Congress for Bronchology and Interventional Pulmonology, Athens (2021)	21.00
RIHS PhD retreat, Nijmegen (2022)	14.00
Cancer Research Retreat, Berg en Dal (2022)	14.00
World Conference on Lung Cancer, Vienna (2022)*	40.00
World Congress for Bronchology and Interventional Pulmonology, Marseille (2022)*	28.00
Technical Innovations In Medicine conference, Utrecht (2023)	8.00
Conference of American Association for Bronchology and Interventional Pulmonology, Chicago (2023)*	35.00
PhD Retreat, Den Bosch (2023)*	17.00
Cancer Research Retreat, Berg en Dal (2024)*	19.00
Technical Innovations In Medicine conference, Utrecht (2024)*	16.00
The International Joint Meeting on Thoracic Surgery, Barcelona (2024)*	28.00

Other	
Journal Club department of Pulmonary Diseases (2021–2022)	14.00
Radboudumc - Thoracic Oncology Research Meetings (2023–2025)	30.00
Teaching activities	
Supervision of internships	
Daily supervision of 10-week M2 internship Technical Medicine (2021)	28.00
Supervision of Grant Proposal – Medicine/Biomedical Sciences (2020–2021)	49.00
Daily supervision of 10-week Bachelor Assignment, 4 students (2021)	28.00
Supervision of Grant Proposal – Medicine/Biomedical Sciences (2021–2022)	49.00
Daily supervision of 20-week internship Biomedical Sciences (2022)	54.00
Total	1014.50

* Oral presentation(s)



Curriculum Vitae

Desi (Karina Maria) ter Woerds was born on the 20th of July 1995 in Enschede, the Netherlands. After obtaining her Gymnasium degree in 2013 at the Marianum college in Groenlo, she studied Technical Medicine at the University of Twente in Enschede. During her Bachelor, she performed a research project where a set-up with a test lung was used to calculate the work of breathing needed to overcome the resistance of an endotracheal tube. She continued her education and completed the Technical Medicine master-track Medical Imaging and Intervention in 2021. Her interest in data to improve healthcare was further expanded by her role as datamanager in the Meetbaar Beter project at the Medisch Spectrum Twente in Enschede. During her Master's, she interned at Medisch Spectrum Twente in Enschede, Ziekenhuis Groep Twente in Hengelo and Radboudumc in Nijmegen to obtain clinical experience. The research performed at these institutes mostly involved imaging – namely CT, SPECT and MRI - and the thorax, where cardiovascular diseases and lung cancer were investigated. The title of her master thesis was “Towards endobronchial treatment of early-stage lung cancer by means of radioactive contrast agents”. This project was partly continued into her PhD trajectory, which she started directly after obtaining her Master's degree, under supervision of Prof Dr. Michel van den Heuvel, Prof. Dr. Erik van der Heijden, Dr. Erik Aarntzen en Dr. Roel Verhoeven. Her studies were expanded to the domain of Thoracic Surgery and therefore Prof. Dr. Ad Verhagen joined the promotion team as well. A sentinel lymph node procedure was implemented in navigation bronchoscopy and lung surgery procedures to determine its feasibility and added value to lung cancer staging in the Radboudumc, which involved the majority of her work as a PhD student. The results of the studies performed during this PhD trajectory are described in this thesis and publications will follow in the near future.



During her PhD project, her interest in (interventional) oncology grew. After completion of her PhD trajectory at the Radboudumc, Desi started as a Science Liaison at KWF Kankerbestrijding. She currently lives in Arnhem with her husband Max. After her PhD defense, she plans to move to Houston (Texas, USA) to work temporarily as a post-doctoral researcher on liver ablations at the Division of Diagnostic Imaging from the Department of Interventional Radiology at the MD Anderson Cancer Center.



Dankwoord

De afgelopen jaren in het Radboudumc waren een bijzonder traject waarin ik veel heb mogen leren, samenwerken en groeien als onderzoeker. Ik kwam op de afdeling Longziekten als tweedejaars Masterstudent en heb mezelf uiteindelijk mogen ontwikkelen tot een onderzoeker die studenten begeleidt en kennis over kan dragen. Dit proefschrift is niet alleen het resultaat van mijn eigen inspanningen, maar van een heel team aan collega's, begeleiders, vrienden en familie die mij op allerlei manieren hebben ondersteund. Ik wil dan ook graag iedereen bedanken die hier direct of indirect aan heeft bijgedragen.

Daarnaast wil ik **alle patiënten** die hebben deelgenomen aan de klinische studies of anderzijds hebben bijgedragen aan mijn kennis over het (mogelijk) hebben van longkanker, bedanken. Jullie betrokkenheid heeft niet alleen deze onderzoeken mogelijk gemaakt, maar mij ook gevormd als Technisch Geneeskundige, onderzoeker en als persoon.

Graag wil ik mijn promotieteam bedanken voor de fijne begeleiding. Beste **Erik van der Heijden**, ik wil jou heel graag bedanken voor de klinische blik die je mijn projecten altijd gaf en de manier waarop je mij uitdaagde om met een helikopter-blik naar mijn onderzoek te kijken. Ik zal nooit vergeten hoe erg ik ooit met de planning in de knoop zat en dat jij mij mailde dat je het al geregeld had. Toen ik je ervoor bedankte mailde je: "geen probleem, we zijn een team!" en dat was ook echt zo. Jij bent daarnaast ook iemand waar ik tegenop kijk als het gaat om het schrijven van artikelen. De snelheid waarmee je teksten kon herzien en tegelijkertijd de diepte in ging, is vrij ongekend, denk ik.

Beste **Roel**, jou wil ik ten eerste graag bedanken voor het feit dat ik me nooit druk heb hoeven maken om de financiën of de relaties met externe partijen, want dat nam jij allemaal op je. Af en toe kwam je daarom wel in een CPU-overload en moest je even navigeren naar het plekje in jouw hoofd waar bepaalde informatie opgeslagen stond, maar je kwam er altijd. Maar wat bovenaan staat, is jouw visie. Mijn toch wat uiteenlopende projecten waren nooit zo mooi bij elkaar gekomen, als jouw visie op het longkankeronderzoek in Nederland en daarbuiten niet zo breed was geweest. Naast mijn project heb jij ongeveer overal een visie op. Of dit nu in het onderzoek, in huis of bij de NVvTG is; je kunt er altijd vanuit gaan dat Roel er al over na heeft gedacht. Dat neemt absoluut niet weg dat je je visie niet wilde aanpassen aan nieuwe informatie, inzichten of meningen. Ik denk dat ik daarvan, nog steeds, veel kan leren en ik hoop dat in de toekomst ook nog te kunnen doen.

Ik wil je dan ook bedanken voor jouw begeleiding in het vormen van mijn eigen visie en het sparren hierover.

Beste **Erik Aarntzen**, ik ben dankbaar voor jouw betrokkenheid in mijn project en met name jouw blik op de horizon omtrent mijn lering en mijn loopbaan na mijn PhD. Jouw rol in mijn project was met name gericht op het Nucleair Geneeskundige stuk, maar je zette ook vaak andere petten op, puur om mij of de rest van het team een heel ander, objectief en vaak verrassend perspectief te geven. Dit heeft meermaals geleid tot het voorzien van mogelijke problemen in de toekomst, die we direct tijdens onze vergaderingen het hoofd konden bieden. Ook waren jouw connecties in het werkveld onmisbaar tijdens het pionieren in de wereld van SPECT en PET. Ik wil je bedanken voor de inbreng van jouw nucleair geneeskundige expertise, maar vooral ook jouw onafhankelijke, objectieve kijk op mijn project.

Beste **Ad**, hoewel je pas later werd toegevoegd aan mijn promotieteam, hebben we al vroeg kennis gemaakt op de OK en tijdens de tumorwerkgroep. Jij hebt toen vooral de taak van opleider op je genomen en ik heb veel geleerd van jouw rustige manier van vragen stellen, hardop denken en anatomisch inzicht. Het bekijken van de lymfeklieren was een grotere uitdaging dan we van tevoren hadden voorspeld, maar de leercurve die we daarin hebben doorlopen was vrij steil. Ik kijk met veel plezier terug op de tijd die we op de OK hebben doorgebracht. Ik wil je bedanken voor de stabiliserende rol die je hebt ingenomen in mijn promotieteam en de diepgaande input die je hebt geleverd voor de projecten uit dit proefschrift.

Beste **Michel**, jouw betrokkenheid bij het begin van mijn project was heel waardevol. Als afdelingshoofd kon je alle onderzoek goed overzien en me bepaalde richtingen op sturen om op ontdekkingstocht te gaan. Je stond dusdanig dichtbij mijn project dat je goed wist waar het over ging, maar je stond er ook dusdanig ver vanaf om naar het algehele traject en lering te kijken en me daar goed advies over te geven. Ook kon ik je altijd in vertrouwen nemen en heb ik veel geleerd over jouw manier van werken en hoe snel je kon schakelen.

Geachte leden van de manuscriptcommissie, **Jurgen, professor Annema** en **Olga**, ik wil jullie hartelijk bedanken voor het kritisch lezen van mijn proefschrift en de mooie woorden hierover. Ik kijk ernaar uit om het tijdens de verdediging met jullie te bediscussiëren.

Door de groei van de afgelopen jaren, kunnen we nu zeggen dat er een Onderzoeksgroep Interventiepulmonologie is. Oorspronkelijk bestond dit clubje

uit de (co)promotoren, mij en **Stephan**. Als congresbuddies hebben we meerdere congressen uitgespeeld en leerden we het spelletje goed kennen. Daarnaast konden we goede discussies voeren; over bevers, cappuccino en soms ook Longziekten en met name daar wil ik je voor bedanken. Lieve **Inge**, wat was ik blij toen jij je bij de club voegde. Jij weet van een groep een team te maken en zorgt ervoor dat iedereen zich welkom voelt. We konden goed sparren over technisch inhoudelijke vraagstukken en programmeren, maar ik wil je ook bedanken voor je hulp bij de CBCT, jouw positiviteit en onvermoeibaarheid. **Ferhat**, bedankt voor jouw enorme enthousiasme, de eerlijkheid waarmee je overal over praat en het lachen dat we samen hebben gedaan. **Annick**, gedeeld leed is half leed, dat hebben wij zeker gemerkt. Bedankt dat je me al je vragen stelde en andersom weer met mij meedacht, daardoor heb ik ook echt veel zelfvertrouwen gekregen. **Aniek**, bedankt voor je gezelligheid, de babyfeitjes en het delen van de uitdagingen van uitvoeren van een klinische studie. Lieve **Judith**, ook jou wil ik enorm bedanken voor jouw expertise, luisterend oor, de hulp die je me gaf bij het goed uitvoeren van de studies en data-analyse, de monitoring en algemene PhD-dingen.

Ook **Leila** wil ik hier benoemen, want jouw gezelligheid bij de WCLC en kennis nemen van hoe jij je begaf in het congresveld waren heel fijn. Last but not least, **Milou**, sidekick van de Interventielongziekten, bedankt dat je me in het begin hebt laten zien wat het inhield om een PhD te doen; jij was echt een voorbeeld voor mij en jouw doorzettingsvermogen is denk ik een inspiratiebron voor velen.

Ik wil ook heel graag de **afdeling Endoscopie** bedanken voor alle lering, het begrip voor de technologische en logistieke uitdagingen van het klinisch onderzoek en het altijd goede en duidelijke handelen omtrent de apparatuur. In het bijzonder wil ik **Ineke**, **Hennie** en **Annelou** bedanken voor jullie enthousiasme, behulpzaamheid, interesse in de studie en in mij en de altijd aanwezige gezelligheid op de OK of Angiokamer. Jullie oplettendheid en harde werken hebben het mogelijk gemaakt om dit er allemaal maar éven bij te doen, naast de al enorm complexe procedures die dagelijks uitgevoerd worden.

Beste **Stefan** en **Wilson**, ook jullie wil ik graag bedanken voor jullie betrokkenheid tijdens de klinische studie op de OK. Ik heb veel van jullie geleerd, niet alleen op anatomisch en chirurgisch vlak, maar ook op organisatorisch vlak. Daarnaast wil ik ook graag de **operatieassistenten van de CTC**, in het bijzonder Marjos, Inge en Maie, bedanken voor de fijne tijd die ik gehad heb op de OK. De communicatie verliep altijd heel soepel en ik heb me mede door jullie enorm thuis gevoeld en daardoor ook fouten durven maken, waar ik veel van geleerd heb. Ik wist altijd

dat ik en de studie in goede handen waren en dat jullie je er ook voor de volle 100% voor wilden inzetten. Ik vond het ook heel leuk hoe gaaf iedereen (ikzelf ook absoluut) de groene lymfeklieren altijd vond en hoeveel interesse er was vanuit het hele team.

De **afdeling Beeldvorming, Daphne, Steffie, Milou, Pieternel en Gerben** zou ik graag willen bedanken voor alle hulp, ondersteuning, gezelligheid en met name het vertrouwen bij het opzetten van toch wel een vrij complexe studie op radioactief vlak. Niet alleen de *ex vivo* studies – eerst bij het dierenlab en daarna op de SPECT/CT scanner – maar ook voorbereiding rondom de in-vivo studie verliep heel soepel en jullie hulp en de fijne samenwerking daarin vond ik heel waardevol. In het bijzonder wil ik ook **Maarten** enorm bedanken voor de hulp bij het (last-minute) inplannen van de scans en de flexibiliteit, snelheid en ruimte die je ons project daarin gaf en **Eddy, Marga en alle andere laboranten** die ik heb lastig gevallen tijdens het maken van de SPECT-scans wil ik ook enorm bedanken.

Als het gaat over diagnostiek van longkanker, is er één gouden speler in het werkveld en dat is de Pathologie. Ik wil **Shoko** heel erg bedanken met de hulp rondom het opzetten van de projecten, het interpreteren van de uitkomsten en ook het last minute bekijken van een zoveelste versie van een artikel. Jouw rustige, kritische blik en vastberadenheid waren een vaste kracht in mijn onderzoeken. Beste **Monica**, jou wil ik ook graag bedanken voor de weefselbeoordeling en het meedenken in het protocol. Ik wil ook heel graag de **pathologisch assistenten** bedanken voor de assistentie en het vertrouwen rondom het opspuiten van het weefsel tijdens de CAELC-studie, de soms krappe planning hiervan en de organisatie van de lymfeklierbak. Ik ben met name enorm dankbaar voor jullie oprechte interesse in het onderzoek, het enthousiasme als ik weer met de lymfeklierbak aankwam en jullie soepele, laagdrempelige communicatie daarin.

Alle andere **promovendi** van de afdeling Longziekten en binnen de **Thoracic Oncology Research Group** wil ik graag bedanken voor het enthousiasme tijdens onze maandelijkse vergaderingen en de hoeveelheid die ik van het hele werkveld heb geleerd. Ook wil ik graag de **onderzoeksassistenten** van de afdeling Longziekten bedanken voor de algehele ondersteuning in het uitvoeren van studies, monitoring en het reilen en zeilen binnen het Radboudumc en daarvan **Femke** in het bijzonder voor haar bijdrage aan de opstart van de klinische studies en het reilen en zeilen rondom de opslag van studiemateriaal. Ook wil ik graag het secretariaat Longziekten, **Rob, Hilda, Joyce en Jolanda** bedanken voor het beantwoorden van mijn eindeloze stroom vragen, het meedenken over logistieke

puzzels, de behulpzaamheid rondom alle andere administratieve en logistieke zaken en het lachen. De **backoffice Longziekten** wil ik graag bedanken voor het verwerken van alle opgestuurde patiëntgegevens en hulp bij postzaken. Ook de andere **verpleegkundigen, A(N)IOS en longartsen van de Longziekten** wil ik graag bedanken voor de gezelligheid op de afdeling, tijdens het jaarlijkse Longfeest en alles wat ik hier geleerd heb. Specifiek wil ik graag **Saartje** en **Nicolle** bedanken. De hoeveelheid werk die jullie namens de INITIATE-studie op de poli en ook in het kader van planning hebben gedaan is heel uitzonderlijk. Het samenwerken met jullie was heel fijn en ik kreeg enorm het gevoel onderdeel uit te maken van jullie kleine team en de strakke en efficiënte manier waarop jullie samenwerken. Jullie blik op de psychosociale ruimte die patiënten wel of niet hadden voor studie-informatie heeft mij altijd heel goed voorbereid op gesprekken en jullie feedback daarop gaf me veel vertrouwen. Daarvoor wil ik jullie heel erg bedanken!

Tijdens de opzet en uitvoering van de onderzoeken heb ik samengewerkt met meerdere bedrijven, maar met name de samenwerking met **Philips** was intensief. Ik wil daarom **Ronald** enorm bedanken voor jouw eerlijkheid, het vertrouwen in ons als team in het werken met het IVUS-systeem, maar met name ook de prachtige INITIATE-taart en natuurlijk de mozartkugln. Ook wil ik **Sander** graag bedanken voor de bijna-standaard worstenbroodjes en de open gesprekken die we hadden over samenwerkingen binnen het klinisch onderzoek. I would also like to thank the **Interventional Oncology team at Johnson&Johnson** for their valuable input and informing us of new insights quickly, to enable adaptation of the research to the latest information and making it even more clinically valuable.

Dan wil ik ook graag mijn collega's bij **KWF Kankerbestrijding** bedanken voor de fijne tijd die ik hier heb, de ruimte die ze mij geven om mijn PhD af te ronden en alle adviezen die ik daarover heb gekregen van jullie als ervaringsdeskundigen.

Ook wil ik graag de docenten en studieadviseurs van de **opleiding Technische Geneeskunde** en al mijn begeleiders tijdens de klinische stages bedanken. Mijn stages hebben de basis gelegd voor mijn interesse in onderzoek en me het vertrouwen gegeven meer werk te maken van deze interesse.

Als laatste wil ik natuurlijk mijn vrienden en familie bedanken. Dan wil ik graag beginnen met mijn lieve **dispuutsgenoten**, die ook mijn studiegenoten waren. Beste **Mirte** en **Jenske**, enorm bedankt voor de fijne gesprekken tijdens onze kopjes koffie, waarbij we konden sparren over het leven als onderzoeker, TG'er en alles daarbuiten. Ook **Auke** wil ik graag bedanken, voor de gezelligheid, jouw eerlijkheid

en onze sparringsessies over van alles en nog wat. Lieve **Nicolien**, ondanks dat we ook collega's zijn, zie ik jou meer als vriendin. Wij kunnen samen heel goed zeuren over de kleinste dingen, wetende dat het er ook allemaal niet toe doet, maar dat het gewoon lekker is om dat af en toe uit ons systeem te halen. Bedankt voor deze uitlatingen en alle gezelligheid en het lachen dat daarbij kwam kijken!

Ik wil mijn teamgenootjes van **Hydrofiel** en nu **ENC Arnhem** heel erg bedanken voor de interesse in mijn onderzoek en mijn werk, maar vooral de afleiding en daarmee steun die ik altijd bij jullie allen kon vinden. Ik wil ook mijn oud-huisgenoten van de **Batjas** bedanken dat ik hen altijd als klankbord kan gebruiken voor de alledaagse zaken. Tijdens mijn studie heb ik enorm genoten van de gezelligheid en ik ben blij dat we ook nu nog een goede band hebben en ik nieuwe levensfasen met jullie kan delen. Mijn lieve **vriendinnen van thuis-thuis (Lichtenvoorde)**, mijn cheerleaders, mijn OG's, waar ik altijd op terug kan vallen of waar ik terecht kan met mijn klaagzang wil ik heel erg bedanken voor hun onvoorwaardelijke steun. Jullie juichen mee met mijn successen en zijn er voor me als het allemaal even wat minder gaat. Vooral onze bijna wekelijkse snapchat-vlogs over het leven als werkenden hielpen mij enorm om wat meer perspectief te krijgen in mijn eigen werk en waar we allemaal wel niet dankbaar voor kunnen zijn. De vriendschap die we alweer meer dan 15 jaar hebben, koester ik enorm.

Lieve **Nienke**, jou wil ik ook heel graag bedanken, omdat ik me enorm aan jou optrek, gezien jij echt een goed voorbeeld bent van een TG'er in haar element. Jij weet wat je wilt in het leven en jouw vastberadenheid en veerkrachtigheid daarin is bewonderenswaardig. Ons schrijfweekend – wat voor mij meer een analyse-weekend was, maar absoluut niet minder waardevol – was dan ook echt heel tof, vooral omdat we ook echt goed kunnen lachen, naast het sparren over onze onderzoeken.

Ik wil mijn lieve **schoonfamilie Lhoest** bedanken voor hun oprechte interesse, het oefenen om mijn onderzoek uit te leggen aan leken en de fijne, eerlijke gesprekken die we met z'n allen kunnen hebben. Door af en toe naar het zuiden af te reizen, kon ik echt even loskomen van alle drukte en me even helemaal ergens anders op focussen, zoals bijvoorbeeld carnaval, Rieu of de volgende fles bubbels.

Beste **Sven** en **Lars**, jullie wil ik graag bedanken voor jullie interesse in mijn onderzoek en mijn studie. Ook al sluit deze niet aan bij jullie – toch ook technische – achtergrond en interesse in auto's, ik voel me altijd gehoord en gesteund door jullie. Ik zie dat jullie trots zijn op hoe we alle drie ons leven leven en ik ben ook enorm trots op jullie!

Lieve **mam** en **pap**, ik wil jullie enorm bedanken voor jullie onvoorwaardelijke steun, ook toen ik mijn eerste jaar Technische Geneeskunde niet ging halen, maar ik het heel graag nog een keer wilde proberen. We hadden hier met z'n allen zeker twijfels over, maar jullie vertrouwen en trots, ook als het af en toe even wat minder ging qua studie, maakte dat ik het toch aandurfde. Jullie hebben me de mogelijkheid gegeven zo ver mogelijk te komen en zo gelukkig mogelijk te worden in het leven en daar ben ik jullie heel dankbaar voor.

Lieve **Max**, mijn man en beste vriend, bij wie ik me altijd thuis heb gevoeld en van wie ik enorm veel houd. Ik wil je graag bedanken voor jouw tolerantie van mijn strebergedrag in onze studietijd, jouw interesse in wat mij interesseert en jouw altijd luisterend oor. Jouw onvoorwaardelijke steun zorgt ervoor dat ik ook daadwerkelijk mijn doelen na kan streven, omdat ik altijd op jou terug kan vallen als het niet goed uit zou pakken. Ik houd enorm veel van jou als persoon en als de rots in de branding van mijn leven. Ik ben heel benieuwd wat het leven ons samen gaat brengen in Houston. Gelukkig kan ik met jou aan mijn zijde de hele wereld aan.

